N 70 14569

NASA CONTRACTOR REPORT

NASA CR-61316

LONG RANGE SOLAR FLARE PREDICTION

By Dr. J. B. Blizzard

Department of Physics
Denver Research Institute
University of Denver
Denver, Colorado 80210

October 1969

Final Report

Prepared for

NASA-GEORGE C. MARSHALL SPACE FLIGHT CENTER
Marshall Space Flight Center, Alabama 35812

TECHNICAL REPORT STANDARD TITLE PAGE

1. REPORT NO. NASA CR-61316	2. GOVERNMENT ACCESSION NO.	3. RECIPIENT'S CATALOG NO.
4. TITLE AND SUBTITLE LONG RANGE SOLAR FLARE PREDICTION		5. REPORT DATE Oct. 1969
		6. PERFORMING ORGANIZATION CODE
7. AUTHOR(S) J. B. Blizard		8. PERFORMING ORGANIZATION REPORT # 4130-10
9. PERFORMING ORGANIZATION NAME AND ADDRESS Department of Physics, Denver Research Institute, University of Denver, Denver, Colorado 80210		10. WORK UNIT NO.
		11. CONTRACT OR GRANT NO. NAS8-21436
12. SPONSORING AGENCY NAME AND ADDRESS Aero-Astrodynamics Laboratory, NASA - George C. Marshall Space Flight Center, Marshall Space Flight Center, Alabama 35812		13. TYPE OF REPORT & PERIOD COVERED Contractor 6-68/8-69
		14. SPONSORING AGENCY CODE

15. SUPPLEMENTARY NOTES Distribution of this report is provided in the interest of information exchange. Responsibility for the contents resides in the author or organization that prepared it.

16. ABSTRACT

Statistical studies of solar cycles show a high correlation between solar perturbations and proton events. It is hypothesized that the motion of the sun and planets about the center of mass of the solar system could trigger solar disturbances in unstable zones in the solar subphotosphere at active longitudes. The results of this study indicate that many of the major recorded proton events occurred near major planet conjunctions.

(The publication of this report does not constitute agreement with its conclusions by NASA. It is published only for the exchange and simulation of ideas.)

17. KEY WORDS

18. DISTRIBUTION STATEMENT

PUBLIC RELEASE STAR Announcement

E. D. Geissler
Director, Aero-Astrodynamics Laboratory

19. SECURITY CLASSIF. (of this report)	20. SECURITY CLASSIF. (of this page)	21. NO. OF PAGES	22. PRICE
UNCLASSIFIED	UNCLASSIFIED	75	

MSFC - Form 3292 (May 1969)

<u>TABLE OF CONTENTS</u>

LIST OF TABLES

LIST OF FIGURES

ACKNOWLEDGMENTS

The author expresses gratitude to the Aero-Astrodynamics Laboratory, NASA Marshall Space Flight Center, Alabama, under whose sponsorship this work was performed as partial fulfillment of Contract NAS8-21436. Further acknowledgment is due to the University of Denver, Denver Research Institute for assistance in preparation of the line drawings and typing of the text. The author acknowledges much reference material supplied by J. P. Cox and R. N. Thomas of JILA, University of Colorado, and C. Warwick-Sawyer and M. Haurwitz of ESSA.

The author acknowledges very useful discussions with Col. L. L. DeVries, C. L. Hasseltine, W. T. Roberts, H. C. Euler, C. C. Dalton, and others of the Aero-Astrodynamics Laboratory, NASA Marshall Space Flight Center.

The encouragement of Lt. Col. D. T. Sherry, Col. C. K. Anderson, Lt. Col. Wm. O. Banks and Capt. Boright of the Solar Forecast Facility, 4th Weather Wing, Ent AFB, is acknowledged. Many thanks to R. M. Wood of McDonnell-Douglas for useful discussions and references, and to K. D. Wood of University of Colorado for contributing Section 9 of the Final Report.

Many thanks are due for helpful discussions with D. Billings, A. Skumanich, and J. Eddy of HAO: C. Sawyer-Warwick, M. Haurwitz, P. McIntosh, M. Dryer, R. Olson, R. Donnelly and T. Gray of ITSA-ESSA. Many thanks to J. P. Cox for reading the entire manuscript and for continuous encouragement during the course of the investigation.

DISCLAIMER

The contents of the report reflect the viewpoint of the author, who is responsible for the accuracy of the results presented. Section 9 represents solely the views of Prof. K. D. Wood. Publication of this technical report does not necessarily reflect the views or policy of NASA Marshall Space Flight Center or the U. S. Government.

1. INTRODUCTION

INTRODUCTION

The purpose of the current program has been to develop a long range solar flare prediction technique, and if possible, to determine the mechanisms involved in solar system dynamics correlating with proton events. Prediction of solar flare proton events is vital for the space program. The space crew could receive a lethal radiation dose from a single event. Communications are disrupted by polar cap blackouts and by ionospheric disturbances caused by accompanying X-rays. Upper atmosphere densities are sensitive to X-rays, protons and geomagnetic disturbances, all caused by proton events.

The current study has the following bases. (1) Studies were made only of flare-active sunspot groups, a subgroup of about 5% of all sunspots; (2) predictions have been made over a four year period and compared to actual solar activity, so that the method could be checked and improvements made; (3) the method is empirical and not dependent upon any theory.

An experimental method was used partly because a complete theoretical solution to planetary influence on solar activity requires a very large number of variables, even if a suitable theory is available. In addition, the sun displays cyclic behavior (Babcock, 1961) (Leighton, 1969) and latitudinal and longitudinal asymmetries which are probably not related to planetary configurations. Experience during several years of forecasting showed that significant results could be obtained with a small number of parameters, but some strictly solar parameters had to be included for a solution. It was necessary to include the solar active longitudes as a variable. The active longitudes are critical for proton events during the rising part of the cycle, less so during the declining part, when they are broader (i.e., at lower latitudes) and the sun is more flare-active (Gnevishev and Krivsky, 1966).

The outstanding examples of any phenomenon are worth special study for clues that may shed light on the general behavior of the whole class. Therefore outstanding proton event centers on the sun have been studied in detail. The study of large active centers established the correlation between solar activity and geomagnetic disturbances and their accompanying auroras. Giant active centers have been the means by which several other solar phenomena have been discovered (i.e., radio bursts from the February 1942 active center). Ground Level Events (GLE) were chosen for study because: (a) longer period of observation; (b) Trellis (1966) has shown that planetary influence is much greater for "centers of activity" (large, long-lived spot groups) than for all sunspots; (c) Four years' experience with a trial prediction system confirmed this non-linear effect. The prediction is excellent for major proton events, not as good for spot and flare activity. (d) A statistical analysis of the cycle 19 events showed that all of the GLE events could be explained by 4-planet configurations, whereas only about 80% of all the proton events and smaller centers of activity could be satisfactorily explained by 4 planet configuration. In the statistical analysis more events could be explained in the declining portion of the 11 year cycle than in the rising portion.

GLE's included by most authorities are: 28 Feb. 1942; 25 Jul. 1946; 19 Nov. 1949; 23 Feb. 1956; 16 Jul. 1959; 12, 15 Nov. 1960 and 18, 20 Jul. 1961, during cycles 17-19. (See Smith and Smith "Solar Flares," p. 219, and McDonald, "Solar Proton Manual," NASA TR-R169, pp. 12-13.) When ambiguity about the characteristic spectrum exists, the integrated intensity was used as a criterion. The May 1960 and Sept. 1961 events yielded proton fluxes a factor of 100 or more lower than the events discussed. Events of cycle 20 are listed in ESSA Solar Geophysical Data. Ground level events are: 7 July 1966; 28 Jan. 1967; 28 Feb., 30 Mar., 10 Apr., 1969.

Nearly all authorities agree on the first four GLE events because of the limited number of observing stations and methods. Discrepancies between lists begin to occur in late 1956. Before this time GLE's were measured by meson counters. These were later replaced by neutron monitors, and beginning at about the same time balloon and rocket soundings were obtained. The neutron monitors in turn have been replaced and/or supplemented by super-neutron monitors of greater sensitivity and by satellite measurements. The total number of neutron monitors has increased dramatically, located at many northern latitudes, and, beginning during the IQSY, at the south pole stations. Even longitude makes a difference since some events register strongly in Europe and not in the U. S. and vice versa. The seasonal tilt of the earth's axis also affects detection: the 28 Jan 1967 GLE event registered more strongly at the south pole stations than at the north pole stations. Therefore differences after 1956 are due largely to different monitoring techniques and different instrument locations. The four active centers studied during cycle 19 were responsible for 90% of the proton flux during that solar cycle.

It is hoped that the study will be useful in at least two contexts. First, to the person engaged in predicting solar, atmospheric or ionospheric parameters, it is hoped that the discussions of individual events are complete enough to explain the use of the technique. It is suggested that a person with such interests concentrate on the events from 1956 through 1969, and on such topics as active longitudes and major activity by phase of the 11-year cycle. Secondly, for the scientist interested in the causes of solar activity, it is hoped that sufficient information and reference material is included so that progress can be made on a very challenging theoretical problem. Solar system dynamics and its relationship to solar activity has undergone a very rapid growth in recent years. Much of the reference material is scattered throughout an extensive international literature not ordinarily read by astronomers. Progress to date has been accomplished by aerodynamicists, meteorologists, physicists and engineers and not by astronomers except in Soviet Bloc countries. It is sincerely hoped that such an unfortunate gap can be bridged in the near future.

2. ORGANIZATION OF REPORT

ORGANIZATION OF REPORT

Various phases of the study are described in separate sections which are largely self-contained. Some definitions and explanations are restated, and appropriate references are listed with each section.

Section 3 describes the prediction technique developed over 4½ years of forecasting. Conjunction dates for 94 years are given.

Sections 4 through 7 describe major active centers on the sun over a 110 year period. Probable events before 1942 are discussed on the basis of criteria developed in the study of events of cycles 17-19. Events after 1900 are described by conjunctions, 7 planet tidal force and derivative of tidal force. Ground level events and white light flares are described from 1942-1951. The latter two active centers are traced by 10-cm. radio flux for two months before the events. Four active centers of cycle 19 produced over 90% of the particle flux. The origins of the centers and the triggering of the events is described using 10 cm. radio flux enhancement on conjunction dates as an indicator for two months before proton events. Four active centers of cycle 20 are described using both X-ray and radio flux enhancements on conjunction dates. The development of each center is traced for three months. An evaluation of cycle 20 predictions is given, and forecasts of events in 1970-71 presented.

Section 8 enumerates three topics of importance for prediction: active longitudes, major activity by phase of solar cycle, and ultra-long-range forecasts of cycles 20, 21 and 22.

Section 9 by K. D. Wood, Ph.D., describes long range prediction of the solar cycle based on configurations of the outer planets.

Section 10: Conclusions and recommendations. Several recommendations are based on improvements in solar monitoring.

Section 11 (Appendix) discusses the solar system in three dimensions. If planet latitude has an effect on the sun, it would be related to the solar equator, not the ecliptic. A new coordinate system is developed.

3. EMPIRICAL APPROACH
(Planet Conj)

3. EMPIRICAL APPROACH

The problem of long range prediction of solar activity is discussed. Fluctuations in solar activity are influenced by motion of the sun about the center of mass of the solar system. Solar motion is caused by the motion of nine planets in eccentric orbits, resulting in a very large number of variables. In addition, the sun itself displays longitudinal and latitudinal asymmetries.

Therefore planetary influence on solar activity was first studied from the empirical point of view. It was found that sunspots, flares and proton events could be predicted by the position of four significant planets plus an active longitude on the sun. Conjunctions of these planets in alignment with an active solar longitude is followed by solar activity. Tables of planetary conjunctions over a 94 year period are given, for comparison to geomagnetic storm data which is available from five observatories from 1874 (Greenwich, Abinger, Huancayo, Watheroo and Slutsk-Pavlovsk).

A variety of planetary functions have been studied in an effort to understand solar system dynamics. Very long range modulation of the sunspot cycle seems to be related to motion of the outer planets, affecting solar displacement or velocity (Wood, 1968) or angular momentum (Jose, 1965) dominated by the outer planets. On the other hand, flares and proton events seem to follow conjunctions of Jupiter, Earth, Venus and Mercury (Blizard, 1968) which have high values of tidal force and rate of change of solar acceleration (jerk).

Finally, there is a discussion of the rank order of planetary influence on solar activity. Triple conjunctions of the four major planets are listed. Dates of triple conjunctions are given for a 70 year period, showing repetition patterns.

I. EMPIRICAL APPROACH TO FLARE PREDICTION

An empirical approach has been used to determine the mechanisms involved in solar-system dynamics correlating with sunspots, flares, X-ray emission, and proton events. First, the large flares and proton events of solar cycles 19 and 20 were examined in detail to determine the relationship between planetary parameters and proton events or flares. A correlation study was made using Chi-Square analysis (Blizard, 1965). It was found that conjunctions of two or more tidal planets increased solar activity. In particular, only three combinations of the four tidal planets correlate with 2/3 the proton events noted during 1956-1961. The possibility of such a correlation occurring by chance alone is less than 5 in 10,000 ($p = .0005$) using the Chi-Square Test of statistical significance. Other planetary combinations may be followed by X-ray flares. Conjunctions of three or more of these planets were even more likely to be followed by high solar activity. Planetary conjunctions are a necessary but not a sufficient condition for solar activity. In addition, active longitudes on the sun must be approximately in alignment with the longitude of conjunction.

A trial prediction method has been attempted over a period of 2-1/2 years (Blizard, 1968) indicating the approximate date and location of solar active centers which could result in proton events. This was the first long-range forecasting technique designed specifically to predict proton events, as distinguished from sunspots or radio emission. These forecasts were begun in June, 1965, predicting solar activity 120 days in advance. The predictions apply to events on the sun and not to transmission of radiation in interplanetary space. Proton events which have been successfully predicted by this method include:

Jul 9 Jul 28 Aug 28 Sep 2	1966
Jan 28 (Ground Level Event)	1967
Oct 31	1968

II. THEORETICAL APPROACH TO FLARE PREDICTION

It would be desirable to represent solar perturbations as continuous functions, but the crucial conditions preceding solar proton events have not as yet been successfully plotted in this manner. An approximation to the sunspot no. and/or 10 cm radio flux has been made by several investigators using the following functions:

(1) Jose (1964) - rate of change of solar angular momentum

(2) Wood and Wood (1965) - rate of change of solar acceleration

(3) Takahashi (1967) - tidal force squared

(4) Bigg (1968) - rate of change of tidal force

and for solar radio bursts by:

(5) Nelson (1952) - planetary conjunctions and 90° configurations,

and for solar particle events by:

(6) Blizard (1965) - rate of change of tidal force and resonance sequences of planetary conjunctions

(7) Head (unpubl.) - square of the modulus (gravity vector)

One reason for the inconsistent results in these approaches is that two functions may possibly be involved. Evidence for this includes:

(1) Influence of all nine planets on solar activity (Nelson etc.). Nearly all reasonable functions emphasize either the inner or outer planets. (K. D. Wood, 1968).

(2) Influence of planets in 90° configuration. No physical explanation is reasonable, except for rare occasions when the tidal function undergoes a sudden decrease due to a 90° configuration of 3 or 4 tidal planets. Recent examples are July 1966 and June 1968.

III. RANK ORDER OF PLANETARY EFFECTS

If the effects of individual planets were additive and linear, then one could examine the influence of the planets singly. However, that does not seem to be the case. If either sunspot number or proton events is used as a criterion, then the influence on solar activity of two planets in conjunction is usually greater than the sum of their separate influences. Computer analysis of the influence on sunspot numbers of Mercury alone and in combination with Venus, Earth or Jupiter shows a very complex curve (Bigg, 1965). Table 4 shows a simplified listing of tidal and jerk values for a variety of conjunctions, subject to the cautions above, that the individual effects are not strictly additive. These values are therefore considered only as a first approximation.

Theoretically, one finds that Venus-Jupiter conjunctions would be the most likely to be followed by proton events. However, when Jupiter's longitude lies between 0° and 90°, Mercury-Jupiter conjunctions are possibly more important (the perihelions of Jupiter and Mercury lie in this quadrant). Jupiter was located in this quadrant at the beginning of cycle 18, 19 and 20 and early in each cycle the monthly mean sunspot number shows a 90-day periodicity (the synodic period of Mercury-Jupiter conjunctions). Toward the end of these cycles, the 8-month Venus-Jupiter synodic period is clearly dominant in solar activity (for example, July 1959, May, November 1960, July 1961). Among triple conjunctions, it is no surprise to find Mercury-Venus-Jupiter to be of paramount importance.

CONCLUSIONS

Long range prediction of solar activity has become possible as a result of the study of solar system dynamics. Although a complete solution to the problem requires a very large number of parameters, realistic predictions can be made using as few as 5 variables. This method was the only one to successfully predict the July 7, 1966 proton event and the Jan. 28, 1967 ground level event from a flare on the far side of the sun.

The planetary conjunctions used empirically can be visualized in computer plots of tidal force (or jerk) as rapid variations. (Bollinger, 1960, Takahashi, 1968). These fluctuations are caused by sequences of conjunctions, by triple conjunctions and occasionally by sharp dips due to quadratures of tidal planets.

A variety of planetary functions have been offered to explain solar activity. The highest correlation with flares and proton events is with either:

(1) Rate of change of tidal force (or of tidal force squared),

(2) Rate of change of solar acceleration (jerk), both of which can explain events even at the beginning of the 11-year solar cycle.

TABLE 1. Dates of Planetary Conjunctions 1876-1970
(American Ephemeris)

Year	Mercury-Venus	Mercury-Earth	Mercury-Jupiter	Venus-Jupiter	Earth-Jupiter
1876	Jan 21 Jun 2 Oct 25	Feb 12 Jun 15 Oct 12	Mar 7 Jun 5 Sep 4 Dec 3	Jun 10	May 17
1877	Mar 30 Aug 1	Jan 26 May 26 Sep 26	Mar 4 Jun 1 Aug 30 Nov 28	Feb 2 Sep 26	Jun 19
1878	Jan 4 Jun 8 Oct 19	Jan 10 May 5 Sep 9 Dec 27	Feb 28 May 29 Aug 27 Nov 25	May 19	Jul 21
1879	Mar 17 Aug 14 Dec 20	Apr 16 Aug 23 Dec 9	Feb 24 May 25 Aug 23 Nov 21	Jan 10 Sep 5	Aug 30
1880	May 25 Oct 14	Mar 28 Aug 4 Nov 23	Feb 17 May 18 Aug 16 Nov 14	May 5 Dec 31	Oct 6
1881	Feb 28 Aug 2 Dec 13	Mar 10 Jul 17 Nov 7	Feb 13 May 13 Aug 10 Nov 7	Aug 27	Nov 12
1882	May 12 Oct 11	Feb 21 Jun 27 Oct 22	Feb 5 May 5 Aug 2 Oct 29	Apr 17 Dec 14	Dec 17
1883	Mar 7 Jul 20 Dec 21	Feb 5 Jun 7 Oct 6	Jan 27 Apr 27 Jul 24 Oct 21	Aug 6	
1884	Apr 25 Sep 29	Jan 20 May 17 Sep 18	Jan 20 Apr 18 Jul 17 Oct 14	Mar 28 Nov 25	Jan 19
1885	Feb 23 Jul 4 Dec 10	Jan 3 Apr 26 Sep 2 Dec 18	Jan 10 Apr 10 Jul 7 Oct 5	Jul 15	Feb 18
1886	May 4 Sep 14	Apr 8 Aug 15 Dec 2	Jan 7 Apr 8 Jul 5 Oct 3 Dec 31	Mar 9 Nov 1	Mar 21
1887	Feb 20 Jul 4 Nov 24	Mar 21 Jul 28 Nov 17	Mar 29 Jun 27 Sep 26 Dec 25	Jun 20	Apr 20
1888	Apr 27 Aug 30	Mar 3 Jul 8 Oct 31	Mar 24 Jun 22 Sep 21 Dec 21	Feb 9 Oct 6	May 21
1889	Feb 3 Jul 6 Nov 7	Feb 14 Jun 18 Oct 15	Mar 22 Jun 20 Sep 18 Dec 17	Jun 3	Jun 24
1890	Apr 15 Sep 16	Jan 29 May 29 Sep 29	Mar 18 Jun 17 Sep 15 Dec 14	Jan 17 Sep 15	Jul 29
1891	Jan 19 Jun 25 Nov 13	Jan 13 May 9 Sep 12 Dec 28	Mar 13 Jun 11 Sep 9 Dec 7	May 10	Sep 5
1892	Mar 31 Sep 2	Apr 18 Aug 25 Dec 11	Mar 11 Jun 8 Sep 6 Dec 4	Jan 10 Sep 5	Oct 12
1893	Jan 17 Jun 8 Nov 6	Mar 31 Aug 7 Nov 25	Mar 2 May 30 Aug 27 Nov 24	Apr 26 Dec 21	Nov 17
1894	Mar 15 Aug 19	Mar 13 Jul 20 Nov 10	Feb 22 May 22 Aug 19 Nov 15	Aug 19	Dec 22
1895	Jan 22 May 25 Oct 30	Feb 24 Jun 30 Oct 25	Feb 14 May 14 Aug 12 Nov 9	Apr 8 Dec 6	
1896	Mar 31 Aug 3	Feb 8 Jun 9 Oct 8	Feb 3 May 3 Jul 31 Oct 28	Jul 22	Jan 23
1897	Jan 8 May 31 Oct 14	Jan 21 May 20 Sep 21	Jan 27 Apr 27 Jun 25 Oct 23	Mar 21 Nov 12	Feb 22
1898	Mar 20 Aug 3 Dec 22	Jan 5 Apr 30 Sep 5 Dec 21	Jan 20 Apr 19 Jul 18 Oct 16	Jul 8	Mar 25
1899	May 29 Oct 5	Apr 11 Aug 18 Dec 5	Jan 14 Apr 14 Jul 14 Oct 12	Feb 26 Oct 20	Apr 25
1900	Mar 5 Aug 7 Dec 10	Mar 24 Jul 31 Nov 19	Jan 10 Apr 11 Jul 11 Oct 9	Jun 16	May 27
1901	May 16 Oct 15	Mar 7 Jul 12 Nov 4	Jan 9 Apr 9 Jul 8 Oct 5	Feb 6 Sep 22	Jun 30
1902	Feb 19 Jul 26 Dec 19	Feb 18 Jun 23 Oct 19	Jan 9 Apr 9 Jul 8 Oct 7	May 30	Aug 5
1903	Apr 30 Oct 4	Feb 2 Jun 3 Oct 3	Apr 2 Jun 30 Sep 8 Dec 26	Jan 24 Sep 17	Sep 11
1904	Feb 18 Jul 9 Dec 12	Jan 17 May 13 Sep 15 Dec 31	Mar 26 Jun 23 Sep 21 Dec 20	Apr 23	Oct 18
1905	Apr 22 Sep 19	Apr 23 Aug 29 Dec 15	Mar 20 Jun 17 Sep 14 Dec 12	Jan 8 Sep 1	Nov 23
1906	Feb 20 Jul 3 Nov 29	Apr 4 Aug 12 Nov 29	Mar 12 Jun 9 Sep 7 Dec 5	Apr 26 Dec 19	Dec 28
1907	May 2 Sep 7	Mar 17 Jul 24 Nov 14	Mar 3 May 31 Aug 28 Nov 25	Aug 12	
1908	Feb 8 Jul 7 Nov 12	Feb 28 Jul 4 Oct 28	Feb 22 May 21 Aug 18 Nov 16	Apr 5 Nov 28	Jan 29
1909	Apr 18 Sep 2	Feb 11 Jun 14 Oct 12	Feb 14 May 15 Aug 13 Nov 12	Jul 20	Feb 28
1910	Jan 24 Jun 30 Nov 7	Jan 25 May 25 Sep 25 Dec 31	Feb 9 May 8 Aug 7 Nov 4	Mar 13 Nov 2	Mar 30
1911	Apr 3 Sep 6	May 5 Sep 9 Dec 25	Feb 3 May 3 Jul 6 Oct 30	Jun 23	Apr 30
1912	Jan 13 Jun 13 Nov 12	Apr 15 Aug 21 Dec 8	Jan 28 Apr 29 Jul 28 Oct 26	Feb 17 Oct 11	May 31
1913	Mar 21 Aug 24	Mar 27 Aug 4 Nov 22	Jan 25 Apr 25 Jul 24 Oct 25	Jun 5	Jul 5
1914	Jan 16 May 29 Nov 4	Mar 10 Jul 16 Nov 7 Transit	Jan 24 Apr 24 Jul 23 Oct 22	Feb 1 Sep 26	Aug 10
1915	Mar 23 Aug 8	Feb 21 Jun 26 Oct 22	Jan 18 Apr 18 Jul 17 Oct 15	May 23	Sep 17
1916	Jan 13 May 21 Oct 24	Feb 4 Jun 5 Oct 4	Jan 15 Apr 13 Jul 11 Oct 9	Jan 15 Oct 15	Oct 23
1917	Mar 22 Jul 28 Dec 28	Jan 18 May 16 Sep 18	Jan 6 Apr 5 Jul 4 Oct 1 Dec 28	May 8 Dec 28	Nov 28
1918	Jun 3 Oct 5	Jan 2 Apr 26 Sep 1 Dec 18	Mar 27 Jun 24 Sep 22 Dec 21	Aug 21	
1919	Mar 9 Aug 4 Dec 12	Apr 7 Aug 15 Dec 2	Mar 18 Jun 16 Sep 12 Dec 11	Apr 16 Dec 7	Jan 1
1920	May 19 Oct 5	Mar 19 Jul 26 Nov 15	Mar 9 Jun 6 Sep 4 Dec 3	Jul 31	Feb 2
1921	Feb 21 Jul 27 Dec 5	Mar 2 Jul 7 Oct 30	Feb 28 May 28 Aug 26 Nov 25	Mar 23 Nov 13	Mar 4

TABLE 1. (Continued)

Year	Mercury-Venus	Mercury-Earth	Mercury-Jupiter	Venus-Jupiter	Earth-Jupiter
1922	May 4 Sep 6	Feb 13 Jun 17 Oct 14	Feb 23 Mar 25 Aug 22 Nov 20	Jul 6	Apr 4
1923	Feb 14 Jul 16 Dec 12	Jan 28 May 28 Sep 28	Feb 21 May 21 Aug 18 Nov 17	Mar 1 Oct 23	May 5
1924	Apr 19 Sep 23	Jan 12 May 7 Sep 11 Dec 26	Feb 15 May 15 Aug 13 Nov 12	Jun 15	Jun 5
1925	Jan 17 Jun 25 Dec 3	Apr 18 Aug 25 Dec 11	Feb 12 May 15 Aug 13 Nov 11	Feb 7 Oct 6	Jul 10
1926	Apr 22 Sep 6	Mar 31 Aug 7 Nov 26	Feb 10 May 12 Aug 10 Nov 9	Jun 2	Aug 15
1927	Feb 11 Jun 23 Nov 17	Mar 13 Jul 19 Nov 10	Feb 4 May 6 Aug 2 Oct 31	Jan 26 Sep 22	Sep 22
1928	Apr 20 Sep 10	Feb 24 Jun 29 Oct 24	Jan 31 Apr 31 Jul 29 Oct 26	May 18	Oct 29
1929	Jan 27 Jun 28 Nov 6	Feb 7 Jun 9 Oct 8	Jan 23 Apr 22 Jul 19 Oct 17	Jan 9 Sep 2	Dec 3
1930	Apr 9 Sep 4	Jan 22 May 20 Sep 21	Jan 14 Apr 13 Jul 12 Oct 9	Apr 26 Dec 19	
1931	Jan 11 Jun 18 Nov 4	Jan 6 Apr 30 Sep 5 Dec 21	Jan 6 Apr 5 Jul 3 Sep 30 Dec 28	Aug 14	Jan 6
1932	Mar 22 Aug 24	Apr 10 Aug 17 Dec 4	Mar 26 Jun 24 Sep 21 Dec 20	Apr 6 Nov 28	Feb 7
1933	Jan 8 Jun 22 Nov 1	Mar 23 Jul 30 Nov 19	Mar 19 Jun 18 Sep 15 Dec 14	Jul 21	Mar 9
1934	Mar 14 Aug 13	Mar 6 Jul 11 Nov 3	Mar 14 Jun 12 Sep 9 Dec 10	Mar 14 Nov 5	Apr 8
1935	Jan 17 May 23 Oct 23	Feb 17 Jun 21 Oct 18	Mar 10 Jun 8 Sep 7 Dec 4	Jul 3	May 10
1936	Mar 18 Jul 30	Jan 31 May 31 Oct 1	Mar 7 Jun 4 Sep 2 Dec 1	Feb 21 Oct 14	Jun 10
1937	Jan 2 Jun 6 Oct 7	Jan 14 May 11 Sep 14 Dec 30	Feb 28 May 29 Aug 30 Nov 30	Jun 2	Jul 15
1938	Mar 12 Jul 26 Dec 16	Apr 21 Aug 28 Dec 14	Feb 27 May 27 Aug 27 Nov 23	Feb 1 Sep 26	Aug 21
1939	May 19 Sep 23	Apr 3 Aug 10 Nov 28	Feb 19 May 21 Aug 19 Nov 19	May 26	Sep 27
1940	Feb 27 Jul 31 Dec 4	Mar 15 Jul 22 Nov 11	Feb 16 May 16 Aug 31 Nov 10	Jan 20 Sep 11	Nov 3
1941	May 8 Oct 9	Feb 26 Jul 2 Oct 27	Feb 8 May 8 Aug 5 Nov 2	May 8 Dec 29	Dec 8
1942	Feb 9 Jul 19 Dec 12	Feb 9 Jun 12 Oct 11	Feb 1 May 1 Jul 29 Oct 26	Aug 24	
1943	Apr 21 Sep 27	Jan 24 May 23 Sep 24	Jan 20 Apr 20 Jul 19 Oct 16	Apr 17 Dec 9	Jan 11
1944	Feb 7-8 Jul 2 Dec 1	Jan 8 May 2 Sep 6 Dec 23	Jan 13 Apr 12 Jul 12 Oct 10	Aug 2	Feb 11
1945	Apr 13 Sep 9	Apr 13 Aug 9 Dec 7	Jan 10 Apr 9 Jul 8 Oct 6	Mar 26 Nov 17	Mar 14
1946	Feb 11 Jun 19 Nov 20	Mar 26 Aug 2 Nov 21	Jan 2 Apr 1 Jun 29 Sep 28 Dec 27	Jul 11	Apr 13
1947	Apr 20 Aug 25	Mar 8 Jul 14 Nov 5	Mar 27 Jun 28 Sep 21 Dec 21	Mar 5 Nov 28	May 14
1948	Jan 31 Jun 24 Nov 5	Feb 20 Jun 24 Oct 20	Mar 22 Jun 21 Sep 19 Dec 19	Jun 24	Jun 15
1949	Apr 14 Aug 27	Feb 2 Jan 3 Oct 3	Mar 22 Jun 20 Sep 18 Dec 17	Feb 10 Oct 11	Jul 20
1950	Jan 16 Jun 17 Oct 29	Jan 17 May 14 Sep 17	Mar 17 Jun 15 Sep 13 Dec 11	Jun 5	Aug 26
1951	Mar 29 Aug 28 Dec 31	Jan 1 Apr 25 Aug 31 Dec 17	Mar 8 Jun 7 Sep 4 Dec 3	Jan 28 Sep 23	Oct 3
1952	Jan 1 Jun 6 Nov 8	Apr 5 Aug 12 Nov 30	Mar 5 Jun 3 Aug 30 Nov 28	May 18	Nov 8
1953	Mar 13 Aug 1	Mar 18 Jul 25 Nov 14	Feb 25 May 25 Aug 22 Nov 20	Jan 13 Oct 9	Dec 13
1954	Jan 10 May 22 Oct 25	Mar 1 Jul 6 Oct 29	Feb 16 May 16 Aug 14 Nov 11	May 2 Dec 21	
1955	Mar 15 Aug 1	Feb 12 Jun 16 Oct 13	Feb 8 May 8-9 Aug 7 Nov 1	Aug 17	Jan 15
1956	Jan 6 May 14 Oct 13	Jan 27 May 25 Sep 26	Jan 31 Apr 30 Jul 28 Oct 25	Apr 9 Nov 30	Feb 16
1957	Mar 12 Jul 20 Dec 21	Jan 9 May 5 Sep 9 Dec 25	Jan 23 Apr 23 Jul 20 Oct 19	Jul 23	Mar 17
1958	May 20 Sep 24	Apr 16 Aug 23 Dec 9	Jan 17 Apr 17 Jul 16 Oct 14	Mar 16 Nov 8	Apr 17
1959	Feb 18 Jul 25 Dec 6	Mar 29 Aug 5 Nov 24	Jan 13 Apr 13 Jul 13 Oct 11	Jul 2	May 18
1960	May 12 Sep 24	Mar 10 Jul 16 Nov 7 Transit	Jan 10 Apr 9 Jul 9 Oct 7	Feb 24 Oct 17	Jun 20
1961	Feb 14 Jul 22 Nov 26	Feb 21 Jun 27 Oct 27	Jan 6 Apr 7 Jul 6 Oct 4	Jun 12	Jul 25
1962	Apr 26 Sep 30	Feb 5 Jun 7 Oct 6	Jan 3 Apr 3 Jul 2 Sep 30 Dec 30	Feb 5 Sep 2	Aug 31
1963	Feb 2 Jul 7 Dec 4	Jan 20 May 17 Sep 20	Mar 28 Jun 26 Sep 23 Dec 22	May 28	Oct 8
1964	Apr 11 Sep 17	Jan 4 Apr 27 Sep 2 Dec 18	Mar 20 Jun 18 Sep 15 Dec 4	Jan 20 Sep 14	Nov 13
1965	Feb 6 Jun 18 Nov 25	Apr 8 Aug 15 Dec 2	Mar 13 Jun 9 Sep 17 Dec 5	May 11	Dec 18
1966	Apr 11 Aug 30	Mar 21 Jul 28 Nov 17	Mar 5 Jun 2 Aug 30 Nov 27	Jan 5 Aug 27	
1967	Feb 4 Jun 12 Nov 10	Mar 4 Jul 9 Nov 1	Feb 24 May 25 Aug 22 Nov 19	Apr 22 Dec 13	Jan 20
1968	Apr 15 Aug 18	Feb 15 Jun 18 Oct 15	Feb 17 May 16 Aug 14 Nov 11	Aug 5	Feb 20
1969	Jan 19 Jun 21 Oct 25	Jan 29 May 29 Sep 29	Feb 9 May 10 Aug 7 Nov 5	Mar 28 Nov 20	Mar 21
1970	Apr 1 Aug 26	Jan 13 May 8 Sep 12 Dec 28	Feb 3 May 4 Aug 2 Oct 31	Jul 13	Apr 21

TABLE 2. Triple Conjunctions of Mercury, Venus and Jupiter
(23.3 Year Series)

1903'	Sept. 28	356°
1910	Nov. 4	208°
1916	Jan. 16	5°
1917	Dec. 28	67°
1919	Dec. 11	128°
1925	Feb. 12	275°
1927	Feb. 1	336°
1934	Mar. 14	196°
1939	May 21	352°
1941	May 8	57°
1943	Apr. 20	118°
1948	Jun. 21	264°
1950	Jun. 15	326°
1957	Jul. 21	186°
1962	Sept. 30	340°
1964	Sept. 15	45°
1966	Aug. 27	110°
1971	Oct. 20	253°

TABLE 3. Triple Conjunctions of Mercury, Venus and the Earth Within 10° from 1902 to 1969 (40 Year Period)

1898	Dec. 23	1938	Dec. 14
1902	Feb. 18	1942	Feb. 9
1903	Oct. 3	1943	Sep. 24
1905	Apr. 23	1945	Apr. 13
1906	Nov. 29	1946	Nov. 21
1908	Jul. 5	1948	Jun. 24
1910	Jan. 25	1950	Jan. 17
1911	Sep. 9	1951	Aug. 31

TABLE 4. Rank Order of Conjunctions

Planets	Jerk		Tidal	
	Max	Ave	Max	Ave
Me+V	6.1	4.9	4.2	3.0
Me+J	4.7	2.4	4.6	3.1
V+J	3.7	3.5	4.8	4.4
Me+E	4.6	2.4	3.0	1.9
E+J	2.2	2.0	3.6	3.2

REFERENCES

Bigg, E. K., "Influence of the Planet Mercury on Sunspots," Astronom. J., 72, pp. 463-66 (May 1967) (also private communication, Sept. 1968).

Bhargava, B. N. and Subrahmanyan, R. V. "Geomagnetic Sudden Commencements During Solar Cycles 12 to 18," Planet. Spa. Sci. 14, 871 (1966).

Blizard, J. B., "Prediction of Solar Flares Months in Advance," Astronom. J. 70, No. 9, p. 667 (November 1965).

"Solar Activity and Planetary Positions," Bull. Am. Phys. Soc. 13, (June 1968).

Bollinger, C. J., "Atlas of Solar Planetary Climate," Battenberg Press, Norman, Okla., 1960.

Head, R. M., "A Triggering Mechanism for Solar Flares," (Unpublished) also NASA AT64-915 (1964).

Jose, Paul D., "Sun's Motion and Sunspots," Astronom, J. 70, #3, pp. 193-200, (April 1965).

Meldahl, K. G., "Tidal Forces in the Sun's Corona Due to Planets," Berlinske Forlag, Copenhagen, Part I (1938) Part II (1949).

Nautical Almanac Office, "Planetary Coordinates for the Years 1800-1940, 1940-1960, and 1960-1980," H. M. Stationery Office, London, 1933, 1939, 1958.

Nelson, J. H., "Planetary Position Effect on Short-Wave Signal Quality," Electrical Engineering - 421-424 (May 1952).

"Shortwave Radio Propagation Correlation with Planetary Position," RCA Review, pp. 26-34 (March 1951).

"Radio Weather Forecasting Techniques," Trans. I.R.E. CS-2, No. 1, pp. 19-23 (Jan. 1954).

Takahashi, K., "On the Relation between the Solar Activity Cycle and the Solar Tidal Force Induced by the Planets," Solar Physics, 3, pp. 598-602 (April 1968).

Trellis, M., Comptes Rendus, 262, No. 3, pp. 221-24 (Jan. 17, 1966). Nov. 4, pp. 3-2-15 (Jan. 24, 1966), No. 5, pp. 376-77, (Jan. 31, 1966).

"Solar Geophysical Data," ESSA, Dept. of Commerce (monthly) and Preliminary Reports on Solar Activity (weekly).

U. S. Government Printing Office, Amer. Ephemeris & Nautical Almanac, (yearly).

Wood, R. M., and Wood, I. D., "Solar Motion and Sunspot Comparison," Nature 2-8, #5006, pp. 127-31, (Oct. 9, 1965).

Wood, K. D., "Long-Range Prediction of the Solar Cycle Based on Planetary Effects," SECTION 9.

4. MAJOR EVENTS BEFORE 1942

4. MAJOR EVENTS BEFORE 1942

On the basis of studies of cycles 17, 18 and 19, it is possible to establish nine criteria for the occurrence of major proton flares. Most of the features listed below have been recorded over the 130 year period of quantitative solar observations. Thus it is feasible to study earlier solar cycles and determine major proton flare activity, on the basis of one or more of these criteria. The nine criteria are as follows:

(1) The Plage-sunspot region must be in second or later passage.

(2) The sunspot area must be greater than 500 millionths on the same disk passage.

(3) The penumbra must enclose umbra of opposite polarity (delta configuration).

(4) The flare must cause a magnetic crochet, or short wave fade (SWF) which follows the time of the flare maximum intensity.

(5) The flare must cover a significant part of the sunspot umbrae.

(6) The flare must be accompanied on the same disk passage by the loop prominence system.

(7) The spot group must be magnetically complex, beta or beta-gamma.

(8) The flare must occur at an active Carrington longitude.

(9) The flare must occur near one of the three peaks of major activity in the 11 year cycle.

Applying criteria (1) and (2), a search for early proton flares could begin by scanning the Greenwich records of recurrent sunspots of area >500 millionths of the solar hemisphere.

The discussion will concentrate on events later than 1900 for the following reasons:

1. A complete 59.5 year Jupiter-Saturn cycle is covered, and almost one-half of a Uranus-Neptune cycle. For this reason, 7-planet tidal forces have been computed from 1900-1959 (Bollinger, 1960).
2. Sunspot polarities from 1913 and magnetic field strengths from 1917 are available (Hale and Nicholson, 1938).
3. Daily maps of the chromosphere and prominences are available from Meudon Observatory from 1919 to date (d'Azambuja)
4. Systematic sunspot observations were made by both Greenwich and Mt. Wilson Observatories from 1917.

The discussion thus proceeds to solar cycles 14 thru 17, with descriptions of the following proton events: 10 September 1908, 10 August 1917, 24, 25 January 1926, and 14 January 1938. The 1908 event took place following the time of Uranus-Neptune opposition, when the three inner planets Mercury, Venus and Earth were in alignment with the two outer planets. The 1917 event is the first for which we have magnetic field strength measurements. The 1926 events took place in the largest spot group ever measured before 1946 in solar cycle 18. The January 1937 event was one of the first for which a Forbush decrease and short wave fade were observed. Thus each of these events can contribute uniquely to our understanding of the proton flare mechanism.

I. LONG-LIVED GIANT SUNSPOTS

Long-lived large spot groups are considered a prerequisite for proton flare activity. A search for possible proton flares before 1942 might begin by scanning the list of 55 largest sunspots 1874-1954 (Greenwich, 1955). The number of independent spots is actually smaller, since each passage of a large sunspot group is listed. When repetitions are eliminated, the list contains 49 independent sunspots. If spots after 1942 are eliminated (a period which is discussed in other sections), there are 40 remaining sunspots. Five of these spots appeared for only one passage, and are therefore very unlikely to have produced proton flares. A further eight were non-flaring spots which died out quickly, crossing CMP on Oct. 1903, Feb. and July 1905, Mar. 1920, Mar. 1926, and Sept. 1939. The remaining 27 active spot groups (Table 5) have a curious distribution. Almost half (48%) (13) occurred during cycle 17, and five during cycle 13. The remaining cycles have an average of only 2½ active spots, after only two criteria are applied: spot size and lifetime. Application of other criteria - magnetic class, active longitudes penumbral area, etc., would eliminate some of these. Even spots with areas >750 millionths (Table 6) are rare indeed before cycle 17. If the supplemental list of geomagnetic storms, 1840-1874 is scrutinized, one can discover a few other major spot groups (Table 7). Nevertheless the total number still remains amazingly small.

Table 5. Recurrent Large Sunspots, Cycles 12-17 from List of 55 Largest Sunspots, 1874-1954. (Greenwich, 1955).

CYCLE	YEAR	CMP DATE	INTERV. From Rm	MAX. AREA	UMBRA RATIO	LONG.	LAT
12	1882	Apr 19.1	-1.6	2123	.158	64.7°	-28.5°
		Nov 18.8	-1.0	2425	.211	121.0	+19.2
13	1892	Feb 11.9	-2.0	3038	.172	255.7	-28.2
		Jul 10.2	-1.6	2387	.153	83.4	+11.1
	1893	Aug 7.4	-0.5	2621	.161	292.6	-17.6
	1897	Jan 9.4	+2.9	2743	.161	342.2	- 6.8
	1898	Sep 9.2	+4.6	2235	.161	239.1	-12.1
14	1905	Oct 20.2	-1.2	2995	.095	161.9	+13.8
	1907	Feb 12.4	+0.1	2555	.152	306.2	-16.6
		Jun 19.7	+0.5	2072	.152	65.6	-14.4
	1908	Aug 31.2	+1.7	1919	.137	35.2	+ 6.6
15	1917	Feb 7.5	-0.5	3590	.146	9.0	-16.0
		Aug 10.2	0.0	3178	.136	129.2	+16.2
16	1926	Jan 24.5	-2.3	3716	.159	35.0	+20.0
		Sep 19.7	-1.7	2142	.172	129.4	+24.1
	1929	Nov 3.7	+1.2	2003	.166	189.3	+14.8
17	1935	Dec 2.2	+1.5	2435	.172	55.2	-25.5
	1937	Jan 31.1	-0.3	2364	.146	196.3	-10.1
		Apr 24.7	-0.1	2474	.174	173.9	+19.5
		Jul 28.8	+0.2	3303	.159	356.1	+31.5
		Oct 4.4	+0.4	3340	.146	182.3	+ 9.3
	1938	Jan 18.4	+0.6	3627	.176	225.1	+17.1
		Jul 15.1	+1.1	3379	.147	39.8	-12.1
		Oct 11.9	+1.4	3003	.133	305.7	+17.0
		Nov 10.8	+1.5	2245	.174	272.0	- 8.5
	1939	Sep 10.4	+2.3	3034	.164	224.1	-13.8
	1940	Jan 5.5	+2.6	2860	.207	120.2	+10.5
	1941	Sep 16.9	+4.3	3038	.148	210.0	+11.6
	1942	Feb 28.8	+4.8	2048	.191	197.1	+ 7.0

Table 6. Number of Sunspots with Areas >750 Millionths during Solar Cycles 12 thru 18 (Greenwich, 1955)

CYCLE	A >750	A >1000	A >1500	A >2000	A >2500
12	69	40	11	4	0
13	85	46	17	7	3
14	68	35	15	7	4
15	66	46	15	4	3
16	93	60	17	4	3
17	123	79	31	17	8
18	155	92	37	18	8

Table 7. Sunspots with Areas >1000 Millionths before 1874, Associated with Geomagnetic Storms (Greenwich, 1955)

CYCLE	YEAR	DATE, CMP	INTERV. from Rm	AREA
8	1842	Jul 1	+5.3	1500
9	1847	Sep 19[x]	-0.4	3000
		Oct 23[x]	-0.3	2700
		Dec 16	-0.1	1000
	1848	Feb 20	0.0	1000
10	1859	Aug 31[x]	-0.4	2300
	1860	Aug 8	+0.5	2000
		Sep 4	+0.6	1300
	1866	Feb 18	+6.0	1700
11	1870	Sep 21	+0.1	1700
		Sep 25	+0.1	1200
	1871	Aug 20	+1.0	1250

[x]Caused storms of outstanding range

II. PROTON EVENTS BEFORE 1900

Several noteworthy observations of major solar flares before this time are worthy of study. Since flares occur preferentially in giant spot groups, the earlier observations are better than might otherwise be the case. Reliable data, including photographs and/or detailed sunspot drawings, are available for the following flare events, listed with their observers:

1 Sep 1859 - Carrington, Hodgson (Hale, 1931) (Bartels, 1937)

28 Sep 1870 - Young (Lockyer, 1874)

18, 20, 21 Nov 1882 - Maunder (Newton, 1943)

11, 15 Jul 1892 - Rudeaux (Larousse, 1959) (Hale, 1931).

Planetary conjunctions preceding the proton active centers are given in Table 8.

Geomagnetic crochet measurements were obtained on three of these events (Newton, 1943). In both the 1859 and 1892 cases, the crochet maximum followed the white light flare maximum (Newton, 1943), a characteristic of proton flares. The 21 Nov 1882 flare was accompanied by a crochet which preceded the flare maximum.

A still earlier period may be investigated using the supplement to Catalog I: List of Great Storms recorded at Greenwich 1840-1874 (Greenwich, 1955). All sunspot groups with areas >1000 millionths in the list have been included in Table 7.

Table 8. Planetary Conjunctions Prior to Proton Events of 1859, 1870, 1882 and 1892. (American Ephemeris, 1882, 1892) (Stahlman and Gingerich, 1963).

EVENTS	CONJ. DATE	PLANETS	LONGITUDE
1 Sep 1859	Jun 26	Mercury Jupiter (Earth)	97°(277°)
	Jul 23	Venus Jupiter	279°(99°)
	Aug 18	Venus (Mars Saturn)	316°(136°)
	Sep 1	Mercury Venus Earth Neptune	341°
28 Sep 1870	Jun 3	Mercury Earth	253°
	Jul 6	Mercury Venus	33°
	Jul 12	Mercury Jupiter	66°
	Aug 16	Venus Jupiter	68°
18,20 21 Nov 1882	Oct 11	Mercury Venus	346°
	Oct 22	Mercury Earth L* = 121°	33°
	Oct 26	Mercury Saturn Neptune	55°
	Oct 29	Mercury Jupiter	78°
11,15 Jul 1892	Apr 18	Mercury Earth Uranus	207°
	May 9	Venus Saturn (Jupiter)	192° (12°)
	Jun 4	Mercury Jupiter	13°
	Jun 16	Mercury Neptune (Venus)	72°(252°)
	Jul 4	Venus Earth Mars	287°

*Active solar longitude, see Table 1 for sunspot data

III. PROTON EVENT OF 10 SEPTEMBER 1908

The active center of September 1908 was observed visually, photographically and spectroscopically in the wavelength of calcium and Hα (Hale, 1931). The features observed on the sun were:

1. Giant Sunspot Groups - several groups were involved in the flare which crossed the solar equator. The maximum area at S 5.6^{o} was 568 millionths of the solar hemisphere, and at N 12^{o} the area as 1121 millionths, making a total of 1689 millionths. The average Carrington longitude was 270^{o}, which was an active longitude in cycle 14 for the northern hemisphere (Vitinsky 1965) and possibly at low latitudes for the south.

2. Hα Flare - began in the southern spot and stretched to the north in two branches. Three spectroscopic photographs were taken in sequence at Yerkes Observatory.

3. Magnetic Field - was of the complex type as determined by the sunspot configuration. Actual polarities and field strengths had not yet been measured.

The following solar-terrestrial effect was noted:

1. Geomagnetic storm - followed 26 hours later. A crochet was not measured for this event.

Interpretation - Noteworthy is the succession of four conjunctions involving 3 or more planets each (Fig. 1). The spot group developed rapidly following the five planet conjunction of Mercury, Venus, Earth and Uranus in opposition to Neptune, and reached an area of 1070 millionths on its August passage. The two months preceding the event witnessed rapid changes in planetary tidal force. (Bollinger, 1960.) The tide rose from a minimum of 3195 units on 1 June 1908 to a maximum of 6136 units on 27 July, followed by a dip to 5267 on 4 August and a rise to 6448 on 12 August. A long steep decline followed to a value of 3559 on 21 September.

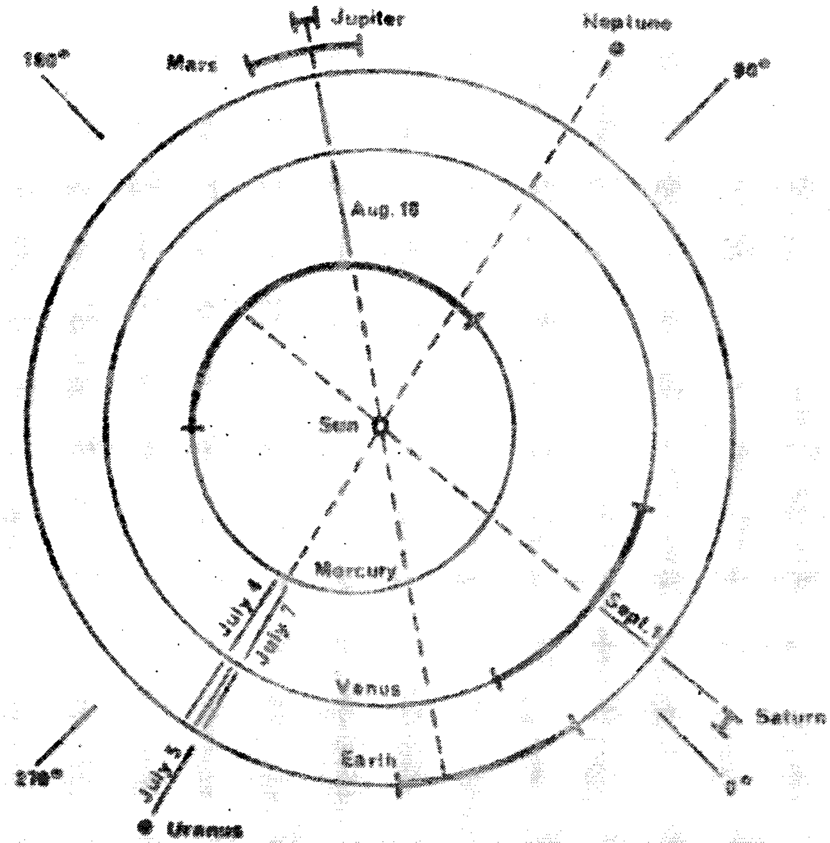

Fig. 1 Planetary Configuration One Month Prior to Proton Event of 10 September 1908

DATE	PLANETS	LONGITUDE
Jul 4	Mercury Earth	280°
Jul 5	Venus Earth	282°
Jul 7	Mercury Venus Uranus(Neptune)	284° (104°)
Jul 27	Mercury Saturn	15°
Aug 11	Mercury Neptune (Uranus)	104° (284°)
Aug 18	Mercury Mars Jupiter (Earth)	147° (327°)
Sep 1	Venus Saturn (Mercury)	15° (195°)

IV. PROTON EVENT OF 9 AUGUST 1917

In the middle of July 1917 a large region developed at N 18° and Carrington longitude $L_o = 130°$. On the first passage in July the spot group had a maximum area of 1412 millionths. On the August passage the following features were noted:

1. Giant Sunspot Group. The maximum area during the August passage was 3178 millionths, the largest spot group ever measured up to that time at Greenwich, with the exception of the February 1892 spot.

2. Hα Flares. Major flares occurred on 8 and 9 August. Photos show the flare crossing between umbrae of opposite polarities within the main penumbra (the delta configuration) on 9 August; the umbrae were largely covered by the spreading flare. Umbral coverage has been noted as a condition for proton emission.

3. Magnetic Fields - of up to N-2900 and S-3300 gauss were found in the βγ group (Hale, Ellerman, Nicholson and Joy, 1919).

The following solar-terrestrial effects were noted:

1. Geomagnetic Storms - were recorded on 9 and 13 August.

Interpretation. On 8 May there was a conjunction of Venus and Jupiter; on 16 May of Mercury and Earth, on 4 July a triple conjunction of Mercury, Mars and Jupiter, and finally on the 28th of July a conjunction of Mercury and Venus (Fig. 2). The Carrington solar longitude $L = 130°$ which produced the flares was opposite (180° degrees away) the triple conjunction on 4 July. In terms of the Bollinger planetary tidal index, there were successive maxima of 6314, 5191 and 5176 on 17 May, 4 July and 13 August, and minima of 4350 and 4198 on 18 June and 20 August (Bollinger, 1960).

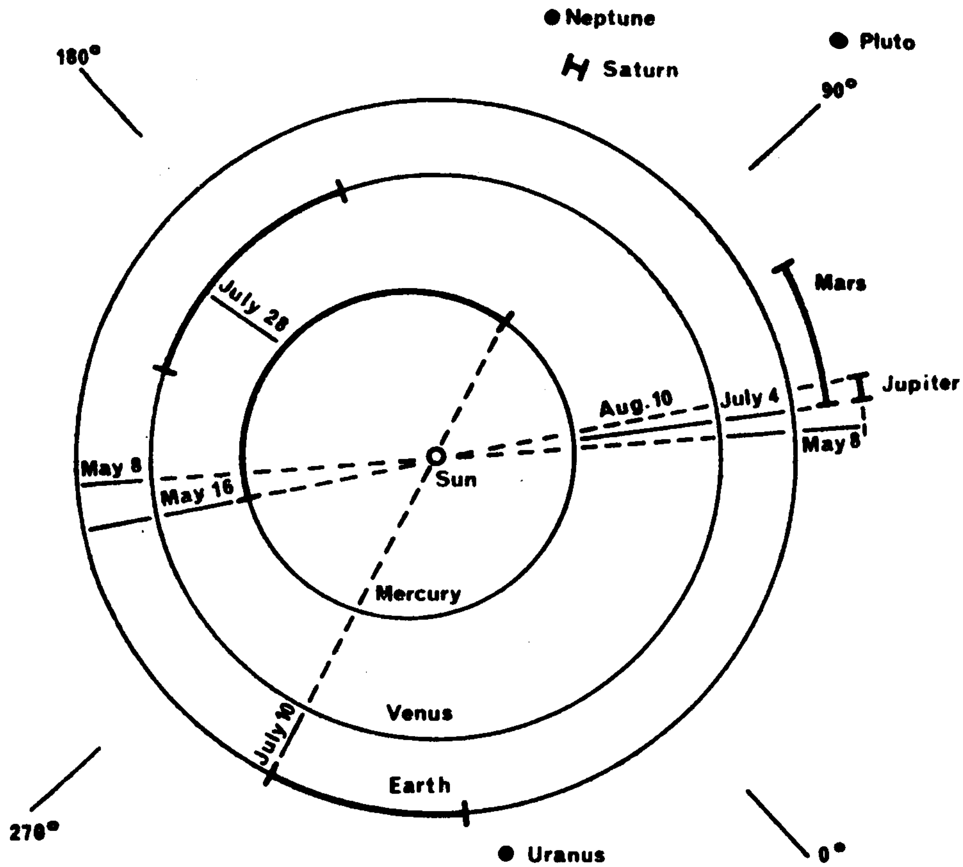

Fig. 2 Planetary Configuration One Month Prior to Proton Event of 9 August 1917

DATE	PLANETS			LONGITUDE
May 8	Venus	Jupiter	(Earth)	51° (231°)
May 16	Mercury	Earth		239°
Jun 14	Mercury	Uranus		326°
Jul 4	Mercury	Mars	Jupiter	56°
Jul 10	Mercury	Earth		112, 292°
Jul 12	Mercury	Saturn		120°
Jul 14	Mercury	Neptune		126°
Jul 28	Mercury	Venus		190°
Aug 10	Mercury	Jupiter		238°, 58°

V. PROTON EVENT OF 25 JANUARY 1926

The sixth largest spot group ever recorded at Greenwich was observed in January 1926. It was the largest sunspot measured up to that time. During the December 1925 passage the spot had already reached an area of 2934 millionths. The features observed on the sun during the January passage were as follows:

1. Giant Sunspot Group - the N 20° sunspot reached a maximum area of 3716 millionths with a very large bright plage (d'Azambija, 1926).

2. Carrington Longitude - the longitude 35° is one of three stable active centers in the sun's northern hemisphere (Vitinsky, 1965). However, early in the 11 year cycle, spots are usually at such high latitudes that only the longitude region from 180-220° is usually the location in early active centers, as has been the case for the July 1946, February 1956, and July 1966 events.

3. Hα Flares - on 24, 25 January and 22 February were observed visually, photographically and spectroscopically in calcium and Hα wavelengths. The first two had the largest areas for flares in historical records: 11,000 and 10,000 millionths. The third on 22 Feb lasted for 7 hours.

4. Sunspot Magnetic Fields - were classified as βV. the major spot penumbra enclosed two large umbrae of opposite polarity (delta configuration) and all three flares covered the umbrae. Fields ranged up to 3000 gauss.

The following solar-terrestrial effects were noted:

1. Great Magnetic Storms - sudden commencements began 48, 24 and 37 hours after the January and the February flares. The second was the most intense in five years, resulting in brilliant aurora.

Interpretation. On 6 October there was a conjunction of Venus and Jupiter (Fig. 3); on 11 November a conjunction of Mercury and Jupiter, on 3 December a Mercury-Venus conjunction, and finally 11 December a conjunction of Mercury and Earth, at which time the active longitude L = 35° was opposite from Mercury and Earth. The spot group developed rapidly and was of outstanding size on the December passage (CMP-28·6 December). A triple conjunction of Mercury, Mars and Saturn took place on 14 January. Using the Bollinger planetary tide index, there was a maximum of 6510 on 20 Sept. 1925 followed by a plateau at 4500-4600 lasting from 14 Oct to 15 Nov. A minimum of 3455 on 1 Dec was followed by a rapid rise to a maximum of 5696 on 17 Dec and a minimum of 5230 on 2 Jan 1926.

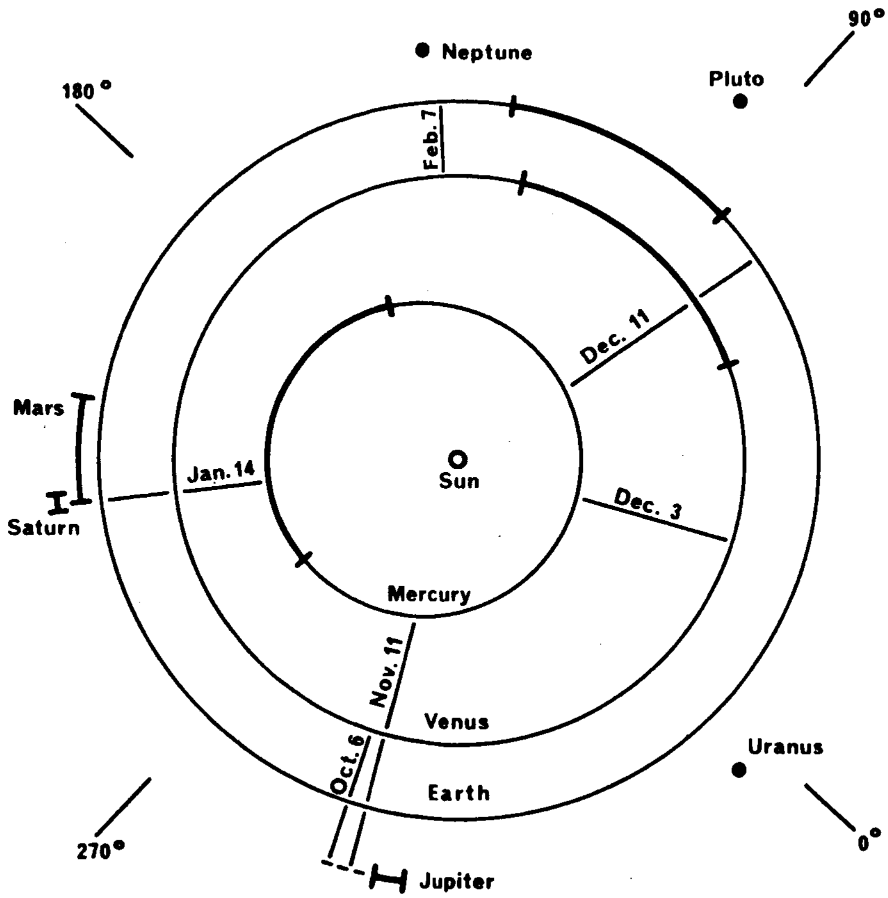

Fig. 3 Planetary Configuration One Month Prior to Proton Event of 26 January 1926

DATE	PLANETS			LONGITUDE
Oct 6	Venus	Jupiter		297°
Nov 9	Earth	Saturn		50°, 230°
Nov 11	Mercury	Jupiter		298°
Nov 13	Venus	Uranus		355°
Nov 26	Mercury	Uranus		355°
Dec 3	Mercury	Venus		25°
Dec 11	Mercury	Earth		76°
Dec 17	Mercury	Jupiter		120°, 300°
Jan 14	Mercury	Mars	Saturn	230°
Jan 25	Earth	Jupiter		124°, 304°

VI PROTON EVENT OF 24 JANUARY 1938

Although the active center itself was not seen until December there had been activity in neighboring centers since October. On 21 Dec a large plage at N 26^{o} and L = 240^{o} crossed CMP and then faded, probably to merge with the nascent center forming at N 17^{o} and L 225^{0}, which appeared at East limb on 11 January (d'Azambuja, 1937, 1938). Features observed included:

1. Giant Sunspot Group - reach its maximum area three days after CMP. It was the 7th in order of size in the Greenwich catalog.
2. Hα Flares - were observed on 14, 20 and 24 January.
3. Sunspot Magnetic Fields - the sunspot type was complex (γ), with fields of up to 3600 gauss.

The following solar-terrestrial effects were noted:

1. Short Wave Fadeout
2. Polar Cap Absorption on 16 January (Svetska, BAC, 1966)
3. Magnetic Storm - one of the 11 greatest storms followed the 24 Jan flare by 29 hours. Aurora were visible in the tropics and both the northern and southern hemisphere.
4. Forbush Decrease - of 6% took place on 14 Jan, following a flare on the eastern hemisphere (Forbush, 1938).

Interpretation. The active longitude was in alignment with the 30 Nov conjunction of Mercury and Jupiter, with the 26 December conjunction of Mercury and Venus, the 30 December conjunction of Mercury and Earth and the 3 January conjunction of Mercury and Jupiter. The Bollinger planetary tide index had the following values; maxima of 6454 and 6566 on 7 October and 3 January; and minima of 3846 and 5630 on 2 December and 27 January. There was a very steep rise in tidal force from 18 December through 3 January.

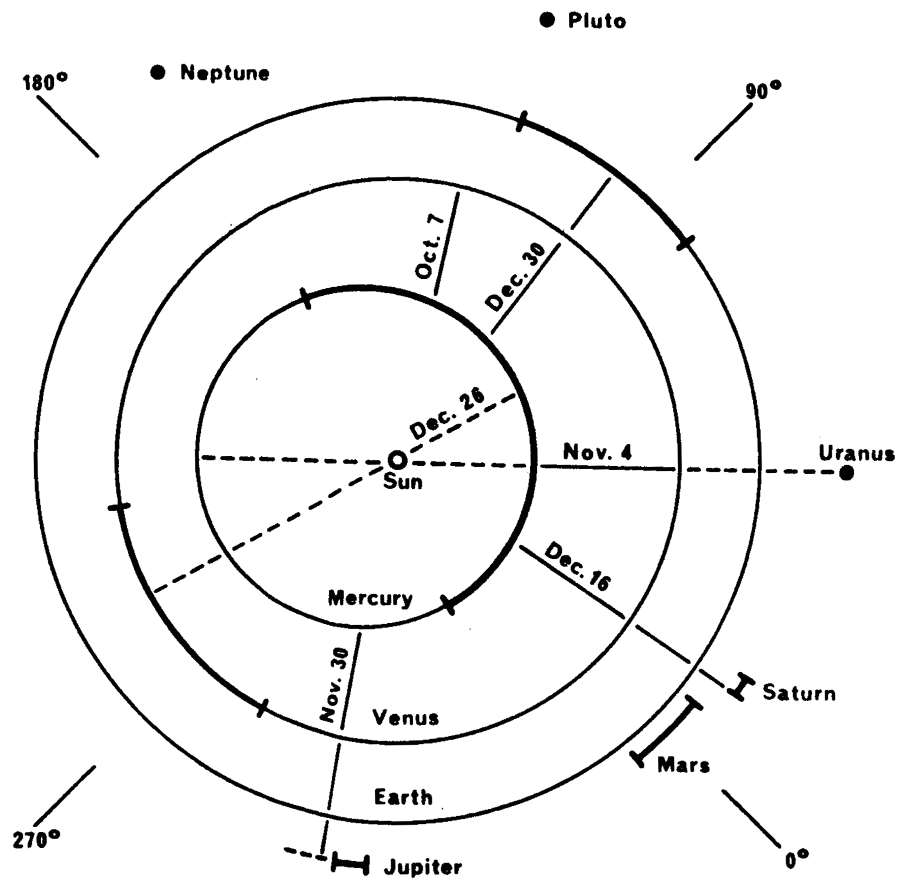

Fig. 4 Planetary Configuration One Month Prior to Proton Event of 24 January 1938

DATE	PLANETS			LONGITUDE
Oct 7	Mercury	Venus	(Jupiter)	120° (300°)
Nov 4	Mercury	(Earth	Uranus)	226° (46°)
Nov 30	Mercury	Jupiter		304°
Dec 16	Mercury	Saturn		10°
Dec 26	Mercury	Venus		73°, 253°
Dec 30	Mercury	Earth		98°
Jan 3-4	Mercury	Jupiter		130°, 310°
Jan 12	Mercury	Neptune		168°

CONCLUSIONS

It is possible to establish evidence for one or more proton flares in every solar cycle from 10 through 20, despite changes in peak sunspot number and the proportion of large sunspots, and the limited amount of earlier solar observation. Even in cycle 18 only 3 to 5 proton events were detected regardless of the proliferation of monitoring techniques and observatories. The earlier observations, although limited to optical methods, still provided coverage of a large fraction of the major events.

Active centers in earlier cycles are of great importance for long range forecasting of future solar activity. The span from cycle 10 to 20 covers more than one secular 90-year solar cycle. At some time it may be possible to investigate the distribution of largesunspots back to 1826, when Schwabe began systematic spot counts, but flares as such were probably not known before 1859.

Events of early cycles occur after sequences of conjunctions of the planets Mercury, Venus, Earth and Jupiter. Occasionally other planets are involved if conjunctions of more than two planets occur. During the two month period preceding major solar events, the number of conjunctions of the four tidal planets is 2 or 3 times the average for a two month period. The concentration of conjunctions is definitely non-random before the solar events.

BIBLIOGRAPHY

Bartels, J., "Solar Eruptions and Their Ionospheric Effects - A Classical Observation and its New Interpretation," Terr. Magn. 42, No. 3, pp.235-239 (Sept. 1937).

d'Azambuja, M., "Cartes Synoptiques de la Chromosphere Solaire," 1917, 1925-1926, 1937-1938, Observatoire de Meudon, Paris.

Dellinger, J. H., "Sudden Ionospheric Disturbances," Terr. Magn. and Atmos. Elect. 42, pp.49-53 (1937).

Dodson, H. W. and Hedeman, E. R., "Crochet-Associated Flares," Ap. J. 128, pp.636-645 (1958).

Forbush, S. E., "On Cosmic Ray Effects Associated with agnetic Storms," Terr. Magn. 43, pp.203-218 (Sept. 1938).

Hale, G. E., Ellerman, F., Nicholson, S. B., and Joy, A. H., "The Magnetic Polarity of Sunspots," Ap. J. 47, pp.153-178 (1919).

Hale, G. E., "The Spectrohelioscope and Its Work: III Solar Eruptions and Their Apparent Terrestrial Effects," Ap. J. 73, pp.379-412 (1931).

Hale, G. E. and Nicholson, S. B., 'Magnetic Observations of Sunspots, 1917 to 1924," Carnegie Inst. of Washington, Washington, D.C. 1938.

"Larousse Encyclopedia of Astronomy," by Rudeaux and G. De Valcouleurs, Prometheus Press, N.Y., 1959.

Lockyer, J. N., "Solar Physics," Macmillan, London, 1874.

McNish, A. G., "Terrestrial-Magnetic and Ionospheric Effects Associated with Bright Chromospheric Eruptions," Terr. Magn. 42, pp.109-118 (1937).

'Mt. Wilson Magnetic Observations, Summary," Publ. Astron. Soc. Pacific 50, pp.129-133 (1938).

Mogel, H., "On the Relation Between Reception of Short Wave Radio and Earth Magnetic Storms," Telefunken-Zeitung 11, p.14-20 (1930).

Newton, H. W., "Solar Flares and Magnetic Storms," Mon. Not. Roy. Ast. Soc. 103, pp.244-257 (May 1943).

Newton, H. W., "The Lineage of the Great Sunspots," In Vistas in Astronomy, Vol. 1. ed. by A. Beer, pp.666-674, Pergamon Press, N.Y., 1955.

Pinter, S. and Knoska, S., "On the 11-Year Cycle of Solar Flares and Geomagnetic Crochets," Bull. Astron. Czech. 19, pp.40-42, (1968).

Royal Greenwich Observatory, "Sunspot and Geomagnetic Storm Data, 1874-1954," Her Majesty's Stationery Office, London, 1955.

Stahlman, W. D. and Gingerich, O., "Solar and Planetary Longitudes for Years - 2500 to +2000," The Univ. of Wisconsin Press, Madison, 1963.

Svestka, Z., "Proton Flares Before 1956," BAC 17, pp.262-270 (1966).

Svestka, Z., "Optical Observations of Solar Flares," Spa. Sci. Rev. 5, pp.388-418 (1966).

Vitinsky, Y. I., "The Problem of Active Longitudes on the Sun," NASA TT-F-249, Washington, D.C., Sept. 1965.

5. MAJOR EVENTS: 1942-1951

5. MAJOR EVENTS: 1942-1951

A variety of indirect observations of solar particle events are available for over a century. Geomagnetic crochets and storm sudden commencements were recorded at Greenwich as early as 1840, and at Slutsk-Pavlovsk from 1878, and at Abinger, Huancayo, and Watheroo from 1882 to the present. Optical observations of flares date from the great white light flare of 1 September 1859 observed by Carrington and Hodgson.

Nevertheless, the quantity and reliability of data concerning solar particle events took a sudden quantum jump in 1942 when ground level events (GLE) and solar radio emission from flares were first noted. Therefore, the catalog of events begins at that time, with occasional references to historical great flares with comparable planetary configurations.

Estimation of atmospheric density changes from solar proton events requires only a study of the few largest centers and events. A catalog of the 30 major events in cycle 19 (McDonald, 1963) shows that they occurred in only 16 different active centers. During the latter half of the cycle, this tendency was even more pronounced, for 18 separate events were associated with only five active centers. Four active centers produced over 90% of the particle emission during the six year period 1956-1961. Therefore, the study of solar activity from 1942-1951 has concentrated on the most active centers.

Planetary effects on solar activity are discussed three ways in most cases: (1) The maximum tidal and jerk (rate of change of solar acceleration) values preceding proton events, calculated on conjunction dates; (2) Maximum rates of change of tidal force and (3) Dates and types of planetary conjunctions two and three months preceding proton events. In the latter case, an attempt is made to trace the cause of the active center, and later the configuration which triggers the proton event.

I. PROTON EVENTS OF 28 FEBRUARY, 7 MARCH 1942

The ground level event (GLE) of 28 February 1942 was an outstanding event, resulting in the discovery of cosmic ray emission from the sun and solar radio bursts. The events observed on the sun were:

1. Giant Sunspot Group - the maximum area was 2048 millionths of the solar hemispheres (Greenwich, 1955), located at active Carrington longitude 190°.

2. H α Flare - the line width measured 30 minutes after the peak was double the normal line width. Two narrow filaments merged to a "Y" configuration, since then found typical of proton flares.

3. Sunspot Magnetic Field - was the complex (γ) type with field strengths of 5100 and 3800 gauss. The former was the highest ever recorded to that time at Mt. Wilson (Ellison et al., 1961).

The following solar-terrestrial effects were detected:

1. Radio Fade-Out (indicating X-ray emission) was observed on all channels 5-20 Mc/s, and persisted for eight hours, an abnormally long period for a Short Wave Fade (SWF).

2. Magnetic Crochet, simultaneous with the beginning of the SWF, also indicating X-ray emission.

3. Radio Noise - a burst 10^5 times the calculated blackbody radiation led to the discovery of nonthermal radio emission from the sun (Hey, 1946).

4. Cosmic Rays - the first recorded burst of solar relativistic particles at ground level raised the cosmic ray level above normal at the following stations: Godhavn (8%), Cheltenham (7%) and Christchurch (5%) (Forbush, 1946).

5. Forbush Decrease - an 11% decrease occurred on 1 March (Forbush, 1946).

6. Great Magnetic Storm - a sudden commencement (SC) geomagnetic storm began 19-1/2 hours later, featured by giant pulsations and lasting three days.

Further observations and measurements on this outstanding event and the 7 March event from the same sunspot group can be found in the extensive literature on the subject.

Interpretation. The 1942 events, although 4.6 years later than the peak of the 11 year cycle, occurred soon after a maximum in the solar velocity function (Figure 3, K. D. Wood, 1968) (the highest during this century). Similarly, the highest value in 50 years of the seven-planet tidal force occurred in 1941 (Bollinger, 1960) (Takahashi, 1968). The two months preceding the events witnessed rapid changes in planetary tidal force from a maximum of 6191 units on 29 December 1941, to a minimum of 5433 units on 14 January 1942, followed by a rise to 6571 on 30 January, and a rapid decline to 3415 on 23 February 1942, (Bollinger,1960) (see Tables 9 and 10). The planetary configuration is shown in Figure 5. Noteworthy is the grouping of Mars, Jupiter, Saturn and Uranus (with Jupiter at the longitude of maximum sunspot effect); and the grouping of Mercury, Venus and the Earth approximately in quadrature to Saturn and Uranus. Dates of planetary conjunction are given below Figure 5. The configuration is similar to the planetary arrangements at the time of the first solar flare ever observed, Carrington's great white light flare of 1 September 1859. At that time Jupiter was also at the 100° longitude of maximum sunspot effect, and Mercury, Venus and Earth were grouped near 0° longitude.

TABLE 9. Energy Spectrum (Rigidity) of Ground Level Events Over 25 Year Period, Compared to Maximum Tidal Forces and Maximum Rate of Change of Solar Acceleration (Jerk). Jerk and Tide Values from K. D. Wood, 1968. Rigidities from Lockwood, 1968 and Carmichael, 1962.

GLE Date	Rigidity (Mv)	Jerk	Tide
January 28, 1967	600	5.73	5.65
February 23, 1956	195	5.73	5.65
February 23, 1942	--	4.66	4.60
November 19, 1949	--	4.66	4.60
November 12, 1960	127	4.57	3.05
July 18, 1961	102	3.47	4.53
July 10, 1959	104	3.47	4.42
July 25, 1946	--	3.47	4.42

TABLE 10. Dates and Values of High Rate of Change of Seven-Planet Tidal Force (dT/dt) (Bollinger, 1960) During Solar Cycles 17 and 18, followed in Last Column by Dates of Proton Events (Svetska, 1966). Underlined Events are Ground Level Events Discussed in This Report.

Year	Date	dT/dt	Event
1941	February 4 - 20	-1.03	February 26
	May 11 - 27	-1.13	July 3
	July 14 - 30	1.0	September 18
1942	February 1 - 23	-1.33	February 28
	July 17 - 25	1.88	Sol. Min
1946	February 1 - 26	1.0	March 27
	June 2 - 10	1.0	July 26
	August 21 - 30	1.33	September 21
1949	January 17 - 25	1.75	January 23
	April 15 - 23	2.13	May 8
	July 20 - 30	-1.06	August 3
	October 24 - 30	-1.13	November 19

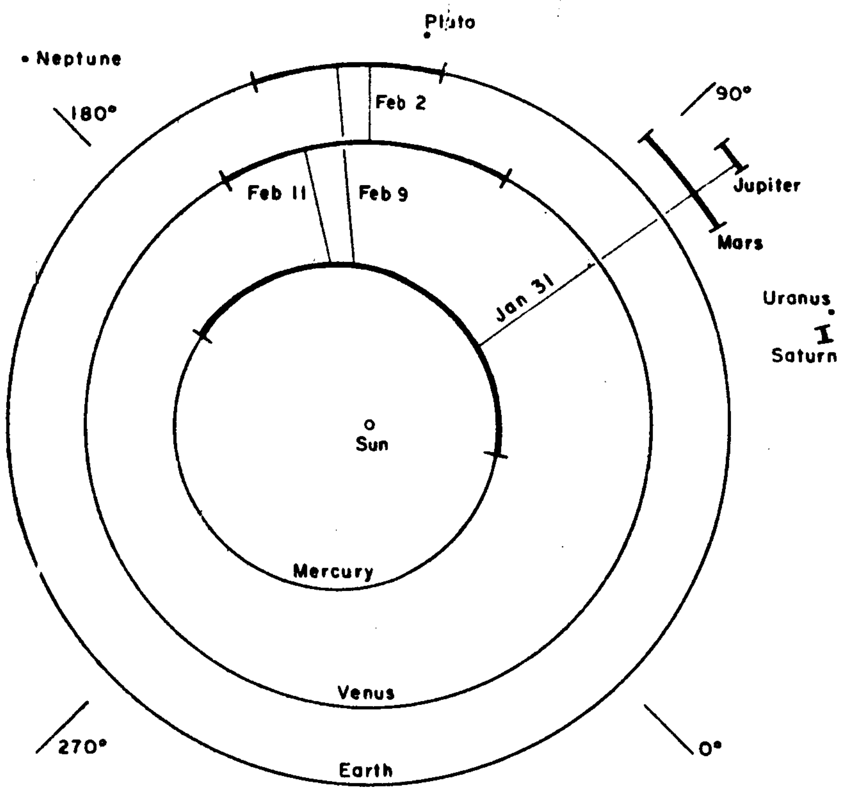

Figure 5. Planetary Configuration One Month Prior to the Proton Events of 28 February, 7 March 1942 (American Ephemeris)

Date*	Planets		Longitude
Dec 8	Earth	Jupiter	76°
Dec 30	Venus	Jupiter	78°
Jan 27	Mercury	Saturn	57°
Jan 27	Mercury	Uranus	59°
Jan 31	Mercury	Mars	79°
Jan 31	Mercury	Jupiter	81°
Feb 3	Mars	Jupiter	81°
Feb 2	Venus	Earth	134°
Feb 9	Mercury	Earth	140°
Feb 11	Mercury	Venus	148°
Feb 18	Mercury	Neptune	178°
Feb 27	Saturn	Uranus	59°

*Dates of lesser importance are indented.

II. PROTON EVENT OF 25 JULY 1946

The events observed on the sun during the 25 July 1946 GLE were as follows:

1. Giant Sunspot Group - the maximum area was 4720 millionths; a reappearance of a giant spot seen at central meridian passage (CMP) on 6 February through 2 May (Ellison et al., 1961).

2. Carrington Longitude - the active longitude 190° was again the site of a proton flare (Guss, 1964) (Warwick, 1965) (Haurwitz, 1968).

3. H α Flare - the line width was 15Å and showed a very rapid rise to maximum brightness of 300% of the continuum. Two parallel bright filaments ran between the N and S spots.

4. White Light Flare - 10% enhancement over the continuum, now considered to be indicative of an X-ray flare.

5. Sunspot Magnetic Field - classified as (βγ) but all the N poles were collected at one end and the S poles at the other. Fields ranged up to 4000 gauss.

The following solar-terrestrial effects were noted:

1. Radio Fade-Out lasted 5-1/2 hours (X-ray emission).

2. Magnetic Crochet recorded at 3 stations (X-ray emission).

3. Radio Noise at 4.7 and 4.2 meters, exceeded 10^8 times the blackbody values.

4. Cosmic Rays - relativistic protons were recorded to be 20% (Cheltenham) and 18% (Mt. Wilson) above steady state values.

5. Forbush Decrease of 7% lasted for 10 days.

6. Great Magnetic Storm - a sudden commencement began 26.3 hours later.

Interpretation. The July 1946 event came at the beginning of the 18th cycle, and as such, resembles the February 1956 event with its high solar latitude and an active center producing a single isolated large event. On the other hand, the conjunctions preceding the July 1946 event far more resemble the conjunctions preceding the July 1959 multiple events. On 19 June 1946 there was a conjunction of Mercury and Venus (Figure 6); on 29 June a conjunction of Mercury and Jupiter, and finally on 12 July a conjunction of Venus and Jupiter, with Earth and Saturn in quadrature. The Carrington active longitude 190° which produced the proton event was approximately in line with the Mercury-Venus conjunction on 19 June. At the time of the 29 June Mercury-Jupiter conjunction, the active longitude was at right angles, approximately in line with the Earth-Saturn opposition. On 12 July, the date of the Venus-Jupiter conjunction, the active solar longitude had made half a revolution and was again in line with the Earth-Saturn line, and in quadrature with the Jupiter-Venus conjunction. The massive spot group then was first seen from the earth at east limb on 19 July, after which it grew in size for ten days to a maximum area of 4720 millionths, the third largest spot group ever recorded at Greenwich (Jones, 1955). In terms of the Bollinger planetary tidal index, there were successive minima on 9 May, 10 June and 28 July and maxima on 25 May and 26 June (tabulated every eight days).

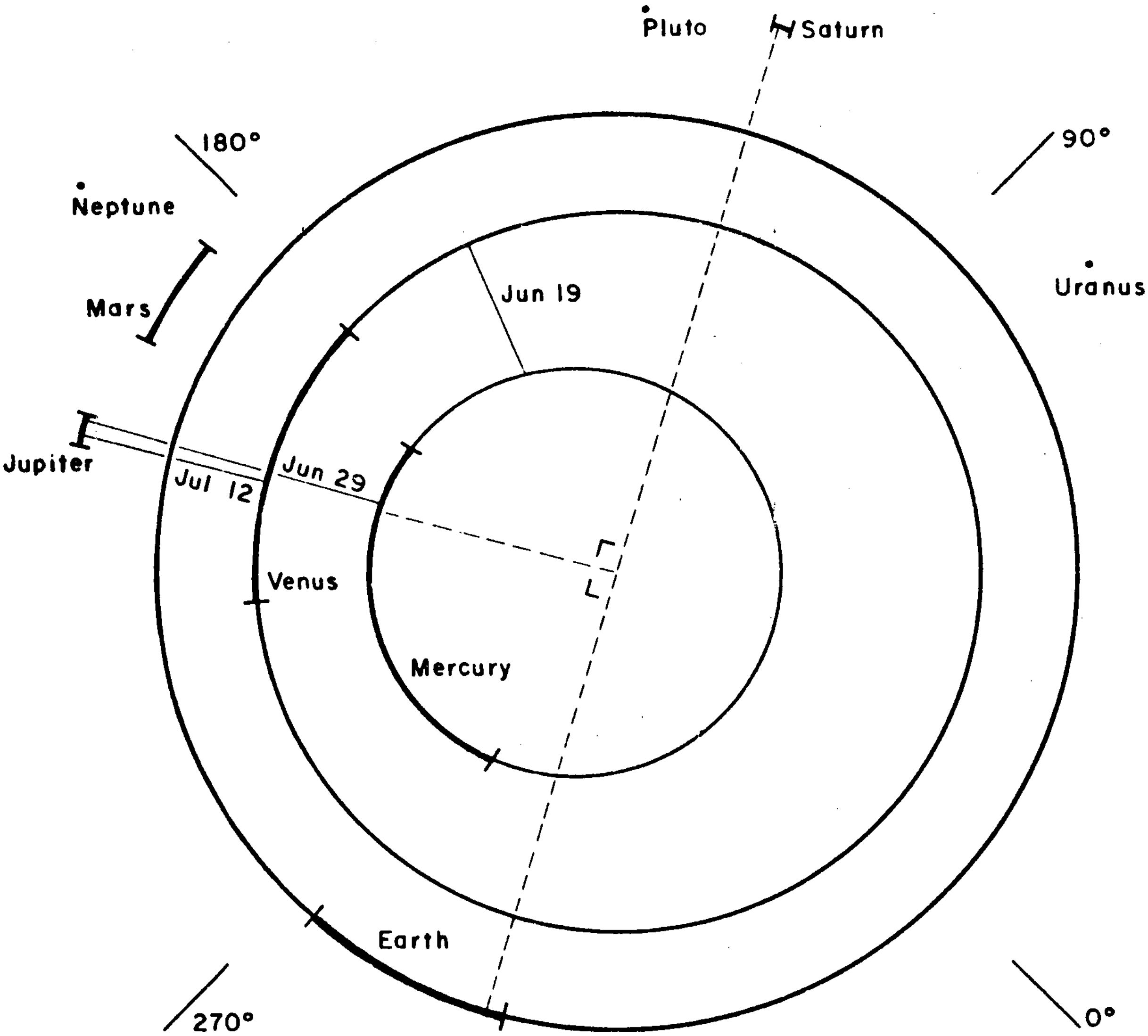

Figure 6. Planetary Configurations One Month Prior to Proton Event of 25 July 1946

Date	Planets		Longitude
Jun 19	Mercury	Venus	170°
Jun 25	Venus	Mars	185°
Jun 28	Venus	Neptune	187°
Jun 29	Mercury	Jupiter	208°
Jun 30	Mars	Neptune	187°
Jul 12	Venus	Jupiter	209°

III. PROTON EVENT OF 19 NOVEMBER 1949

The events observed on the sun during the 19 November 1949 event were as follows:

1. Large Sunspot Group of maximum area 1280 millionths on its second passage. A southern spot, the Carrington longitude was 115°, conforming to one of the active longitudes (Vitinsky, 1965), although less is known about the southern active longitudes as related to proton events because of the excessive northern activity of the last few cycles.

2. H α Flare - the maximum line width was 22.9Å, the largest maximum measured prior to 15 November 1960.

3. White Light Flare. 8% enhancement of the continuum (X-ray flare).

4. Sunspot Magnetic Field; the peak magnetic field was 2700 gauss, and on the day before the spot group was classed as β, unusual for a cosmic ray flare.

5. High Green Coronal Emission. The magnitude of green coronal emission (indicating a temperature of 2×10^6 degrees K) increased markedly both North and South toward the end of the 18th cycle (Kiepenheuer, 1957). Proton flares have a tendency to occur near a maximum of green coronal line intensity (Gnevyshev and Krivsky, 1966).

The following solar-terrestrial effects were noted:

1. Radio Fade-Out lasted five hours. A Sudden Enhancement of Atmospherics (SEA) lasted about two hours.

2. Magnetic Crochet was recorded at four stations.

3. Radio Noise was recorded at 73 Mc/s, 158 Mc/s and 545 Mc/sec; at the lower frequency continuing for an hour.

4. Cosmic Rays were recorded at 16 stations including the neutron monitor at Manchester, the first time solar particles has been thus detected.

5. No Forbush Decrease, No Magnetic Storm due to the flare location at 70°W so near to the solar limb.

Interpretation. The interpretation of this event is more difficult than the previous two, because although the plage was visible on the previous rotation (d'Azambuja, 1949), the sunspot region developed suddenly and was observed for only seven days (Jones, 1955). Most high energy events occur on the second or third rotation of a large complex sunspot group. However, it occurred during the most flare active portion of the eleven year cycle, and the proton event occurred on the west limb, which placed it optimally for interception at the earth, because of the co-rotation garden hose shape of the interplanetary extension of the sun's general magnetic field.

Therefore, it is not clear whether the 6 October conjunction of Venus and Jupiter and the 23 October superior conjunction of Mercury and Jupiter apply to the case in question, (Figure 7). Nevertheless there is an increase in mean daily radio flux on 6 October, (Table 11). On 30 October, a triple conjunction of Mercury, Venus and Saturn occurred approximately in line with the Carrington longitude which produced the flare.

On Bollinger's chart of the seven-planet tidal force, one observes a rapid decrease from 24 October through 9 November, at which time the plage and latent sunspot region was at the east limb (Table 2).

TABLE 11. Ottawa 10.7 cm Radio Flux Daily Means for October, November 1949. (Quarterly Bulletin, IAU) Units - 10^{-22} Watts/m^2 (c/s^{-1}). The Passages of the Active Center are Shown, and the Date of the Venus, Jupiter Conjunction (6 October).

1949 Date		October		November
1		127		129
2		140		131
3		142		144
4		166		144
5		187		148
6	V, J Conj	[206]	East Limb	--
7		191		176
8		198		191
9	East Limb	204		183
10		196		157
11		196		161
12		--		146
13		185	CMP	--
14		172		153
15		163		170
16		163		172
17	CMP	148		187
18		131		174
19		127		161
20		123	West Limb	--
21		125		133
22		129		131
23		--		133
24	West Limb	140		144
25		114		146
26		112		146
27		123		135
28		125		146
29		127		--
30		--		159
31		129		--

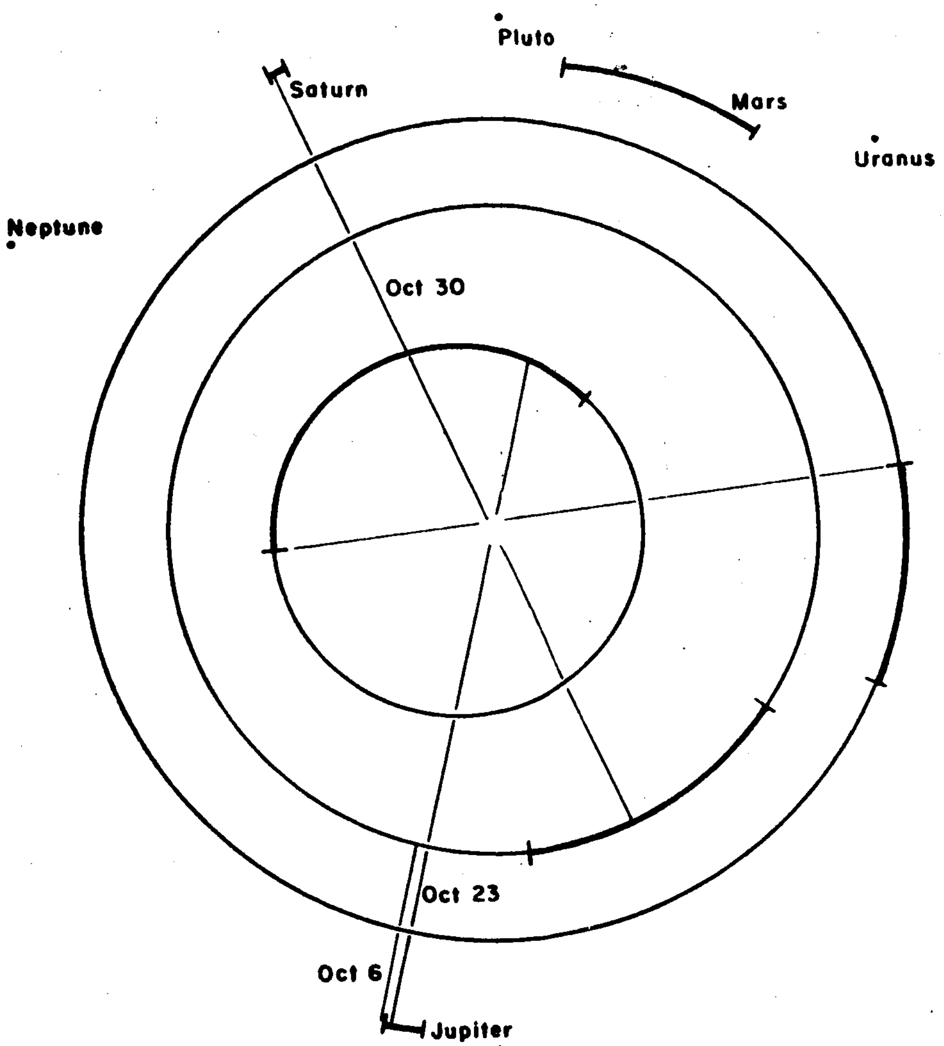

Figure 7. Planetary Configurations One Month Prior to Proton Event of 19 November 1949

Date	Planet	Longitude	Planet	Longitude
Oct 6	Venus	304°	Jupiter	304°
Oct 21	Mercury	112°	Mars	114°
Oct 23	Mercury	124°	Jupiter	305°
Oct 30	Mercury	160°	Venus	341°
			Saturn	161°
Nov 8	Mercury	196°	Neptune	195°
Nov 19	Mars	127°	Jupiter	307°

CONCLUSIONS

In order to establish periodicities in the occurrence of proton events, it is necessary to study solar flare effects over as long a time period as possible. Therefore the active centers of cycles 17-18 are of great importance for possible prediction of future proton events and active centers.

The events of February-March 1942 originated from a persistent active center, typical for the late portion of the 11-year cycle. The planetary configuration preceding the activity involved a close conjunction of three outer tidal planets (Jupiter, Saturn and Uranus) followed by a near triple conjunction of Mercury, Venus and Earth.

The 25 July 1946 event occurred at the beginning of cycle 18 from a non-recurrent center, similar to the 23 February 1956 and 28 January 1967 events. Although automatic monitoring equipment had now been widely installed, no further high energy (GLE) events were detected for a 3-1/2 year period at the peak of the sunspot cycle until 19 November 1949.

The antecedents of the 19 November 1949 event resemble those of the November 1960 events. Similar event(s) are predicted for November 1970, following the triple conjunction of Venus, Earth and Saturn on November 10-11 in opposition to Jupiter and Neptune.

Comparable to the February-March 1942 and July 1961 active centers, occurring near the time of Jupiter-Saturn conjunction or opposition, would be an active center producing either protons or high radio flux is predicted for May-June 1971.

The overall activity of cycles 18 and 19 may be compared on various grounds, particularly: (1) Events of great magnitude; (2) 10.7 cm radio flux and (3) Sunspot number (or area). On the basis of (1) or (2) the two cycles are of approximately equal activity. On the basis of (3) sunspot number, cycle 19 is far more active than cycle 18. This is because the frequency of small and average size sunspots has been higher than normal in cycle 19 and lifetimes have been shorter than before (14% of all sunspots lasted only one passage) (Kopecky, 1967). It has been noted that proton events occur almost exclusively from the second, third and subsequent passages of giant sunspot groups (Anderson, 1966). The frequency and size of giant sunspot groups was greater during cycle 18 than during the remainder of the entire 120 year period when areas have been measured at Greenwich (Jones, 1954). The five largest spot groups ever measured were seen in 1946, 1947 and 1951 in cycle 18. The magnetic fields of sunspots have been declining over the last few cycles, (Kopecky, 1967) and typically the 28 February 1942 (cycle 17) spot had very high fields of up to 5100 gauss. Thus there are long range changes in many solar characteristics which should be taken into account in projections of future solar activity.

BIBLIOGRAPHY

American Ephemeris and Nautical Almanac, U. S. Naval Observatory (yearly).

Anderson, C. K., "Forecasting Solar Activity and Geophysical Responses," Weather Man. 4WWM 105-1, Dept. Air Force, Ent AFB, Colo. (Dec. 1966).

Bailey, D. K., "Polar-Cap Absorption," Planet. Spa. Sci. 12, pp. 495-541 (1963).

Bell, B., "Type IV Solar Radio Bursts, Geomagnetic Storms, and Polar Cap Absorption (PCA) Events," Smithsonian Contrib. to Astrophys. 8, No. 3, pp. 119-131 (1963).

Blizard, J. B., "A Long Range Solar Flare Prediction Technique," Trans. Am. Geophys. Un. 46, No. 3, p. 533 (September 1965).

Bollinger, C. J., "Atlas of Solar Planetary Climate," Battenberg Press, Norman, Okla. (1960).

Byrne, F. N., Ellison, M. A., and Reid, J. H., "A Survey of Solar Flare Phenomena," Spa. Sci. Rev. 3, pp. 319-341 (1964).

Carmichael, H., "High Energy Solar Particle Events," Spa. Sci. Rev. 1, pp. 28-61 (1962).

d'Azambuja, M., "Cartes Synoptiques de la Chromosphere Solaire," 1940-1944, 1945-1948, 1949-1952, Observatoire de Meudon, Paris.

Dodson, H. W., Hedeman, E. R., and Covington, A. E., "Solar Flares and Associated 2800 Mc/s (10.7 cm) Radiation," Ap. J. 119, pp. 541-553 (1954).

Ellison, M. A., McKenna, S. M., and Reid, J. H., "Cosmic Ray Flares," Dunsink Obs. Publ. 1, No. 3 (1961).

Ellison, M. A., "The Sun and Its Influence," Am. Elsevier Publ. Co., Inc., New York (1968).

Enger, I., Podsiadlo, R. T., Jensen, D. C., and Ward, F. W., "Solar Flare Occurrence as a Function of Sunspot Size," AFCRL-66-293, 28 pp., Bedford, Mass. (1966).

Fitchel, C. E., and McDonald, F. B., "Energetic Particles from the Sun," Ann. Rev. Astron. Astrophys. 5, p. 351 (1967).

Fletcher, J. D., "Solar Radio Emission as a Criterion for Solar Proton Event Warning," AIAA J. 2, pp. 2193-2197 (Dec. 1964).

Forbush, S. E., "Three Unusual Cosmic-Ray Increases Possibly Due to Charged Particles from the Sun," Phys. Rev. 70, pp. 771-772 (1946).

Gnevyshev, M. N., "The Corona and the 11 Year Cycle of Solar Activity," Soviet A. J. 7, pp. 311-318 (1963).

Gnevyshev, M. N., and Krivsky, L., "The Relation between Proton Flares and the Corona Over the 11 Year Cycle," Soviet A. J. 10, pp. 304-307 (1966).

Guss, D., "Distribution in Heliographic Longitude of Flares which Produce Energetic Solar Particles," Phys. Rev. Letters 13, pp. 363-364 (1964).

Haurwitz, M., "Solar Longitude Distributions of Proton Flares, Meter Bursts, and Sunspots," Astrophys. J. 151, pp. 351-364 (Jan.1968).

Hey, J. S., "Solar Radiation in the 4-6 Meter Radio Wavelength Band," Nature 157, p. 47 (1946).

Jones, H. S., Editor, "Sunspot and Geomagnetic Storm Data Derived from Greenwich Observations, 1874-1954," Her Majesty Stationery Office, London (1955).

Kiepenheuer, K. O., "Solar Activity," in The Sun edited by G. Kuiper, Univ. of Chicago Press, Chicago, Ill. (1957).

Kopecky, M., "The Periodicity of the Sunspot Groups," Advances in Astronomy and Astrophysics, Vol. 5, pp. 189-266 (1967).

Krivsky, L., and Kopecky, M., "Proton Flares and Types of Spot Groups in the 11 Year Cycle," Bull. Astron. Czech 17, No. 6, pp. 360-365 (1966).

Lockwood, J. A., "Cosmic-Ray Solar Flare Effect of Jan. 28, 1967, as Recorded by Neutron Monitors," J. Geophys. Res. 73, No. 13 (Jul. 1968).

Maksimov, I. V., and Smirnov, N. P., "A Tidal Effect in the Disturbances of Solar Activity," Soln. Dannye, No. 10, pp. 104-108 (Oct. 1967).

McDonald, F. B., "Solar Proton Manual," NASA TR R-169 (Dec. 1963).

Nelson, J. H., "Planetary Position Effect on Short-Wave Signal Quality," Electrical Engineering, pp. 421-424 (May 1952).

"Quarterly Bulletin on Solar Activity," International Astronomical Union, Zurich, Switzerland, Nos. 93, 94, 95 (Jan.-Sept. 1951).

Romanchuk, P. R., "Magnetism of the Sun and the Process of Sunspot Formation at the Time of Quadrature and Conjunction of the Planets," Soln. Dannye, No. 8, pp. 66-70 (1965) (In Russian).

Shain, C. A., and Mitra, A. P., "Effects of Solar Flares on the Absorption of 18.3 Mc/s Cosmic Noise," J. Atmos. and Terrest. Phys. 5, pp. 316-321 (1954).

Svestka, Z., "Proton Flares Before 1956," BAC 17, pp. 262-270 (1966).

Svestka, Z., "Optical Observations of Solar Flares," Space Sci. Reviews 5, pp. 397-418 (1966).

Takahashi, K., "On the Relation between the Solar Activity Cycle and the Solar Tidal Force Induced by the Planets," J. Radio Research Laboratories, 14, pp. 237-240 (Jul.-Sept. 1967).

Vitinsky, Y. I., "The Problem of Active Longitudes on the Sun," NASA TT F-249, Washington, D. C. (Sept. 1965).

Warwick, C. S., "Longitude Distribution of Proton Flares," Ap. J. 141, pp. 500-504 (1965).

Warwick, C. S., and Haurwitz, M. W., "A Study of Solar Activity Associated with Polar Cap Absorption," J. Geophys. Res. 67, pp. 1317-1332 (1962).

6. PROTON EVENTS OF CYCLE 19

6. PROTON EVENTS OF CYCLE 19

Four active centers produced over 90% of the solar particle emission during the six year period 1956-1961. Therefore, the study of solar activity from 1956-1961 has concentrated on the four most active centers, plus a GLE with lower flux.

In order to establish periodicities in the occurrence of proton events, it is necessary to study solar flare effects over as long a time period as possible. Therefore the four active centers of cycle 19 are compared to active centers of other cycles for possible prediction of future proton events and active centers.

It has been noted that proton events occur almost exclusively from the second, third and subsequent passages of giant sunspot groups (Jonah, 1967) (Sherry, 1968) with very few occurring on the first passage. The frequency and size of giant sunspot groups has been greater during cycles 18-20 than during the remainder of the entire 100 year period when areas have been measured at Greenwich (Kopecky, 1966).

Planetary effects on solar activity are discussed with respect to three phenomena if data are available: (1) The maximum tidal and jerk (rate of change of solar acceleration) values during the month preceding proton events, calculated on conjunction dates; (2) Maximum rates of change of tidal force and (3) Dates and types of planetary conjunctions two and three months preceding proton events. In the latter case, an attempt is made to trace the cause of the active center, and later the configuration which triggers the proton event.

Four active centers which produced high energy, high flux proton events will be discussed in the 19th solar cycle. These are the centers which caused the 23 February 1956, the 10, 14, 16 July 1959, the 12, 15, 20 November 1960 and the 11, 12, 18, 20 July 1961 events. The 4 May 1960 GLE low flux event is also discussed.

The 23 February 1956 event occurred at the beginning of cycle 19 from the restricted longitudes active at high latitudes, similar to the 25 July 1946 and 28 January 1967 events.

The antecedents of the November 1960 events resemble those of the November 1949 event. Similar event(s) are predicted for November 1970, following the triple conjunction of Venus, Earth and Saturn on 10-11 November in opposition to Jupiter and Neptune.

The July 1961 events occurred during low solar activity, yet repeated proton events and a high flux of X-radiation was produced. The July 1961 activity center is comparable to the February-March 1942 and May 1951 active centers, occurring near the time of Jupiter-Saturn conjunction or opposition. A comparable active center producing protons or high X-ray flux is predicted for May-June 1971.

I. PROTON EVENT OF 23 FEBRUARY 1956

The ground level event (GLE) of 23 February 1956 was the highest energy event during cycle 19. The events observed on the sun were:

1. Giant Sunspot Stream - On its second rotation the area had grown to 2410 millionths of the solar hemisphere with a large bright plage of area 18,000 millionths (Solar Geophysical Data). The flare originated at the longitude L = 190°, the only longitude active at high latitudes. The delta configuration (umbrae of opposite polarity in the same penumbra) was present in several parts of the stream (McDonald, 1963).

2. H α Flare - 98 flares were observed during the 3 most active rotations. The GLE flare had a line width of 18 Ångstroms. It was seen that the flare covered several of the principal umbrae, a characteristic of proton events. (Jonah, 1967) (Dodson and Hedeman, 1964).

3. Sunspot Magnetic Field - The group was of complex (γ) type with maximum field strengths up to 4000 gauss. (Ellison et al., 1961).

4. Loop Prominences - were observed over the active region at east limb 13 days before the GLE flare. Loop prominences are also an indicator of proton flares (Bruzek, 1964) (Jonah, 1967). In addition, coronal yellow line emission was evident during the disc passages of January, February and March (Mac Donald, 1963) indicating a temperature of 4×10^{6} degrees K. in the corona.

The following solar-terrestrial effects were noted:

1. Short Wave Fadeout (SWF) - lasting seven hours.

2. Polar Cap Absorption (PCA) - first case ever observed on the dark hemisphere of the earth.

3. Ground Level Event (GLE) - cosmic ray increase at ground level detected by ion chambers, and neutron monitors at numerous stations including a 6000% increase at Leeds (Ellison, 1961).

4. Magnetic Crochet - indicating X-ray emission recorded at five stations.

5. Great Geomagnetic Storm - beginning 47.4 hours later.

6. Solar Radio Emission - a 10 cm radio burst was recorded in Tokyo lasting 50 minutes. The recorder went off scale, indicating a peak flux in excess of 4700×10^{-22} watts/m^2 (c/s). Bursts were also recorded at 200 Mc/sec, 85 Mc/sec and 20 Mc/sec.

Interpretation. The 23 February 1956 event occurred early in the cycle and consequently from a high latitude active center. The active longitudes are very narrow at high latitudes, as can be seen by the isoline method (Vitinsky) (Warwick, 1965). In fact often only one longitude is represented in the northern hemisphere above 20^{o} latitude. Such has been the case for the beginnings of cycles 18, 19 and 20 in which the northern longitudinal zone from 180^{o} to 210^{o} was the location of nearly all significant early proton centers - July 1946, Jan. - Feb. 1956, and July, Aug., Sept. 1966.

On 6-7 Jan. 1956 a Mercury-Venus conjunction took place (Tables 12 and 13). The 10.7 cm flux was elevated (Table 14) at that time, although no important active centers were on the visible hemisphere (Cartes Synoptiques, 1956). The active center appeared for its first passage on 13 Jan. On 31 Jan. a Mercury-Jupiter conjunction (Table 12) took place, and the 10.7 cm flux was elevated (Table 14) for 5 days (although now another active center had formed at 330^{o} longitude). Radio emission increased 20% on the appearance of the proton active center in February. However, a major increase of 40% in 10.7 flux took place at the time of the triple conjunction of Earth, Jupiter and Pluto on 16 Feb. in alignment with the active center. While the increase in solar activity is clearly noticeable on centimeter wavelengths, the rise is much more striking on the more collimated meter waves. On 16 to 17 February, increases took place in mean daily flux of up to an order of magnitude on all frequencies from 81 Mc/s to 200 Mc/s (Quarterly Bulletin, IAU).

An increase of up to 100% took place on meter wavelengths also at the time of the Mercury-Earth conjunction on 27 Jan., but the change on 10.7 cm cannot be isolated from the passage of the active center at west limb.

The Mercury Jupiter conjunction preceding the proton event had unusually high planetary jerk and tidal values of 4.6 units (Table 12), since both planets were positioned near their maximum sunspot-producing longitudes (which lag behind the perihelion longitudes) (Huntington, 1923). The Bollinger 7-planet solar index shows maxima on 31 Dec. 1955 and 24 Jan. 1956 of 56222 and 53277 units, and minima on 16 Jan. and 17 Feb. of 44308 and 37577 units (Bollinger, 1960). High rates of change of the 7-planet tide are shown in Table 2 to take place from 8 to 16 Jan. and 1 to 9 Feb.

TABLE 12. Rank Order of Planetary Conjunctions (Wood, 1968) Jerk is defined as the rate of change of solar acceleration.

Planets	Jerk Max	Jerk Ave	Tidal Max	Tidal Ave
Me+V	6.1	4.9	4.2	3.0
Me+J	4.7	2.4	4.6	3.1
V+J	3.7	3.5	4.8	4.4
Me+E	4.6	2.4	3.0	1.9
E+J	2.2	2.0	3.6	3.2

TABLE 13. Dates and Values of High Rate of Change of Seven-Planet Tidal Force (dT/dt) (Bollinger, 1960) During Solar Cycle 19, followed in Last Column by Dates of Proton Events (Jonah et al., 1963). Underlined Events are Ground Level Events Discussed in This Report.

YEAR	DATE	dT/dt	EVENT
1956	Jan 8 - 16	-1.41	
	Feb 1 - 9	-1.25	Feb 23
1957	Oct 1 - 9	-1.88	Oct 21
	Mar 18 - 26	-1.63	Apr 10
1958	Jun 1 - 6	1.38	Jun 6
	Jun 14 - 22	-1.25	Jul 7
	Dec 7 - 15	-1.75	peak sun-spot no.
	May 16 -	1.50	Jun 13
1959	Jun 9 - 17	-1.13	Jul 14
	Sep 13 - 21	1.13	Oct 6

Table 14. Ottawa 10.7 cm. Radio Flux Daily Means for January, February 1956. (Quarterly Bulletin, IAU). Units, 10^{-22} Watts/m^2 (c/s). The Passages of the Active Center are shown, and the dates of the Mercury-Venus, Mercury-Jupiter and Earth-Jupiter-Pluto Conjunctions.

1956 Date		January		February
1		-		114
2		128		116
3		125		116
4		123		116
5		116		106
6		120		103
7	Me, V conj	124		107
8		122		109
9		116		116
10		112	East Limb	121
11		116		133
12		124		154
13	East Limb	135		163
14		136		185
15		156		219
16		161	E, J, P conj	240
17		170		248
18		177		251
19		174		248
20	CMP	173		244
21		174		236
22		181		220
23		177		204
24		174	West Limb	178
25		153		-
26		137		154
27	West Limb	124		142
28		121		143
29		109		157
30		107		-
31	Me, J conj	110		-

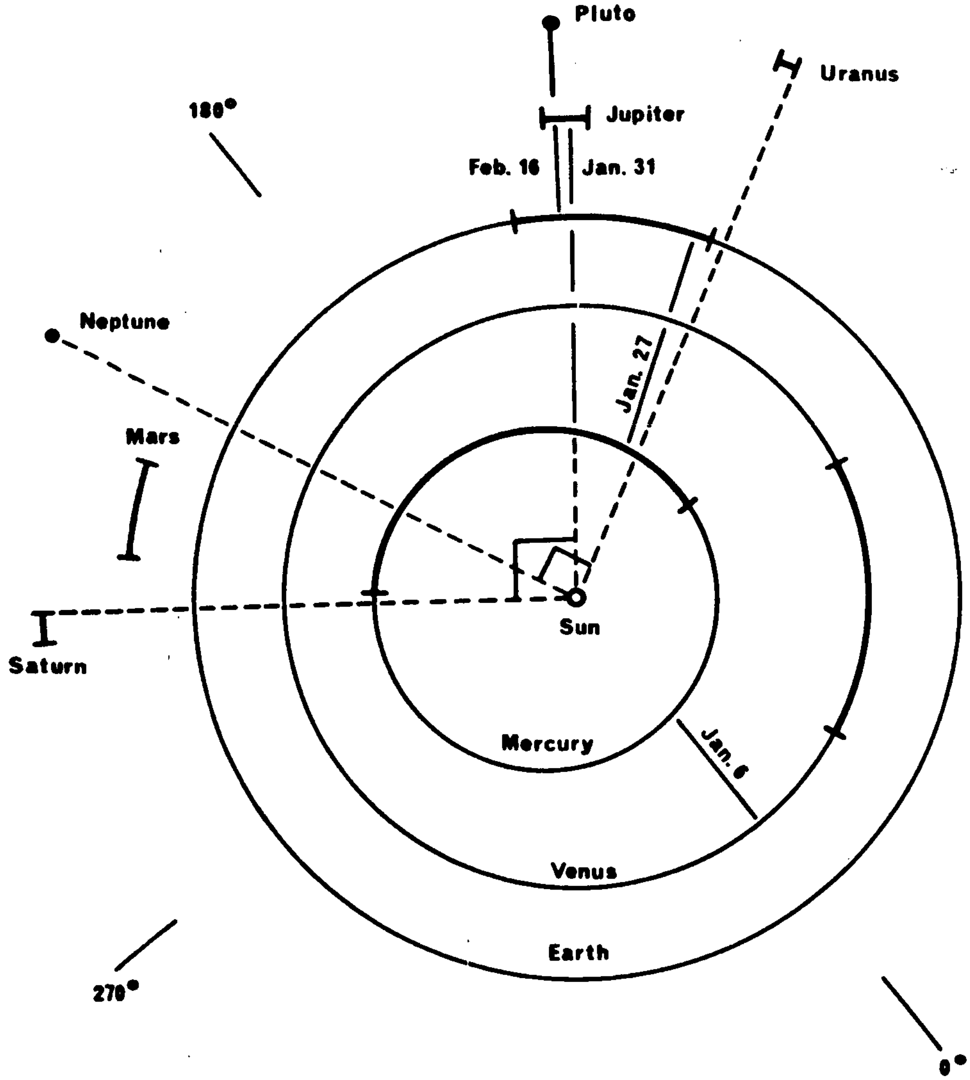

Figure 8. Planetary Configuration One Month Prior to Proton Event of 23 February 1956. (American Ephemeris, 1956)

Date*		Planets			Longitude
	Dec 16	Venus	Jupiter		322°, 142°
Jan 6		Mercury	Venus		0°
	Jan 23	Earth	Uranus		120°
	Jan 24	Venus	Neptune		20°
	Jan 26	Mercury	Uranus		120°
Jan 27		Mercury	Earth		123°
	Jan 30	Venus	Mars		38°, 218°
Jan 31		Mercury	Jupiter	Pluto	145°
Feb 16		Earth	Jupiter	Pluto	146°
	Feb 16	Mercury	Neptune		208°
	Feb 23	Mercury	Mars		230°

*Dates of lesser importance are indented.

II. PROTON EVENTS OF 10, 14, 16 JULY 1959

Late in May 1959, a second region developed behind the group producing the 10 May flare. (McDonald, 1963.) On the second passage in June a bright plage and complex spot group (area = 1111 millionths) produced several large flares. Just before the third passage there were loop prominences (Bruzek, 1964), surges, and radio fade-outs indicating continuing activity. By the 9th of July small flares had occurred and the plage had grown larger and brighter. On the July passage the following features were observed in the active center:

1. Giant Sunspot Group - The maximum area in the July passage was 2100 millionths. The bright plage at CMP was an impressive 12,000 millionths at N16 and Carrington longitude $L_o = 330^o$.

2. H α Flare - The major flares occurred on 10 July, 14 July, 16 July, with the 14 July event producing the highest particle flux during the three year period 1957-1959. The 14, 16 July flares covered all but one of the principal umbrae. Umbral coverage has been noted as a condition for proton events and radio bursts (Dodson and Hedeman, 1964) (Jonah, 1967) (Malville and Smith, 1963).

3. Magnetic Fields - of up to 3200 gauss were recorded in the βγ spot group of Zurich classification H. Umbrae of both polarity were contained in the same large penumbra (the delta configuration).

The following solar-terrestrial effects were noted:

1. Radio Fade-Outs - accompanied all three events. The 16 July event was also associated with SEA and SCNA (Ellison et al., 1961).

2. Radio Bursts - occurred on 10.7 cm on 9 July (peak flux 490 times mean daily flux), 14 July (120 times mean) and 16 July (6500 times mean) (Solar Geophysical Data). All 3 flares were accompanied by Type IV synchrotron radiation.

3. Cosmic Rays - Protons were recorded from all 3 flares despite the unfavorable geometry of the first two located 66E and 06E of CMP. Only the 16 July event produced a GLE of 5% above ambient flux.

4. Magnetic Storms - Sudden commencements were observed on 11, 15 and 17 July with the SC on 15 July the most severe. It should be noted that the flare of 10 July occurred far on the eastern hemisphere, so that the magnetic storm is somewhat remarkable.

Interpretation. The 1959 July event came midway in the 19th cycle, and therefore would not be expected to be as high energy as early and late events such as February 1956, and November 1960.

The conjunctions preceding the July 1959 events resemble the conjunctions preceding the July 1946 event. On 18 May, 1959 there was a conjunction of Earth and Jupiter; on 2 July, Venus and Jupiter, and finally on 12 July a conjunction of Mercury and Jupiter. The Carrington active longitude 330^o which produced the proton event was approximately in line with the Earth-Jupiter conjunction on 18 May. On 12 July, the date of the Venus-Jupiter conjunction, the active solar longitude $L = 330^o$ was approximately in line with the two major tidal planets. Although the spot group was first seen at east limb on 8 July, it grew in size afterwards to a maximum area of 2100 millionths, one of the largest spot groups in cycle 19. (Jonah et al., 1956-1963).

The 10.7 cm radio flux was elevated on the days of Mercury-Jupiter and Mercury-Earth superior conjunctions on 1 and 3 June, and at the time of the Venus-Jupiter conjunction on 1-2 July (Table 15). The Mercury-Jupiter conjunction occurred on 12 July, the day of the first 3+ flare and therefore the increase in radio flux is ambiguous. Again, the increases on meter wavelengths were more impressive, but the generally high fluctuating radio emission during the peak of the 11-year cycle makes interpretation difficult.

In terms of the Bollinger planetary tidal index, there were successive minima on 8 May and 17 June of 35173 and 50026 and maxima on 29 March and 1 June of 51479 and 63376 units (tabluated every 8 days). (Bollinger, 1960.) There was a high rate of change of tidal function from June 9 to 17. (Table 13).

Table 15. Ottawa 10.7 cm. Radio Flux Daily Means for June, July 1959. (Quarterly Bulletin, IAU). Units, 10^{-22} Watts/m^2(c/s). The Passages of the Active Center are shown, and the dates of the Mercury-Earth-Jupiter, Venus Jupiter and Mercury-Jupiter Conjunctions.

1959 Date		June		July
1		193		188
2	Me, J superior	198	V, J conj	174
3	Me, E conjunction	198		171
4		190		177
5		197		176
6		210		188
7		198		192
8		213	East Limb	185
9		223		185
10	East Limb	228		-
11		226		194
12		220		234
13		212	Me, J conj	243
14		208	CMP	264
15		225		245
16		220		261
17	CMP	225		240
18		228		231
19		237		222
20		226		208
21		228		189
22		219	West Limb	178
23		220		178
24	West Limb	232		181
25		233		182
26		238		182
27		240		200
28		224		205
29		219		207
30		196		204
31		-		208

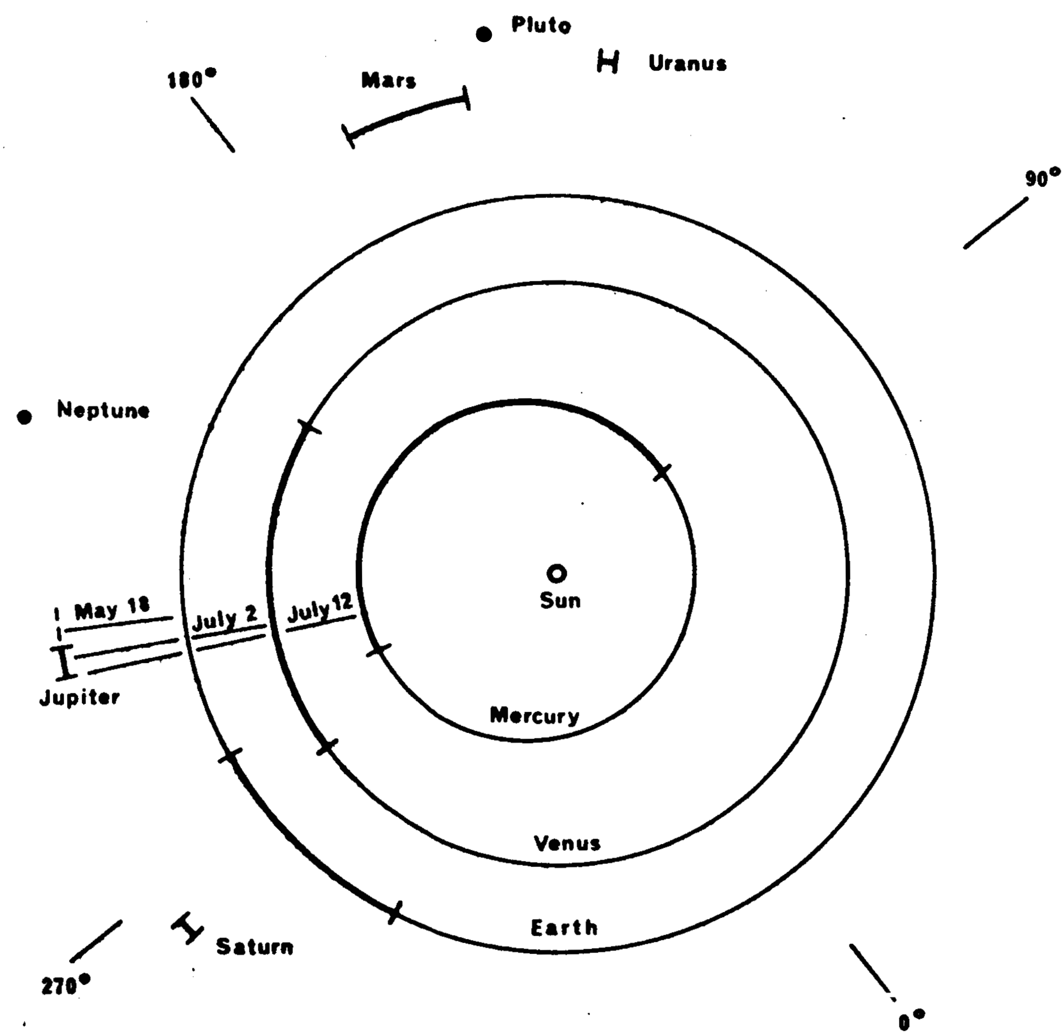

Figure 9. Planetary Configuration One Month Prior to Proton Events of 10, 14, 16 July 1959. (American Ephemeris, 1959).

Date	Planets			Longitude
May 18	Earth	Jupiter		236°
May 19	Mercury	Venus		350°, 170°
Jun 1	Mercury	Jupiter		57°, 237°
Jun 3	Mercury	Earth		72°, 252°
Jun 14	Mercury	Uranus		136°
Jun 16	Venus	Neptune		216°
Jun 17	Mercury	Mars	Pluto	155°
Jun 26	Earth	Saturn		273°
Jul 2	Venus	Jupiter		240°
Jul 4	Mercury	Neptune		216°
Jul 12	Mercury	Jupiter		241°

III PROTON EVENT OF 4 MAY 1960

The region became active near the east limb around March 25. Three polar cap events (PCE) were recorded on the first passage: on March 31, April 1 and 5. The sunspot area reached a peak on 4 April of 2270 millionths with a bright plage of about 3500 millionths. On the second passage the spot group was reduced in size, but the plage grew to almost double by CMP.

1. The Compact Sunspot Group - at N 10° and L = 135° was over 1000 millionths at east and west limb but was smaller than 700 millionths as it crossed CMP.

2. Sunspot Magnetic Field - when measured on the disk reached 2300 gauss in the C, D and E type spot group. (Jonah et al., 1964.)

The 4 May event took place at west limb and the following solar terrestrial effects were noted:

1. Short Wave Fadeout - accompanied the limb flare.

2. Geomagnetic Crochet - was recorded at Hermanus.

3. Radio Noise - a great burst of 2650 flux units (peak) was recorded on 2980 Mc/s in the Netherlands.

4. Cosmic Rays - were recorded at several stations. This cosmic ray shower had the shortest time scale of all those measured up to this time (Ellison, 1961), with a total duration of only two hours. The solar flare which produced the event was also smaller,

fainter and of much shorter duration. However there may have been a special configuration of the interplanetary field which ducted the particles from the favorable west limb location directly to the earth.

5. Magnetic Storm - of minor intensity occurred on 6 May.

6. There was no Forbush Decrease.

Interpretation. Following the triple conjunction of Venus, Jupiter and Mercury on 24 February, in alignment with the active longitude, the 10 cm. radio emission was elevated 5% for three days. Although the spot group was not distinctive until a month later, the I.A.U. Quarterly Bulletin lists the region as being in its third rotation on the late March passage. On this rotation it was already flare-active and a strong radio emitter at 169 Mc/s and 3000 Mc/s. Following the Mercury-Jupiter-L* conjunction on 9 April, the 10 cm. radiation increased 30% in 5 days. The spot group was large on its reappearance on 22 April, but declined in size for several days, although the plage remained large and bright, on 27 April, two sets of conjunctions took place - Earth-Neptune-L* (at CMP) and Mercury-Mars. Following this date the spot group grew rapidly in size and in radio emission. The maximum plage area was reached on 2 May, and maximum spot area on 3 May and the proton event occurred at west limb on 4 May, when the active center was in alignment with the Mars-Uranus conjunction.

Table 16. Ottawa 10.7 cm Radio Flux Daily Means for February-May, 1960. (Quarterly Bulletin, IAU). Units - 10^{-22} watts/m^2 (c/s). The passage of the active center is shown, and the dates of significant planetary conjunctions.

1960 Date	February	March	April	May	Notes
1	225	137	201	152	
2	213	137	184	160	
3	215	138	179	158	
4	209	139	188	156	
5	209	140	182	152	
6	192	135	169	156	
7	187	139	165	162	
8	183	141	147	168	
9	183	143	148	170	MeJ conj (April)
10	178	132	156	170	
11	175	132	159	180	
12	166	129	168	179	
13	167	135	179	170	
14	167	134	183	162	
15	160	137	190	162	
16	158	142	183	155	
17	153	140	178	151	
18	151	130	176	153	
19	-	137	170	153	
20	142	143	175	160	
21	156	145	163	164	
22	149	150	160	164	
23	143	154	166	163	
24	140	158	165	164	
25	147	157	165	164	Me-V-J conj, E-P conj (February)
26	147	-	143	158	E-N-L* conj (March)
27	147	-	140	166	Me-Ma conj (March)
28	140	175	142	171	
29	140	181	153	170	
30	-	193	161	170	
31	-	182	-	159	CMP (March)

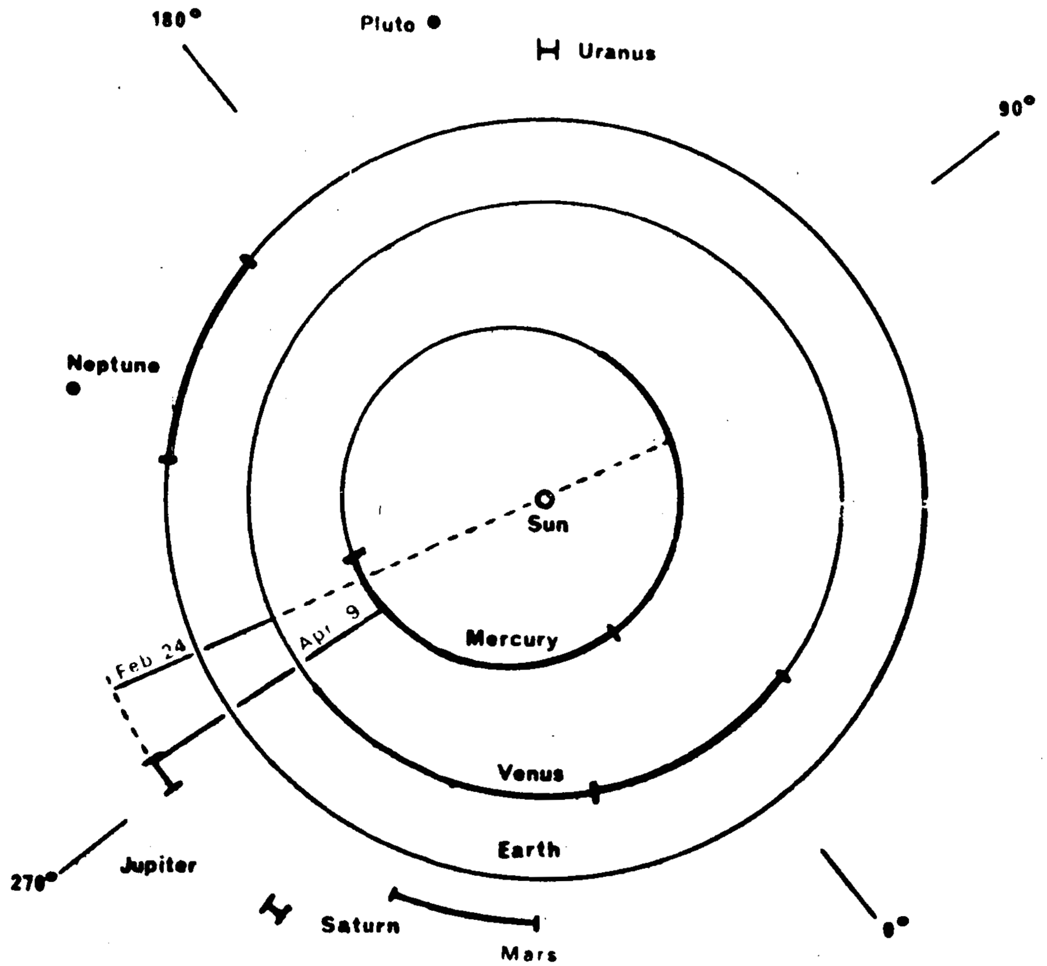

Figure 10. Planetary Configuration One Month Prior to Proton Event of 4 May 1960. (American Ephemeris, 1960).

Date	Planets			Longitude
Feb 24	Venus	Jupiter	(Mercury)	259°(79°)
Feb 24	Earth	Pluto		157°
Mar 2	Mars	Saturn		281°
Mar 4	Mercury	Uranus		139°
Mar 8	Venus	Saturn		281°
Mar 8	Mercury	Pluto		153°
Mar 10	Mercury	Earth		166°
Mar 24	Mercury	Neptune		217°
Apr 9	Mercury	Jupiter		262°
Apr 16	Mercury	Saturn		282°
Apr 27	Earth	Neptune	L*=133°	217°
Apr 27	Mercury	Mars		317°
May 4	Mars	(Uranus)		320°(140°)

IV. PROTON EVENTS OF 12, 15, 20 NOVEMBER 1960

The active region was observed first in October (CMP-15 Oct) with moderate activity, loop prominences, and yellow coronal line emission. When the region reappeared on 4 November the spot group was very large and complex with a very bright plage.

1. The Large Sunspot Group - at N 26° reached a maximum area of 2330 millionths on 13 November, although the maximum plage area of 9200 millionths was observed on 10 November. (HAO Summary.) The Carrington longitude of the F type group was $L_o = 30^{\circ}$, one of the active longitudes listed by Vitinsky (see also Losh, 1938) (Bezrukova, 1961, 1962).

2. H α Flare - The line width on 15 November was 25.2Å, one of the largest ever recorded. The 15 November flare was also observed in white light. The two principal umbra were completely covered by both the 12 and 15 November flares (Dodson and Hedeman, 1963).

3. Sunspot Magnetic Field - On 12 November the peak fields were north - 2800 gauss, and south - 2700 gauss, but by the time of the flare of 15 November the maximum fields had declined to north - 2500 gauss and south - 1500 gauss, and were unobservable on 20 November. The sunspot type was complex (γ), and the large penumbra enclosed umbra of opposite polarity (the delta configuration).

The following solar terrestrial effects were noted:

1. Short Wave Fadeouts - of great severity accompanied all three proton events.

2. Geomagnetic Crochets - were recorded by up to nine stations for all three events, and in each case, the crochet maximum followed the H α maximum, one of the criteria for proton emission (Jonah, 1967).

3. Radio Noise - on 10.7 cm was outstanding on 12 November with a rare great burst of 5500 flux units, possibly related to the umbral coverage (Malville and Smith, 1963). Type IV emission accompanied all three events.

4. Cosmic Rays - were observed from all three events, including the 20 November event which occurred 23° behind the west limb, but at a high altitude in the corona (Athay, 1962).

5. Magnetic Storms and Forbush Decreases - occurred following all three events.

Interpretation. The active region appeared in early October, following the conjunction of Mercury and Venus on 25 September (Fig. 11). The Mercury Jupiter conjunction on 7 October was in alignment with the active center on the sun, and radio emission of up to 100 times average was observed over frequencies from 67 Mc/s to 234 Mc/s for four days following the conjunction. The emission was also elevated on 2800 Mc/s on 7 October (Table 17). Further enhanced radio emission was noted on 17 October, the date of the Venus-Jupiter conjunction (Table 17) and within two days on all frequencies between 67 Mc/s and 234 Mc/s (Quarterly Bull, IAU). On 7 November an inferior conjunction and transit of Mercury took place, and a small radio burst occurred over the active center on that day, according to the radio interferometer observations at 169 Mc/s (Solar Geophysical Data). The correlation between significant conjunctions and elevated solar radio emission is particularly striking for the November 1960 events, on the 169 Mc/s interferometer graphs, because of the bursts accompanying the 7 and 17 October conjunctions.

Table 17. Ottawa 10.7 cm. Radio Flux Daily Means for October, November, 1960, (Quarterly Bulletin, IAU). Units, 10^{-22} watts/m^2 (c/s). The Passages of the Active Center are shown, and the dates of the Mercury-Jupiter and Venus-Jupiter Conjunctions.

1960 Date		October		November
1		115		124
2		112		129
3		120		130
4		132		131
5		132	East Limb	144
6		132		148
7	Me,J conj	144		157
8		143		168
9	East Limb	151		175
10		159		200
11		152		188
12		159	CMP	168
13		162		180
14		166		192
15	CMP	165		183
16		165		174
17	V,J conj	167		164
18		154	West Limb	153
19		153		150
20		149		147
21		144		139
22	West Limb	141		127
23		134		116
24		129		113
25		130		111
26		132		117
27		132		119
28		122		117
29		131		119
30		128		131
31		127		-

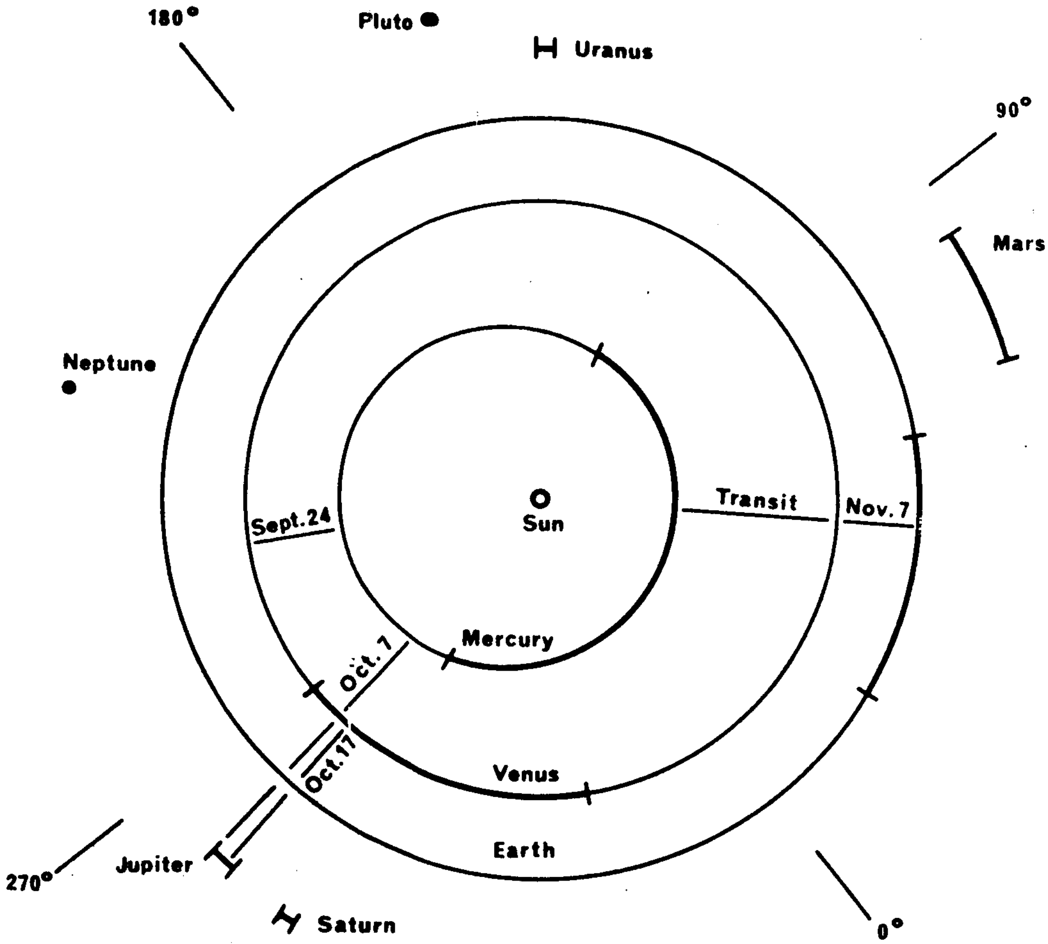

Figure 11. Planetary Configuration One Month Prior to Proton Events of 12, 15, 20 November 1960. (American Ephemeris, 1960).

Date	Planets			Longitude
Sep 24	Mercury	Venus		243°
Oct 7	Mercury	Jupiter		277°
Oct 17	Venus	Jupiter		278°
Oct 21	Mercury	Uranus		322°, 142°
Oct 24	Venus	Saturn		288°
Oct 25	Mercury	Pluto		386°, 156°
Nov 1	Earth	Neptune		38°, 218°
Nov 6	Mercury	Neptune		39°, 219°
Nov 7	Mercury	Earth	Transit	49°
Nov 12	Mercury	Mars		92°

V. PROTON EVENTS OF 11-21 JULY 1961

Although the active center produced proton events on 11, 12, 20 and 21 July, the discussion below is concentrated upon the GLE events of 18 and 20 July. The events observed on the sun were:

1. Giant Sunspot Group - the maximum area was 1570 millionths on 12 July with a bright plage of area 5100 millionths on the second rotation. The active longitude was 70^{o}.

2. H α Flare - The flare on 18 July had 2 distinct flash phases. The 20 July flare was a limb event and displayed the well-known loop prominence system (Bruzek, 1963). On the 18 July flare two bright filaments formed, one covering the north umbrae. Umbral coverage has been found typical of proton flares accompanied by strong radio and X-ray emission.

3. Sunspot Magnetic Field - was the complex (γ) type with field strengths of 2100 and 1500 gauss, with 3 north and one south umbrae in a large single penumbra on 12 July (the delta configuration).

The following solar-terrestrial effects were detected:

1. Radio-Fade Out (indicating X-ray emission) was observed on many frequencies, persisted for 2 hours on the 18th, 7 hours on the 20th, an abnormally long period for a short wave fade (SWF). On 20 July, other unusually strong ionospheric effects were noted, including SEA and SCNA (Bruzek, 1963).

2. Magnetic Crochet - delayed in both cases after the H α flare maximum, found to be characteristic of proton flares (Pinter, 1967) (Jonah, 1967).

3. Radio Noise - strong bursts on 2800 Mc/s occurred on 12, 18 and 20 July. The peak fluxes were 6000, 2400 and 1800 flux units (10^{-22} watts/m^2 (c/s). The meter bursts on 200 Mc/s were 22,000; 1000; and 4000 flux units on the same three days (Bruzek, 1963).

4. X-ray Emissions - Intense X-ray emission was detected directly by the Injun I Satellite (Van Allen et al., 1965). The counting rate increased to 3 times normal on 18 July and 50 times normal on 20 July in the wavelength band 0-14Å (hard X-rays) in synchronization with the two flares described.

5. Cosmic Rays - Increases of 12% on 18 July and 5% on 20 July were noted above galactic background on ground level neutron monitors. However, it is likely that particle emission at the sun may have been greater on the 20th, but failed to reach the earth because of geometry.

Interpretation. The planetary configuration for the month preceding 11 July is shown in Fig. 12, and significant conjunctions are listed below. The time of Jupiter-Saturn conjunction is felt by many authors to be significant for solar activity. The Bollinger tables extend from 1900 to 1959, so that the 7-planet tide and its rate of change cannot be obtained from that source for the November 1960 and July 1961 events. The 2-planet tidal force on 11 June the date of the Venus-Jupiter conjunction was 4.4 (Table 18); 25 days later (one solar revolution) the Mercury-Earth conjunction took place. During the first week of July 1961, the five major tidal planets - Mercury, Venus, Earth, Jupiter and Saturn - were within 40° longitude of each other. On 6 July a significant conjunction took place between Mercury and Jupiter. The sunspot group grew rapidly following that date.

Table 18. Ottawa 10.7 cm. Radio Flux Daily Means for June, July 1961. (Quarterly Bulletin IAU). Units - 10^{-22} watts/m^2(c/s). The Passages of the Active Center are shown, and the dates of the Venus-Jupiter and Mercury-Jupiter conjunctions.

1961 Date		June		July
1		86		104
2		88		99
3		92		104
4		89		103
5		86	Me, J conj	106
6		88		102
7		89	East Limb	105
8		91		107
9		100		112
10	East Limb	102		124
11	V, J conj	110		138
12		108		137
13		114	CMP	141
14		123		136
15		129		136
16		132		132
17	CMP	137		137
18		136		131
19		131		126
20		131	West Limb	123
21		132		118
22		134		119
23	West Limb	135		118
24		117		118
25		111		117
26		108		115
27		99		111
28		95		105
29		102		103
30		103		92
31		-		91

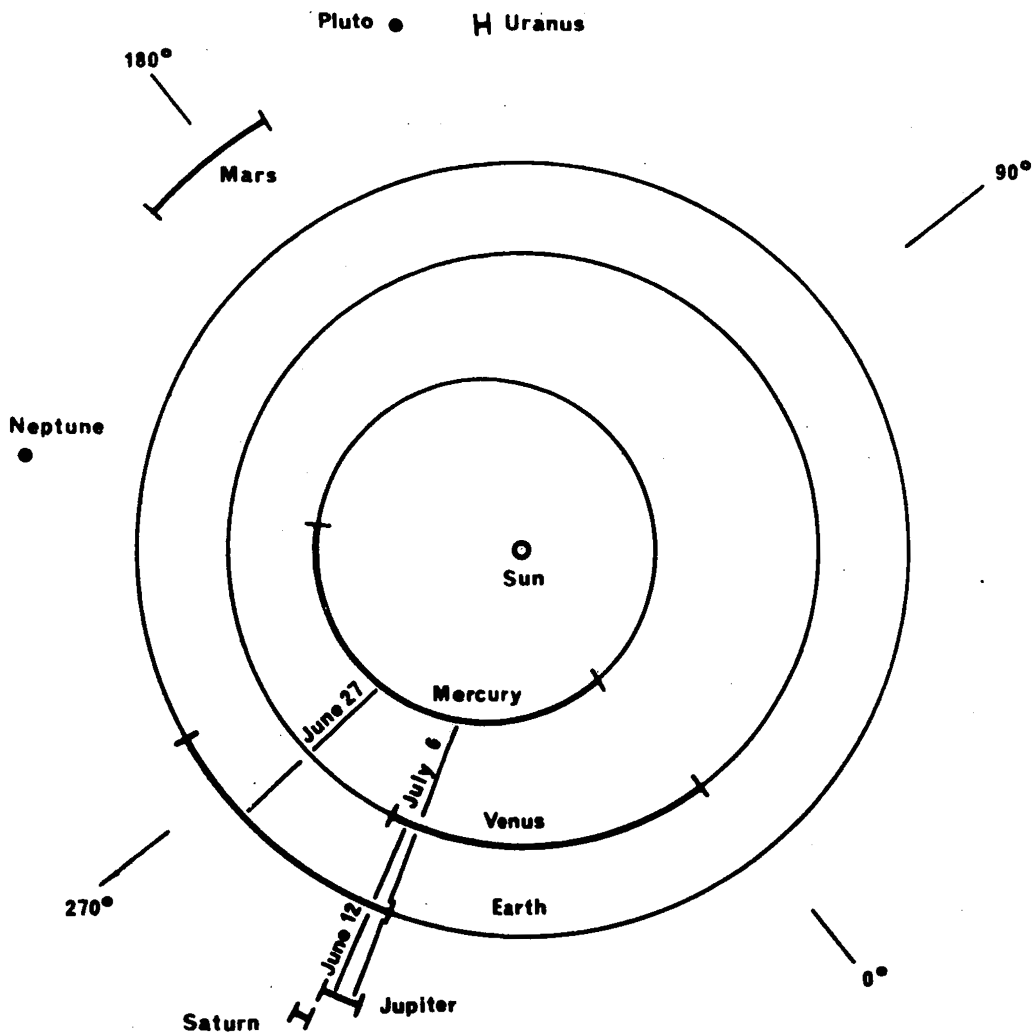

Figure 12. Planetary Configuration One Month Prior to the Proton Events of 11-21 July 1961. (American Ephemeris, 1961).

Date	Planets			Longitude
May 1	Mercury	Earth		35°, 215°
May 5	Mercury	Venus		59°, 239°
May 14	Mercury	Jupiter		115°, 295°
Jun 12	Venus	Jupiter	Saturn	296-8°
Jun 27	Mercury	Earth		274°
Jun 28	Venus	Uranus		324°, 145°
Jul 5	Mercury	Saturn		296°
Jul 6	Mercury	Jupiter		298°
Jul 6	Venus	Pluto		336°, 156°
Jul 13	Mercury	Uranus		325°, 145°
Jul 16	Mercury	Pluto		336°, 156°

CONCLUSIONS

On the basis of studies of cycle 17, 18 and 19, it is possible to conclude that high energy proton events occur in two major peaks about 2 years before and 2 years after the peak sunspot number R_m, followed by a smaller peak occurring 3-4 years after R_m. It can be shown that most characteristics of major solar activity follow the same three-peaked cycle including: areas of giant sunspots, frequency of giant sunspots, frequency of large flares, green coronal line intensity, occurrence of geomagnetic crochets and sudden commencement storms, and E and F_2 layer ionospheric indices, and that where known, these indices show a similar 3-peaked pattern for solar cycles 12-19.

It is now possible to establish nine criteria for the occurrence of major proton flares. Most of the features listed below have been recorded over the 130 year period of quantitative solar observations. Thus it is feasible now to study earlier solar cycles and determine major proton flare activity with a high probability. A long period of proton event cycles is necessary for long range predictions of future solar activity. The nine criteria are as follows:

1. The plage - sunspot region must be in second or later passage.
2. The sunspot area must be greater than 1000 millionths.
3. The penumbra must enclose umbra of opposite polarity (delta configuration).
4. The flare must cause a magnetic crochet, or short wave fade (SWF) which follows the time of the flare maximum intensity.
5. The flare must cover a significant part of the sunspot umbrae.
6. The flare must be accompanied on the same disk passage by the loop prominence system.

7. The spot group must be magnetically complex, beta or beta-gamma.

8. The flare must occur at an active Carrington longitude.

9. The flare must occur near one of the three peaks of major activity in the cycle.

BIBLIOGRAPHY

Acton, L. W., "Some Relationships between Short-Wave Fadeouts, Magnetic Crochets and Solar Flares," J. Geophys. Res. 66, pp. 3060-3063 (Sept. 1961).

American Ephemeris and Nautical Almanac, U. S. Naval Observatory, (yearly).

Athay, R. G., "The Cosmic Ray Flares of July 1959 and November 1960 and Some Comments on Physical Properties and Characteristics of Flares," Space Research II, pp. 837-848, 1962.

Bailey, D. K., "Polar-Cap Absorption," Planet. Spa. Sci. 12, pp. 495-541.

Bell, B., "Type IV Solar Radio Bursts, Geomagnetic Storms, and Polar Cap Absorption (PCA) Events," Smithsonian Contrib. to Astrophys. 8, No. 3, pp. 119-113 (1963).

Bezrukova, A. Ya., "Longitudinal Distribution of Areas of Sunspot Groups in the 19th Cycle of Solar Activity," Soln. Dannye, pp. 58-60 (Feb. 1961) and pp. 69-71 (Jan. 1962).

Blizard, J. B., "Long Range Solar Flare Prediction," Astron. J. 73, No. 5 (June 1968).

" "Solar Activity and Planetary Positions," Bull. Am. Phys. Soc. 13, (June 1968).

Bollinger, C. J., "Atlas of Solar Planetary Climate," Battenberg Press, Norman, Okla., 1960.

Bruzek, A., "Optical Characteristics of Cosmic Ray and Proton Flares," J. Geophys. Res. 69, No. 11, pp. 2386-2387 (June 1, 1964).

Bruzek, A., "Case Histories of Flares: The Large Flares of July 11, 12, 18 and 20, 1961," in "Physics of Solar Flares," NASA SP-50 (1963).

Castelli, J. P., and Michael, G. A., "Flux Density Measurements of Radio Bursts of Proton-Producing Flares and Non-Proton Flares," J. Geophys. Res. 72, No. 21, pp. 5491-5498 (Nov. 1967).

d'Azambuja, L., "Cartes Synoptiques de la Chromosphere Solaire," 1956, 1959, 1960, 1961, Observatoire de Meudon, Paris.

de Jager, C., "Structure and Dynamics of the Solar Atmosphere," in Handbuch de Physik, Vol. 52, ed. by S. Flugge, Springer-Verlag, Berlin, 1959.

Dodson, H. W. and Hedeman, E. R., "Problems of Differentiation of Flares with Respect to Geophysical Effects," Planet. Spa. Sci. 12, pp. 393-418 (1964).

Ellison, M. A., McKenna, S. M. and Reid, J. H., "Cosmic Ray Flares," Dunsink Obs. Publ. 1, No. 3 (1961).

Fitchel, C. E. and McDonald, F. B., "Energetic Particles from the Sun," Ann. Rev. Astron. Astrophys. 5, p. 351 (1967).

Fletcher, J. D., "Solar Radio Emission as a Criterion for Solar Proton Event Warning," AIAA J. 2, pp. 2193-2197 (Dec. 1964).

Gnevyshev, M. N. and Ol', A. J., "Coronal Emission Line Intensity as an Index of Solar Corpuscular Radiation," Soviet A. J. 9, pp. 765-767 (1966).

Hakura, Y., "Polar Cap Absorptions and Associated Solar-Terrestrial Events Throughout the 19th Solar Cycle," NASA TM X-55812, Goddard (June 1967).

Haurwitz, M., "Solar Longitude Distributions of Proton Flares, Meter Bursts, and Sunspots," Astrophys. J. 151, pp. 351-364 (Jan. 1968).

High Altitude Observatory, "Solar Activity Summaries," 1956, 1959, 1960, 1961, by D. Trotter and W. O. Roberts.

Huntington, E., "Earth and Sun," Yale Univ. Press, New Haven, Conn. (1923).

Jonah, F. C., Dodson-Prince, H. and Hedeman, E. R., "Solar Activity Catalogs, 1954-1963," NASA, Houston.

Jonah, F. C., "Analysis of Polar Cap Absorption Events IV - Almost Necessary and/or Sufficient Condition for Solar Proton Warning," LTV Astro. Div., Report 00.882 (Feb. 1967).

Kopecky, M., "The Periodicity of the Sunspot Groups," Advances in Astronomy and Astrophysics, Vol. 5 (1967).

Krivsky, L., "The Relation Between Proton Flares and the Corona Over the 11 Year Cycle," Soviet Astron. AJ 10, No. 2, pp. 304-307 (Sept.-Oct. 1966).

Kundu, M. R., "Centimeter Wave Radio and X-Ray Emission from the Sun," Spa. Sci. Rev. 2, pp. 438-469 (1963).

Losh, H. M., "Distribution of Sunspots in Longitude," Publ. Obser. Univ. of Michigan 7, No. 5, pp. 127-145 (Sept. 1938).

Malville, J. M. and Smith, S. F., "Type IV Radiation from Flares Covering Sunspots," J. Geophys. Res. 68, pp. 3181-3185 (May 15. 1963).

McDonald, F. B., "Solar Proton Manual," NASA TR R-169, Dec. 1963.

Pinter, S., "Geomagnetic Crochets Associated with Proton Flares," Bull. Astron. Czech. 13, No. 1, pp. 282-286 (1967).

"Quarterly Bulletin on Solar Activity," International Astronomical Union, Zurich, Switzerland, 1956, 1959, 1960, 1961.

Roberts, W. T., "Probabilities of Solar Flare Occurrence," NASA TM X-53463 (May 1966).

Rubashev, B. M., "Problems of Solar Activity," NASA TT F-244 (Dec. 1964).

Sawyer, C. G., Agy, V. L., and Haurwitz, M. W., "Early Recognition of a Solar Flare, II - Energetic Protons," Nat. Bu. Standards, Report 9192 (Mar. 1966).

Sawyer, C., "Statistics of Solar Active Regions," Ann. Rev. Astron. and Astrophys. 6, pp. 115-134 (1968).

Sherry, D. T., editor, "Forecasting Solar Activity and Geophysicsl Responses," 4WWM 105-1 revised, Ent Air Force Base, Colorado Springs (June, 1968).

Solar-Geophysical Data, ESSA, Dept. of Commerce, Washington, D. C. (monthly).

Svetska, Z., "On Long-Term Forecasting of Proton Flares," Sol. Phys. 4, pp. 18-29 (1968).

Takahashi, K., "On the Relation between the Solar Activity Cycle and the Solar Tidal Force Induced by the Planets," J. Radio Research Laboratories 14, pp. 237-240 (Jul.-Sep. 1967).

Van Allen, J. A., Frank, L. A., Maehlum, B. and Acton, L., "Solar X-Ray Observations by Injun I," J. Geophys. Res. 70, No. 7, pp. 1639-1645 (April 1, 1965).

Vitinsky, Y. I., "Solar Activity Forecasting," NASA TT F-289 (1965).

Warwick, C., "Longitude Distribution of Proton Flares," Ap. J. 141, pp. 500-504 (1965).

Warwick, C. S. and Haurwitz, M. W., "A Study of Solar Activity Associated with Polar Cap Absorption," J. Geophys. Res. 67, pp. 1317-1332 (1962).

Xanthakis, J., "The Relative Sunspot Numbers and the Time of Rise," Bull. Astron. Czech 17, No. 5, pp. 215-233 (1966).

7. PROTON EVENTS OF CYCLE 20

7. PROTON EVENTS OF CYCLE 20

Proton events usually occur after a closely spaced sequence of conjunctions of the planets Mercury, Venus, Earth and Jupiter, some of which are in alignment with an active longitude on the sun. Occasionally conjunctions of 3 or more other planets may be significant in triggering an event. The number of conjunctions of the four tidal planets is two or three times average during the two month period preceding major solar events. The concentration of conjunctions is definitely non-random before the events.

Since only the first half of cycle 20 is available for study, one non-GLE event will be discussed. The first major active center appeared in March 1966 and is an excellent subject for study because of the previous low level of activity. The consequent isolation from background and other sources of activity eliminates ambiguity.

The first GLE of cycle 20 took place on 7 July 1966. Its antecedents resemble the 23 February 1956 event as does the Carrington longitude involved. The region revived in August to produce events on 28 August and 2 September.

The highest energy event occurred on 28 January 1967 from a region on the far side of the sun with a short previous history as was also the case for 7 July 1966.

High activity in 1969 is also discussed. Ground level events (GLE) occurred in late February and March and on 10 April 1969 from one active center, L = 88°. Solar monitoring shows a great increase in precision and quantity in the period from 1967 to 1969.

Cycle 20 appears to be as active as cycle 18 in radio flux and high energy proton events (GLE), although it is difficult to discount increased sensitivity of instrumentation. On the other hand, the sunspot number is definitely lower than cycle 19.

I. PROTON EVENT OF 24 MARCH 1966

The first important active center of the 20th cycle appeared in late February 1966 at N 18° and longitude 146°. Previous to the appearance of Plage 8207, the sunspot number and 10 cm radio flux had been at a consistently low level. The Zurich sunspot number had been below 50 except for a few days, and many days had been spotless. Following the February passage, the yellow coronal line (indicating $T = 4x10^6$ degrees K in the corona) was observed at west limb, indicating presence of an active center which could produce protons. The longitude was unusual for an active center early in the cycle, but the latitude was low enough to fit the isolines of another longitude group, which appeared for 6 earlier cycles (Vitinsky) (Warwick, 1965).

The March 1966 active center produced 146 optical flares and 155 radio bursts on 10 cm (Fan et al., 1968), and on 24 March produced a proton event. Although activity declined after the March passage, another center approximately 180° away produced frequent 10 cm radio bursts and flares, resulting in the March-April period being the most active radio period during the entire year.

The events observed on the sun during the March passage were as follows:

1. Large Sunspot Group of maximum area 900 millionths on its second passage. The Carrington longitude

was 146°, conforming to one of the northern active longitudes (Vitinsky, 1965). The plage area was 9500 millionths on 22 May (CMP).

2. H α Flare - occurred on 24 March with a proton counting rate 20 times ambient in the energy range 12-70 MeV (Fan et al., 1968).

3. Sunspot Magnetic Field - the magnetic field was beta-gamma, and the spot group was classed as Zurich class G on 24 March.

The following solar-terrestrial effects were noted:

1. X-Rays - Bursts over 10 times ambient flux in the 0–8Å band were recorded on 15, 17, 20, 23, 26 and 29 March (see Table 19).

2. Radio Noise - type IV continuum emission was recorded daily for nine days from the appearance of the active center on 15 March.

3. Protons - above 20 MeV had a peak flux of 15×10^5 particles/cm^2-sec.

4. A Magnetic Storm - occurred the next day, accompanied by a Forbush decrease.

Interpretation: On 3 Jan there was a conjunction of Venus and Jupiter, and on 26 January of Venus and Earth. No opposition of Jupiter and the earth took place, although the two planets were close in longitude in early January. On 13 Feb. a five planet conjunction took place between Uranus and Pluto in opposition to Mercury Mars and Saturn. The active center developed soon after and was a radio and X-ray source beginning on 21 or 22 February. Yellow coronal line emission from the region was noted on the same date. On 8 March, another 5 planet conjunction took place between Earth, Uranus and Pluto in opposition to Mars and Saturn. On 19 March, four planets were in alignment, Mercury Uranus Pluto in opposition to Saturn. Finally on 21 March there was a conjunction between Mercury and the Earth. (See Figure 13).

The 10 cm radio flux was elevated at the time of the five planet conjunctions on 13 Feb. and 8 March, and again on 19 March and 21 March, two other conjunction dates. The SOLRAD Satellite had been monitoring X-rays in four wavelength bands. The flux levels in one X-ray band and 10 cm are shown for February and March 1966 in Table 19. The increase in X-ray flux is much greater on conjunction dates than for 10 cm radio flux.

Table 19. Daily X-Ray and Radio Flux for January-March, 1966. Units: 0-8Å: 10^{-4} ergs/cm^2-c/s); 10 cm. radio: 10^{-22} watts/m^2 (c/s). The passage of the active center is shown, and the dates of significant conjunctions.

DATE 65-66	JANUARY			FEBRUARY			MARCH		
		X-Ray	Radio		X-Ray	Radio		X-Ray	Radio
1		2.37	82		0.35	79		11.0	81
2		1.53	79		1.85	79		0.65	78
3	V J conj	0.33	78		1.49	80		--	77
4		0.28	81		1.59	82		--	77
5		--	81		0.40	83		--	76
6		--	80	MeE conj	0.50	84		--	76
7		0.40	81		0.49	85		--	76
8	MeN-----	--	81		0.50	85	EMaS	--	77
9		--	80	MeV conj	1.24	85	UP conj	3.4	79
10		0.30	80		0.70	85	L* =128°	--	80
11		2.18	81	L*=133°	0.66	86		--	79
12		1.44	84		0.77	85		--	79
13		1.56	87		0.59	86		1.9	80
14		3.31	93		0.60	86		3.34	82
15		2.95	102		0.47	85		11.7	88
16		3.35	106		0.41	84		5.0	94
17	Plage	1.64	102		0.38	84		35.0	105
18	#8131	3.85	105		0.54	84		5.4	110
19	CMP	7.48	109		0.69	84	Me SUP-	7.1	113
20		2.75	102		1.36	85	conj	61.0	114
21	MeJ conj	1.57	99	V-U-P	1.10	88	MeE—	9.8	120
22		1.61	95	conj	0.89	88	conj	5.1	104
23		1.43	94	L* =139°	2.25	84		13.0	97
24		--	92	CMP	1.55	83		8.1	93
25		0.80	88	#8174	1.52	81		3.4	90
26	VE conj	0.96	85		1.64	85		14.0	84
27	L* =141°	0.68	82		3.46	85		6.3	84
28		0.66	81		4.58	85		20.0	87
29		0.54	81		--	--	Plage	19.0	95
30		0.33	78		--	--	#8223	12.0	110
31		--	78		--	--		12.0	110

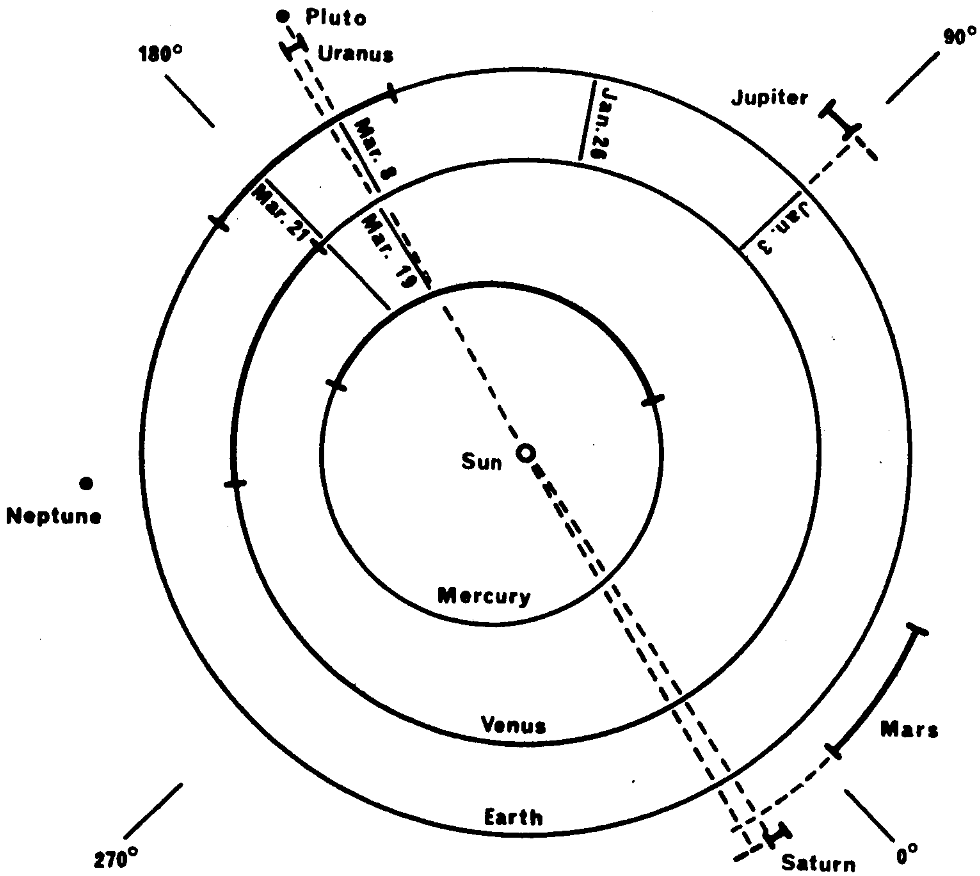

Fig. 13. Planetary Configuration One Month Prior to Proton Event of 24 March, 1966. (American Ephemeris, 1966).

DATE	PLANETS	LONGITUDE
Dec 18	Earth Jupiter	87°
Jan 3	Venus Jupiter	88°
Jan 26	Venus Earth	125°
Feb 6	Mercury Earth	316°, 136°
Feb 9	Mercury Venus	327°, 147°
Feb 13	Uranus Pluto (Mercury Mars Saturn)	167° (347°)
Mar 2	Venus Mars	182°, 2°
Mar 8	Earth Uranus Pluto (Mars Saturn)	167° (348°)
Mar 19	Mercury Uranus Pluto (Saturn)	168° (349°)
Mar 21	Mercury Earth	178°

II. PROTON EVENT OF 7 July 1966

So much has been written about this active center (Svetska, 1968) that only a few highlights will be repeated here. Although the spot group seemed to appear from nowhere on 28 or 29 June, sequential diagrams and photos show that remnants of the plage No. 8331 probably were incorporated in the new plage. (Fortini and Torreli, 1968) (Svetska, 1968).

1. Sunspot Group - The area grew rapidly from less than 100 on 3 July to 1300 millionths on 7 July. The bright plage crossed CMP at 3,4 July at N 35° and Carrington longitude L = 190°.

2. H α Flare - The 7 July flare covered all but one of the principal umbrae. Umbral coverage has been noted as a condition for proton events and radio bursts (Dodson and Hedeman, 1964) (Jonah, 1967).

3. Magnetic Fields - of up to 3300 gauss north (3000 south) were recorded in the βγ spot group (Soln. Dannye, 1966). Umbrae of both polarity were contained in the same large penumbra (the delta configuration). A rapid increase of magnetic flux was noted on 6 July (Severny, 1968) (Svetska, 1968).

The following solar-terrestrial effects were noted:

1. X-ray Emission - significant X-ray emission was detected by satellite (Van Allen, 1967) (Cline et al., 1968).

2. Electrons - the 7 July event was the first recorded case of electron emission from the sun (Anderson and Lin, 1967).

3. Protons - Protons were recorded at many stations due to the favorable geometry near the west center of the disk. The 7 July event produced a GLE of 3% above ambient flux. Events were also recorded from this center on 11 July, 16 July and 28 July. (Dodson and Hedeman, 1969)

4. Radio Bursts - occurred on 10.7 cm on 7 July (peak flux 2650 times mean daily flux), (Solar Geophysical Data), accompanied by Type IV synchrotron radiation.

5. Magnetic Storm - A sudden commencement was observed on 9 July along with a Forbush decrease of 5%.

Interpretation. The 1966 July event occurred early in the 20th cycle, at the one northern active longitude of importance at high latitude $L = 190^{\circ}$. (See Fig. 14 and Table 20).

Again, as in February 1956 event, the Earth Jupiter conjunction seemed to be the triggering factor. Earlier on 2 June there was a conjunction of Mercury and Jupiter, on 15 June a quadruple conjunction of Mercury Uranus Pluto and Venus and finally on 5 July a conjunction of Earth and Jupiter. The Carrington active longitude 190° which produced the proton event was approximately in line with the 15 June quadruple conjunction. On 5 July the date of the Earth Jupiter conjunction, the active solar longitude $L = 190^{\circ}$ was again approximately in line with the conjunction. Although the spot group was born on the disk on 29 June, it grew in size rapidly afterwards to a maximum area of 1300 millionths, one of the larger spot groups thus far in cycle 20.

The 10.7 cm radio flux was elevated on the day of the Mercury-Jupiter conjunction, and increased very significantly at the time of the Earth-Jupiter conjunction on 5 July (Table20). Again, the increases on meter wavelengths were more impressive, but the generally high fluctuating radio emission during the peak of the 11-year cycle makes interpretation difficult. In terms of the Takabashi square of the vertical planetary tidal force, there was minimum during the middle of the year 1966 (Takahashi, 1968).

The proton events of 28 August and 2 September 1966 occurred in an active center located at $L^{*} = 185^{o}$ and latitude N20, very close to the projected position of the active center which caused the 7 July 1966 event. Detailed descriptions of the active center and events can be found in the literature (Dodscn and Hedeman, 1968). A conjunction took place between Mercury and Earth on 28 July (Fig. 2) causing an increase of X-ray and radio flux (Table 2). On 28 August there was a conjunction between Venus and Jupiter. The X-ray flux increased from 0.5 on 16 August to 19.2×10^{-4} ergs/cm^{2}-sec on 27 August in the 0-8Å band.

Table 20. Daily X-Ray and Radio Flux for May-July 1966. Units: 0-8Å: 10^{-4} ergs/cm^2-sec; 10 cm. radio: 10^{-22} watts/m^2-(c/s). The passage of the active center is shown, and the dates of significant conjunctions.

DATE 1966	MAY			JUNE			JULY		
		X-RAY	RADIO		X-RAY	RADIO		X-RAY	RADIO
1		1.33	89		1.6	102		2.4	92
2		1.30	93		1.15	101		1.4	92
3		1.63	93		1.15	100	CMP	1.3	92
4		1.98	91		1.13	99	#8362	1.2	101
5		1.63	88		0.94	99	E-J conj	2.0	102
6		1.12	87		1.2	98		1.3	106
7		1.34	87		0.92	94		1.4	110
8		0.24	86		0.96	96		7.3	111
9		1.48	86		1.00	96		14.0	104
10		1.27	85		0.90	93		14.0	105
11		0.92	87		0.85	94		5.1	106
12	E-Ma-N-L*	1.54	90		1.08	93		4.2	100
13	conj	1.33	91	Me-V-S	1.14	93		1.6	97
14		1.24	95	-U-P	1.4	93		1.7	97
15		1.71	97	conj	0.79	92		1.7	98
16		2.11	98		0.68	94		1.6	99
17		1.71	97		0.67	96		1.6	98
18		1.41	96		0.65	96		1.1	98
19		3.30	105		0.58	94		1.1	98
20		4.07	113		0.92	92		1.3	98
21		5.64	121		0.84	91		1.9	100
22		4.29	115		0.82	93		1.7	102
23		5.64	112		1.2	96		3.6	111
24	Me-Ma-N	7.38	114		1.3	100		6.5	116
25	L*conj	3.24	111		2.4	102		5.5	123
26		2.21	109		1.04	102		6.0	123
27		2.21	105	E Limb	1.17	98		3.1	120
28		1.72	105		1.4	98	Me-E	3.9	121
29		1.58	103		1.4	96	conj	3.7	128
30		1.07	99		1.9	97		2.7	123
31		1.48	102		-	-		2.8	121

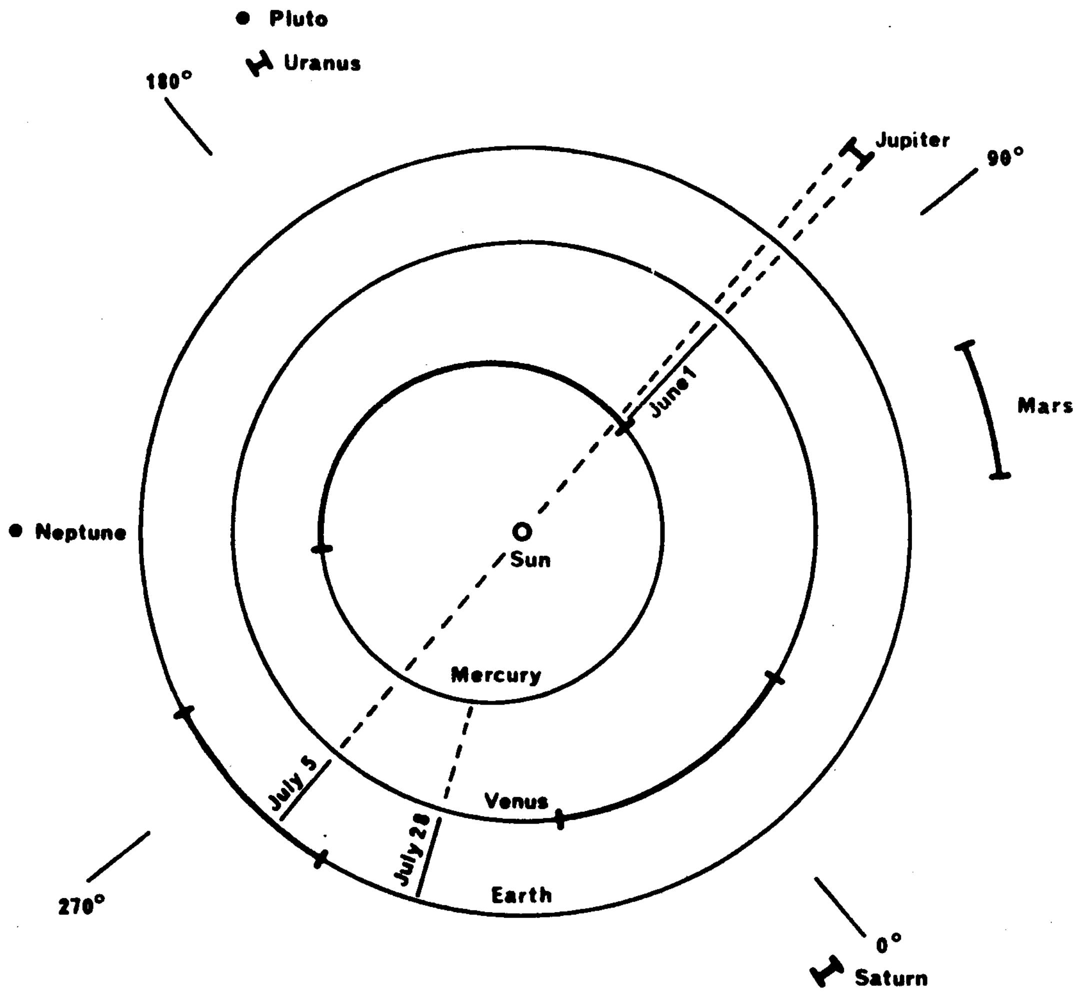

Fig. 14. Planetary configuration One Month Prior to Proton Event of 7 July 1966. (American Ephemeris, 1966)

Date	PLANETS	LONGITUDE
Apr 11	Mercury Venus	246°
May 13	Mercury (Saturn Uranus Pluto)	378°(168°)
May 28	Mercury (Earth Saturn)	70°(352°)
Jun 2	Mercury Jupiter	100°
Jun 15	Mercury Uranus Pluto (Venus)	168°(349°)
Jun 17	Venus Saturn	352°
Jul 3	Mercury Neptune	230°
Jul 5	Earth Jupiter	284°, 104°
Jul 12	Mercury Mars	256°, 77°
Jul 22	Mercury Jupiter	284°, 104°
Jul 24	Venus Neptune	51°, 231°
Jul 28	Mercury Earth	303°

III. PROTON EVENT OF 28 JANUARY 1967

The analysis of the 28 January 1967 event must be based largely on indirect evidence, because the ground level event (GLE) originated on the far side of the sun (60° beyond the West Limb), and from a new unimpressive plage and spot group. The same active longitude was responsible for the 24 March 1966 event, and there had been activity in neighboring centers for almost a year. (Sawyer, 1968). On 12.9 Feb a large plage at N 22° and L =124° crossed CMP, although the spot group was very small. This was a new plage formed from remnants of an old plage at N 26° and L 135, which crossed CMP on 16.0 January. Features observed included:

1. Hα Flares - inferred from GLE on 28 January from the far side of the sun (Lockwood 1968) (Dodson-Hedeman 1969) and observed on 6 and 13 February. The latter was a Class 4 flare, but without protons.

The following solar-terrestrial effects were noted:

1. Ground Level Increase of 16% on 28 January.
2. Forbush Decrease reached maximum on 9 February.

Interpretation. The active longitude was in alignment with the 27 November conjunction of Mercury and Jupiter, with the 24 December conjunction of Venus and Jupiter and the 18-20 January conjunction of Mercury, Earth and Jupiter. In each case there was an increase of radio and X-ray emission on the conjunction dates (Table 21)(Fig. 15). There was a rapid decrease in the vertical tidal function preceding the event (Takahashi, 1967).

Table 21. X-ray and Radio Flux Daily Means for December, 1966 and January, 1967. 0-8Å Units: 10^{-3} Ergs/cm^{2}- Sec; 10 cm. Units - 10^{-22} watts/m^{2} (c/s). The passage of the active center is shown, and the dates of significant planetary conjunctions (Quart Bull IAU) (Solar Geophys. Data).

Date 66-67	November			December			January		
	Conj.	X-RAY	RADIO	Conj.	X-RAY	RADIO	Conj.	X-RAY	RADIO
1		1.44	96		1.15	95			131
2		1.33	98		2.12	97			148
3		1.24	95		2.17	102			161
4		0.83	93		2.41	108			167
5		2.55	100		3.10	115			174
6		2.74	107		3.36	119			167
7		4.08	116		6.52	122			160
8		2.01	119		6.00	128			149
9		1.50	119		13.34	149			152
10		2.51	124		24.09	162			149
11		3.49	129		18.70	168			147
12		2.15	129		9.39	163			145
13		4.39	129		5.89	160			144
14		3.75	127		5.76	153		4.32	139
15		5.34	125		6.60*	148		4.15	131
16		4.09	124			140		8.07	125
17	Me-E conj	3.61	116			129		2.89	122
18		3.23	116			115		5.55	121
19		4.66	114			116		5.75	120
20		2.75	114			111		5.61	132
21		4.21	113			110	Me-E-J conj	8.54	143
22		12.53	119			109		6.08	146
23		2.16	118			114		10.72	153
24		3.59	117			114		5.51	152
25		2.29	114	V-J conj		115		5.16	147
26		2.49	110	V-J conj		115		7.46	160
27	Me-J conj	15.69	114			114		8.81	162
28		8.93	107			111		6.85	162
29		2.36	101			113		6.67	164
30		2.35	97			118		18.40	163
31		--	--			124		11.99	162

*No X-ray measurements from 16 Dec. thru 13 Jan. due to large aspect angle.

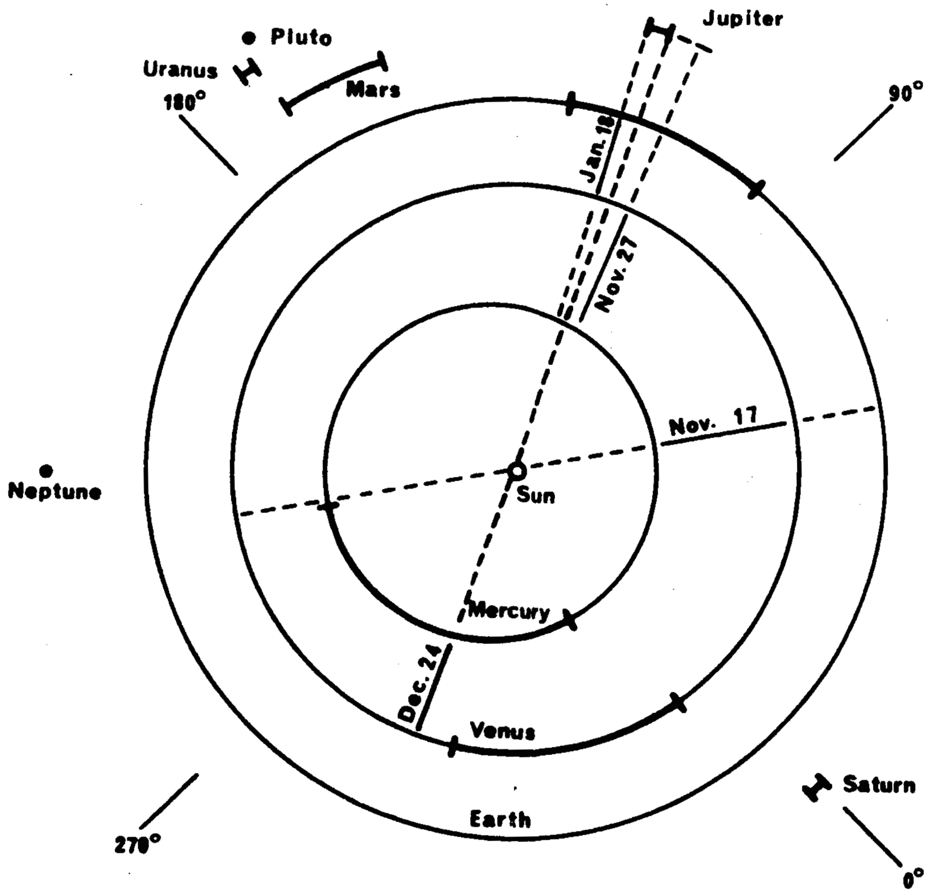

Fig. 15. Planetary Configuration One Month Prior to Proton Event of 28 January 1967. (American Ephemeris, 1969).

DATE	PLANETS			LONGITUDE
Nov 14	Venus	Neptune		233°
Nov 17	Mercury	Earth	(Venus)	58° (238°)
Nov 27	Mercury	Jupiter		115°
Dec 6	Mercury	Mars		161°
Dec 7	Mercury	Pluto		165°
Dec 8	Mercury	Uranus		170°
Dec 24	Venus	Jupiter		297°, 117°
Dec 25	Mercury	Neptune		233°
Jan 20	Mercury	(Earth	Jupiter)	299° (119°)
Jan 28	Venus	(Mars	Uranus)	350° (170°)

IV. PROTON EVENTS OF 30 MARCH, 10 APRIL 1969

The region that was active during February, March and April was first seen in January. At least two separate spot groups merged to form the massive sunspot stream. On the February passage the plage area increased to 10,000 millionths. On 20 February a small GLE (5%) took place near N13°, L = 72°. X-ray enhancements greater than 2 orders of magnitude in the 1-8Å band took place on four occasions during the February passage. On the March passage, X-ray activity was even greater and a GLE was recorded on 30 March. During April high energy proton events were observed by Satellite on 10 April (beyond East limb) and on 30 April (beyond West limb). On the March passage, the features observed on the sun were:

1. Giant Sunspot Stream between N14 and N22 extended over 70° of longitude. The plage reached the enormous size of 28,000 millionths on 21 March, but the accompanying sunspots were less impressive, reaching a maximum area of only 920 millionths on 22 March.

2. Sunspot Magnetic Fields of up to 3000 gauss were measured at various times during the March passage. The strongest fields were located at longitudes L = 100-106° and L = 56-66°.

3. Hα Flare. The proton flare occurred on 30 March when the region was at the West limb, so the exact location in the stream is difficult to pinpoint.

The events observed at the earth and by satellite are as follows:

1. Proton Flux was detected first by VLF paths and by the Pioneer and VELA Satellites and then by ground-based riometers and neutron monitors, on 30 March, 10 April and 30 April.

2. Ground Level Increase of 4.5% was detected on 30 March by the Deep River neutron monitor.

3. X-ray bursts were recorded by the SOLRAD Satellite, with increases of 2 orders of magnitude on at least six occasions during the March passage.

4. Radio Bursts on 2800 Mc/s were recorded on 12, 21, and 27 March of 1600, 1875 and 900 flux units, respectively.

5. Forbush Decrease took place on 24 March following a 2B flare on March 21. Particle enhancement had been observed by satellite.

6. Aurora were visible as far south as Texas on 23 March.

7. Sudden Enhancements of Atmospherics (SEA) occurred also on 22 March.

8. A Short Wave Fade took place on 23 March.

Interpretation. The X-ray and radio daily means were enhanced on 7 January (Table 22) at the time of the Mercury-Mars-Jupiter-Uranus conjunction, in approximate alignment with the solar longitude of the active center. (An earlier conjunction between Venus and Jupiter on 3 December 1968 may have also been significant.) Other conjunctions were not accompanied by X-ray and radio enhancements until the Earth-Jupiter-Uranus conjunction on 21 March, in line with $L = 84^{o}$ on the sun. Enhancements were noted also on 29 March, the date of the Venus-Jupiter-Uranus conjunction. In terms of Takahashi's vertical tidal force, there was a steep increase in late 1968.

Table 22. Daily Solar X-Ray and Radio Flux for January, February and March, 1969. (Quarterly Bull., IAU)(Solar Geophysical Data, ESSA). Units: X-Rays 0-8Å - 10^{-4} ergs/cm^2-Sec; 10 cm. radio-10^{-22} watts/m^2-(c/s). The passage of the active center is shown and the dates of significant conjunctions.

DATE 1969	JANUARY			FEBRUARY			MARCH		
		0-8Å*	RADIO		0-8Å*	RADIO		0-8Å*	RADIO
1		1.51	145		5.30	134		4.9	170
2		1.24	147		0.72	143		1.41	155
3		1.62	149		0.86	143		1.69	150
4		3.32	160		0.55	142		0.65	142
5		0.83	168		0.66	143		0.65	146
6		1.57	182		0.92	143		0.77	142
7	Me-Ma-J-	3.25	189		1.46	144		0.69	140
8	U conj	2.24	189		1.20	138		0.45	142
9		2.11	190	Me-J	1.18	137		1.22	144
10		0.97	175	conj	0.66	134		1.81	140
11		0.58	174		1.49	132		1.06	138
12		0.92	169		0.61	128		17.21	140
13		0.85	163		0.83	129		1.58	136
14		0.88	158		0.66	128		2.04	140
15		1.01	159		0.44	128		3.46	148
16		0.86	158		0.38	131		3.18	177
17		1.67	154		0.51	138		3.08	202
18		3.17	149		0.55	143		4.37	213
19		0.77	136		0.90	154		2.97	210
20	MeV	0.39	132		1.79	163		3.82	220
21	conj	0.89	136	CMP	0.70	173	E-J	39.52	236
22		0.54	138		1.46	189	conj	3.28	224
23		0.36	129	Me-J	3.52	206		11.56	214
24	CMP	2.69	135	conj	5.71	210		2.6	197
25		1.39	138	+ 14	3.66	211		2.46	182
26		0.83	147	days	9.95	193		10.24	204
27		0.58	136		17.89	201		17.68	183
28		0.67	134		5.90	184		3.82	178
29	Me-E	0.51	133		-	-	V-J	4.84	187
30	conj	0.52	130		-	-	conj	7.52	188
31		0.47	130		-	-		1.31	186

*Average of hourly values.

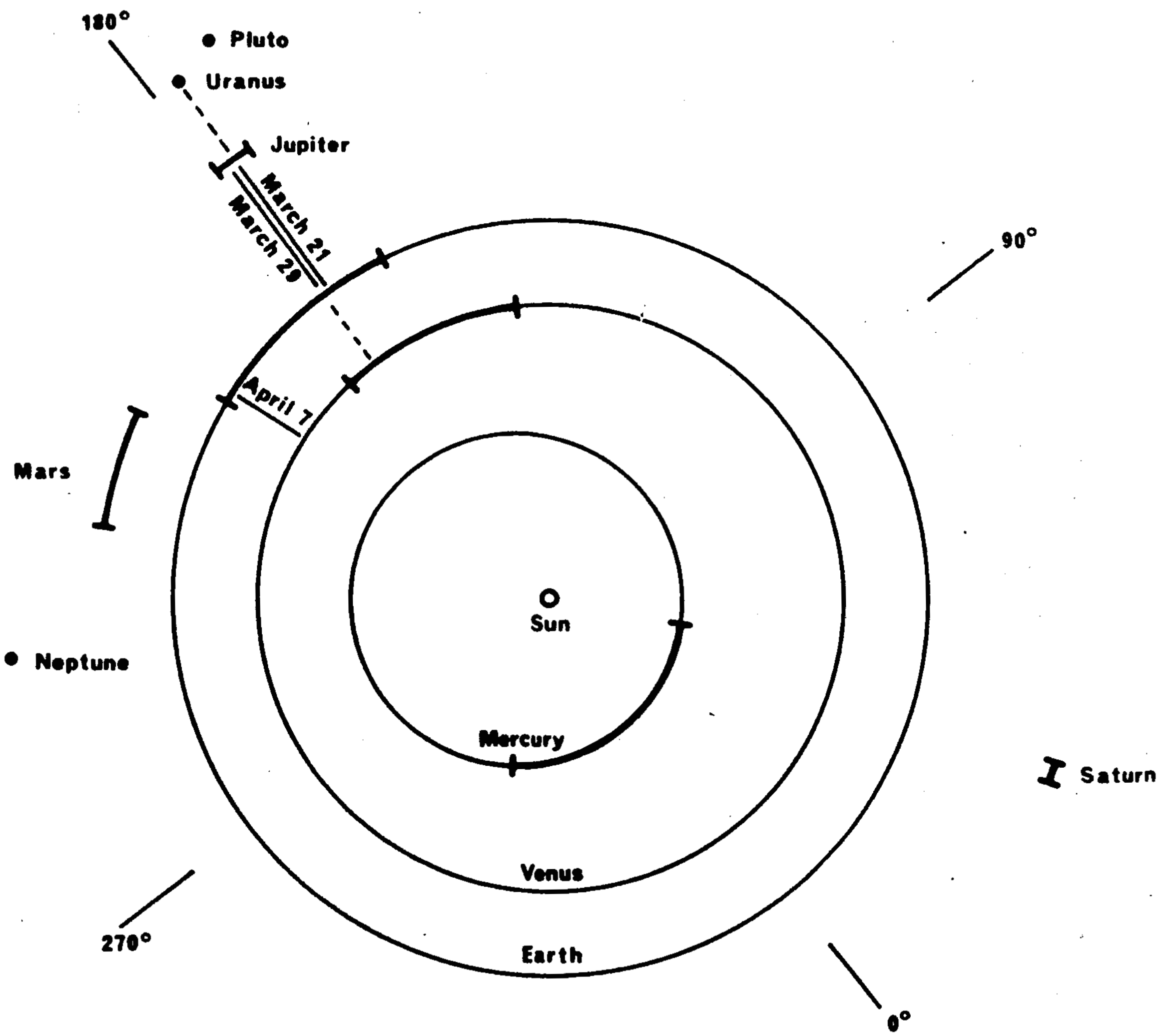

Fig. 16. Planetary Configuration One Month Prior to Proton Event of 10 April 1969 (American Ephemeris, 1969).

DATE	PLANETS				LONGITUDE
Jan 7	Mercury	(Mars	Jupiter	Uranus)	360°(180°)
Jan 20	Mercury	Venus			72°
Jan 29	Mercury	Earth			127°
Feb 9	Mercury	Jupiter	Uranus		180°
Feb 15	Mercury	Mars	(Saturn)		206°(26°)
Feb 26	Mercury	Neptune			235°
Mar 7	Mars	Saturn			207°, 27°
Mar 21	Earth	Jupiter	Uranus		181°
Mar 29	Venus	Jupiter	Uranus		182°
Apr 6	Mercury	(Jupiter	Uranus)		4°(182°)
Apr 8	Mercury	(Venus	Earth)		15°(195°)

V. LONG RANGE PREDICTION, CYCLE 20

A trial prediction method has been attempted over a period of four years, indicating the dates of the 14-day passage of solar active centers which could produce proton events. The forecasts were begun in June 1965, predicting solar activity 120 days in advance. During the first year of forecasting, the active longitudes had not been included, and the method underwent several other improvements. During the latest three years, twelve proton events (PE) have been successfully predicted by the method outlined (Table23). To check the validity of the prediction method, we define three ratios. The first, Sensitivity (S), is the ratio of the number of correctly predicted PE/total number of PE. The second, termed Reliability (R), is the ratio of correctly predicted PE/total number of prediction periods. The S and R ratios are commonly used for evaluating predictions, by ESSA personnel among others. The third, alert time (T), is the ratio of the time during which proton events were forecasted/total time. From the totals in Table 23, one can obtain the three ratios for the period from June 1, 1966, through May 31, 1969:

$$S = \frac{12}{19} = 63\% \qquad R = \frac{12}{17} = 70\% \qquad T = \frac{17\text{x}14 \text{ days}}{1096 \text{ days}} = 22\%$$

Both the Sensitivity (S) and Reliability (R) ratios are high, despite the fact that proton events were predicted only 22% of the total time. Many failures that did occur were due to the slowly changing active longitudes on the sun, or (2) events taking place on a different passage of the same active center or (3) from events on the far side

Table 23. Proton Events from June 1966 through May 1969 Compared to 120-Day Prediction. Ground Level Events are underlined. Parentheses show timing error of less than 4 days.

Year	Predicted 14 d. Periods Starting	Successes	Observed Events (ESSA)
1966	9 Jul	X	9 Jul
	27 Jul	X	28 Jul
	26 Aug	X X	28 Aug, 2 Sep
		X	5 Oct
	12 Nov		
1967	23 Jan	X	28 Jan
	24 Feb	X	11 Mar*
			25, 28 May
	10 Jun	(X)	6 Jun
	7 Aug		
	19 Aug		
	5 Nov	(X)	2 Nov
	13 Dec	X	3, 16 Dec
1968	15 Feb		
	14 Apr		
	22 May	(X)	9 Jun
			8 Jul
	23 Aug		
	22 Oct	X	31 Oct
1969			28 Feb
			30 Mar
	4 Apr	X	10 Apr
TOTAL	17	12	19

*Event on Far Side of Sun

of the sun , or (4) combinations of the other planets. Therefore improved Sensitivity and Reliability would result from further study of the longitude system on the sun and the time development of active centers, and from including all nine planets.

Ground level events (GLE) during cycles 18 through 20 are shown in Fig. 17, compared to Zurich smoothed sunspot numbers. Typically one or two GLEs occur early in the cycle 1.5 to 2 years before sunspot maximum, Rm. Two or three active centers produce GLEs late in the cycle, starting at least one year after Rm, and the majority of polar cap absorptions (PCA or PE) occur at this time.

Predictions for the remainder of the 20th cycle are shown with dotted lines in Fig 17. The predicted smoothed sunspot number is found from a regression formula (Euler 1969) and the GLE dates are estimated from sequences of planetary conjunctions (Blizard, 1969). In the latter case, the total no. of GLEs is also estimated from the overall activity of cycle 20 compared to earlier cycles. The Rm of cycle 20 is about equal to the Rm of cycle 17. On the other hand, the shape of cycle 20 more resembles cycle 18 because both have the same sunspot polarity.

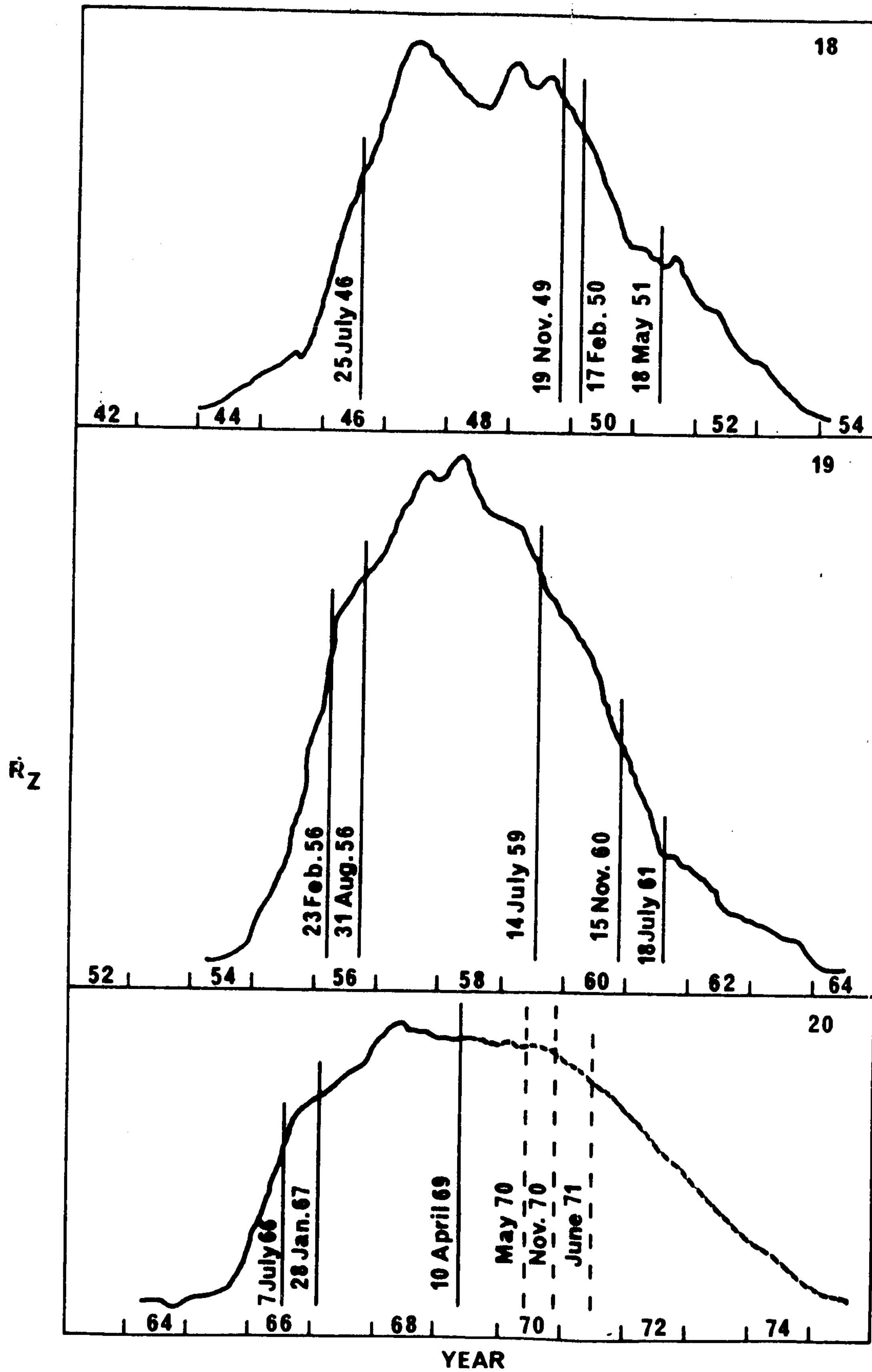

Figure 17. Major Proton Events of Cycles 18-20, by Phase of 11-year cycle. (Fichtel and McDonald, 1967) (Solar-Geophysical Data) (Blizard, 1968).

CONCLUSION

The overall activity of cycles 17 through 20 may be compared by various criteria for example:

1. Events of great magnitude (high energy or high flux proton events).
2. Ten-cm. Radio Flux.
3. Sunspot Number.
4. Sunspot Area

On the basis of (1) Events of Great Magnitude and (2) Radio Flux, and sunspot area cycles 18 and 19 are about equally active. On the basis of (3) Sunspot Number, cycle 19 was the most active ever recorded, and cycle 20 is about equal to cycle 17. During cycle 19, small and average sized spots were more frequent than in earlier cycles and lifetimes were shorter.

The major solar activity of cycle 20 (events thus far) resemble the two-peaked structure of even cycles, and the early and late appearance of GLE's, with an absence of high energy events at the midpoint of the cycle.

The antecedents of the 7 July 1966 event resemble those of the 23 February 1956 event. The first GLE's of three cycles (18, 19, 20) were located at the same active longitude $L_o = 190^o$.

Proton events are predicted for May-June 1970, November 1970 and May-June 1971, provided that solar longitudes active at the time are in alignment with some of the planetary conjunctions involved.

BIBLIOGRAPHY

American Ephemeris and Nautical Almanac, U. S. Naval Observatory (yearly).

Anderson, C. K., "Forecasting Solar Activity and Geophysical Responses," Weather Man. 4WWM 105-1, Dept. Air Force, Ent AFB, Colo. (Dec. 1966).

Anderson, K. A., and Lin, R. P., "Electrons Greater than 40 KEV and Protons Greater than 500 KEV of Solar Origin," Sol. Phys. 1, pp. 446-464 (1967).

Blizard, J. B., "A 200-Day Period in Solar Activity," Bull. A.P.S. 13, No. 2, p. 513 (March 1968).

Boardman, W. J., "A Solar Enhancement in the Extreme Ultraviolet," Astron. J. 73, No. 5 Pt. II, p. 556, June Supp. (1968).

Castelli, J. P., and Michael, G. A., "Flux Density Measurements of Radio Bursts of Proton Producing Flares and Non-Proton Flares," J. Geophys. Res. 72, No. 21, pp. 5491-5498 (Nov. 1967).

Cline, T. L., Holt, S. S., and Hones, E. W., "High-Energy X-Rays from the Solar Flare of July 7, 1966," J. Geophys. Res. 73, pp. 434-437, (Jan 1, 1968).

Dodson, H. W., Hedeman, E. R., Kahler, S. W., and Lin, R. P., "The Solar Particle Event of July 16-19, 1966 and its Possible Association with a Flare on the Invisible Solar Hemisphere," Sol. Physics 6, pp. 294-303 (Feb. 1969).

Dodson, H. W. and Hedeman, E. R., "Solar Circumstances at the Time of the Cosmic Ray Increase on Jan. 28, 1967," Bull. Am. Astron. Soc. 1, (in press).

Dodson, R. F., "The X-Ray and EUV Radiation of the August 28, 1966 Proton Flare as deduced from SID Data," Sol. Phys. 5, pp. 123-6 (1968).

Euler, H. C., "Solar Activity Indices," pp. 188-196, NASA TM-X-53782 (Oct. 1968). and "Solar Activity Prediction," (in press).

Fan, C. Y., et al., "Protons Associated with Centers of Solar Activity and Their Propagation in Interplanetary Magnetic Field Regions Corotating with the Sun," J. Geophys. Res. 73, No. 5 (Mar. 1968).

Fitchel, C. E., and McDonald, F. B., "Energetic Particles from the Sun," Ann. Rev. Astron. Astrophys. 5, p. 351 (1967).

Fortini, T., and Torelli, M., "On the Birth of Some Proton-Flare Regions," pp. 50 55, IAU Symposium #35, D. Reidel Publ. Co., Dorerecht, Holland, 1960.

Goedeke, A. D., Masley, A. J., and Adams, G. W., "Riometer Observations in the Polar Caps of Solar Cosmic Ray Events During the IQSY," Sol. Phys. 1, pp. 285-294 (1967).

Goldreich, P., and Peale, S. J., "The Dynamics of Planetary Rotations," Ann. Rev. Astron. Astrophys. 6, pp. 287-320 (1968).

Haurwitz, M., "Solar Longitude Distributions of Proton Flares, Meter Bursts, and Sunspots," Astrophys. J. 151, pp. 351-364 (Jan. 1968).

Jonah, F. C., "Analysis of Polar Cap Absorption Events IV - Almost Necessary and/or Sufficient Condition for Solar Proton Warning," LTV Astro. Div. Rept. 00.882 (Feb. 1967).

Kahler, S. W., Primbach, J. H., and Anderson, K. A., "Energertic Protons from the Solar Flare of March 24, 1966," Sol. Phys. 2, No. 2, pp. 179-191 (Sept. 1967).

Kopecky, M., Advances in Astronomy and Astrophysics, Vol. 5 (1967).

Krivsky, L., "The Relation Between Proton Flares and the Corona Over the 11 Year Cycle," Soviet Astron. AJ 10, No. 2, pp.304-307, (Sept.-Oct. 1966).

Kundu, M. R., "Centimeter Wave Radio and X-Ray Emission from the Sun," Spa. Sci. Rev. 2, pp. 438-469 (1963).

Lockwood, J. A., "Cosmic-Ray Solar Flare Effect of Jan. 28, 1967, as Recorded by Neutron Monitors," J. Geophys. Res. 73, No. 13 (Jul.1968).

McDonald, F. B., and Cline, T. L., "Relativistic Solar Electrons," Astron. J. 73, No. 5 Pt.II, p. S71 (June 1968).

Sawyer, C. G., "Sunspot Changes Following Proton Flares," pp. 547-552, IAU Symposium #35, D. Reidel Publ. Co., Dordrecht, Holland, 1968.

Sawyer, C., "Statistics of Solar Active Regions," Ann. Rev. Astron. and Astrophys. 6, pp. 115-134 (1968).

Solar-Geophysical Data, ESSA, Dept. of Commerce, Washington, D. C. (monthly); also Preliminary Reports (weekly).

Svetska, Z., "Proton Flare Project," pp. 513-535, IAU Symposium #35, D. Reidel Publ. Co., Dordrecht, Holland, 1968.

Takahashi, K., "On the Relation between the Solar Activity Cycle and the Solar Tidal Force Induced by the Planets," J. Radio Research Laboratories, 14, pp. 237-240 (Jul.-Sept. 1967).

Van Allen, J. A., "The Solar X-Ray Flare of July 7, 1966," J. Geophys. Res. 72, pp. 5903-5911 (Dec. 1, 1967).

Warwick, C., "Longitude Distribution of Proton Flares," Ap. J. 141, pp. 500-504 (1965).

8. PROTON FLARE CRITERIA

8. PROTON FLARE CRITERIA

Several topics of importance for forecasting of solar activity are discussed. First, the non-random distribution in Carrington longitude of sunspots, flares, meter bursts and proton events is surveyed. Short-range predictions depend also upon the solar rotation rate for flare activity, as distinguished from the rotation rate of other identifiable features.

Second, the probability of major flare activity depends upon the phase of the eleven-year cycle. Major flare related activity is not correlated with the smoothed sunspot number, but rather is related to the frequency of large sunspots (or sunspot area). Studies over eight cycles show that large, naked-eye sunspots have a two or three peaked distribution during the eleven-year cycle.

Finally, ultra-long-range forecasting is discussed. Detailed study of the long solar cycle (80-90 year) is necessary for forecasts of the length of cycle 20, and the features of cycles 21 and 22. Regression formulas may not be realistic unless the long cycle modulation is taken into account.

I. ACTIVE LONGITUDES

There is a tendency for sunspot activity to occur in certain longitude zones of the sun. The concentration is far greater for flare activity and even more striking for proton events (Warwick, 1965) and meter bursts (Haurwitz, 1968).

Early studies (Losh, 1938) (Vitinsky, 1960) made use of sunspot data from the Greenwich catalog and showed that:

1. Active longitudes are populated by long-lived large spot groups (Areas >500 millionths).
2. Activity reappears at fixed longitudes which are stable over several cycles (as distinguished from differential rotation) (Rubashev, 1964).

Another investigation has implied that longitudinal zones did not persist throughout cycle 19 (Trotter and Billings, 1962). One explanation for this contradictory result may be the latitudinal extent of the zones, which perhaps can best be visualized by Vitinsky's isoline method (examples in Rubashev, 1964 and Warwick, 1965). Early in the 11-year cycle spots are generally at high latitudes, and not all of the active longitudes are represented. At the beginning of cycles 18-20 high latitude ground level events originated from the northern longitude zone L=180 - 210° (events of 25 July 1946, 23 February 1956 and 7 July 1966). (On the other hand the active center of January 1926 was situated at N20° and L=35°). Furthermore, studies year by year during cycle 19 of sunspot area by longitude (Bezrukova, 1961), flares by longitude (Pratt, 1968) and proton events by longitude (re-plotted from Warwick, 1965) show that activity appeared successively at the northern active longitudes 180°, 320° and finally 80°.

Flare activity early in cycle 20, however, appeared at all three northern active longitudes during the first two years, 1965-1967. But non-GLE groups are included, and flare patrol coverage and other monitoring has greatly improved. The longitudinal distribution of large sunspots and proton events is shown in Tables 24-29.

A related topic is the solar rotation rate for flares and proton events. Although the sunspot rotation rate has been extensively studied, it was shown recently that sunspots of different classes may have different velocities even at the same latitude (Ward, 1966). Other identifiable solar features (plages, faculae, prominences) have a variety of rotation rates (Blizard and Epstein, 1965). Furthermore, different levels in the solar atmosphere have different solar rotation rates (Newkirk, 1967). Of greater importance for flare prediction are the rotation rates for flares and proton events (Warwick, 1965) (Wilcox and Schatten, 1967)(Haurwitz, 1968) (Van Hoven, Sturrock and Switzer, 1968). The importance of statistical methods for such studies cannot be overestimated.

Table 24. Active Longitudes, Cycles 12-20, Determined from Sunspot Data, Cycles 12-18 (Vitinsky, 1964) and from Proton Event Centers, Cycles 19-20 (Solar Geophysical Data, ESSA) (Cartes Synoptiques).

CYCLE	NORTHERN HEMISPHERE			SOUTHERN HEMISPHERE				
	L_1	L_2	L_3	L_1	L_2	L_3	L_4	L_5
12	240°	125°	40°		220°			25°
13	310	190	70	310°		150°		70
14	250	165	45	320		160		40
15	300	135	15	275	200		105°	0
16	290	130	50		220		100	
17	310	190	115	270	190			350
18	260	180	85		220			15
19*	330	190	50	330	230	165	90	50
20	332	153	69	338	265	141	86	53
Average	280°	159°	60°	302°	208°	155°	102°	34°

*1965-1967

Table 25. Solar Coordinates of Flare Centers, Early Cycle 20. (Solar Geophysical Data, ESSA) (P. McIntosh, private communication)

YEAR	CMP DATE	LAT.	LONG.	PCA DATES
1965	Feb 3	$+07^{\circ}$	160°	Feb 5
	May 20	+21	206	
	Oct 2	+18	215	
	Dec 24	+12	205	
1966	Jan 19	+22	225	
	Mar 21	+17	147	Mar 24
	Apr 3	+26	333	
	Jul 3	+33	210	Jul 7, 28
	Aug 28	+20	185	Aug 28, Sep 2, Oct 5
1967	Jan 16	+22	135	Jan 28
	May 24	+24	228	May 25, 28

Table 26. Solar Coordinates of Proton Event Centers, Northern Hemisphere, 1956-1961 (Cycle 19)

YEAR	DATE	LAT.N.	LONG.
1956	Feb 23	23	186
	Aug 31	14	96
1957	Jun 28	10	74
	Jun 30	10	76
	Jul 3	14	76
	Aug 31	25	335
	Sep 3	15	334
	Sep 12	10	191
	Sep 18	21	84
	Sep 21	9	59
	Sep 26	23	329
1958	Aug 22	18	352
1959	May 10	20	60
	Jul 10	21	327
	Jul 14	17	330
	Jul 16	16	331
1960	Mar 29	12	128
	Apr 1	12	128
	Apr 5	12	131
	Apr 29	14	133
	May 4	15	132
	May 13	30	350
	May 26	15	128
	Jun 1	30	342
	Jun 27	21	66
	Aug 11	22	141
	Aug 14	24	140
	Sep 3	20	146
	Oct 29	22	183
	Nov 10	22	31
	Nov 12	26	28
	Nov 15	26	22
	Nov 20	25	34
1961	Sep 28	14	85
	Nov 10	19	1

Table 27. Solar Coordinates of Proton Event Centers, Southern Hemisphere, 1956-1961 (Cycle 19)

YEAR	DATE	LAT. S.	LONG.
1957	Jul 28	24	141
	Aug 28	30	338
	Oct 20	26	66
1958	Jan 25	23	265
	Mar 23	15	85
	Aug 16	14	86
1960	May 6	9	5
1961	Jul 11	6	49
	Jul 12	7	49
	Jul 15	7	51
	Jul 18	7	51
	Jul 20	7	52

Table 28. Solar Coordinates of Ground Level Event Centers, 1942-1961.

YEAR	DATE	LAT.	LONG
1942	Feb 28	+7	201
1946	Jul 25	+22	197
1949	Nov 19	-2	165
1956	Feb 23	+23	186
	Aug 31	+14	96
1959	Jul 14	+17	330
	Jul 16	+16	331
1960	May 4	+15	132
	Nov 12	+26	28
	Nov 15	+26	22
	Nov 20	+25	34
1961	Jul 18	-7	51
	Jul 20	-7	52

Table 29. Recurrent Large Sunspots, Cycles 16-18 from List of 55 Largest Sunspots, 1874-1954. (Greenwich, 1955).

CYCLE	YEAR	CMP DATE	INTERV. FROM Rm	MAX. AREA	UMBRA RATIO	LONG.	LAT
16	1926	Jan 24.5	-2.3	3716	.159	35.0	+20.0
		Sep 19.7	-1.7	2142	.172	129.4	+24.1
	1929	Nov 3.7	+1.2	2003	.166	189.3	+14.8
17	1935	Dec 2.2	-1.5	2435	.172	55.2	-25.5
	1937	Jan 31.1	-0.3	2364	.146	196.3	-10.1
		Apr 24.7	-0.1	2474	.174	173.9	+19.5
		Jul 28.8	+0.2	3303	.159	356.1	+31.5
		Oct 4.4	+0.4	3340	.146	182.3	+ 9.3
	1938	Jan 18.4	+0.6	3627	.176	225.1	+17.1
		Jul 15.1	+1.1	3379	.147	39.8	-12.1
		Oct 11.9	+1.4	3003	.133	305.8	+17.0
		Nov 10.8	+1.5	2245	.174	272.0	- 8.5
	1939	Sep 10.4	+2.3	3034	.164	224.1	-13.8
	1940	Jan 5.5	+2.6	2860	.207	120.2	+10.5
	1941	Sep 16.9	+4.3	3038	.148	210.0	+11.6
	1942	Feb 28.8	+4.8	2048	.191	197.1	+ 7.0
18	1946	Feb 5.7	-1.4	5202	.183	297.2	+26.1
		Jul 26.9	-0.9	4720	.111	195.8	+22.2
		Dec 17.0	-0.5	2099	.138	107.2	- 6.4
	1947	Apr 7.2	-0.2	6132	.133	83.1	-24.4
	1948	Dec 24.0	+1.5	2513	.149	87.0	-14.4
	1949	Jan 22.9	+1.6	2471	.146	53.7	+22.9
	1950	Feb 20.1	+2.6	2856	.151	264.2	+10.1
		Apr* 13.6	+2.8	2000	.140	293.1	+13.4
	1951	May 16.0	+3.9	4865	.158	86.4	+13.0

*Not recurrent

II MAJOR ACTIVITY BY PHASE OF ELEVEN-YEAR CYCLE

Many characteristics of major solar activity occur in two cyclic processes during the 11-year cycle (Gleissberg, 1968; Anatalova and Gnevishev 1968). The shape of the curve of sunspot number depends upon how the two processes overlap. Even cycles characteristically show a two-peaked structure even for smoothed sunspot numbers. Some fine structure is due to different time development of activity on the northern and southern hemispheres. The northern hemisphere has dominated during the last few cycles (Tables 24 – 29). The two-peaked structure of the sunspot cycle could be related to the reversal of the poloidal field of the sun (Leighton, 1969).

Major activity shows the double-peaked time development more strongly than sunspot numbers, and displays it in every cycle (Figures 18 & 19). Therefore it is highly significant for prediction of flares and proton events. The first peak occurs one to one and a half years before the peak sunspot number (Rm), and the second peak occurs about 2 years after Rm, often followed by a minor peak 3 to 4 years after Rm.

Most characteristics of major solar activity follow the same three-peaked cycle including: areas of giant sunspots, frequency of giant sunspots, frequency of large flares, green coronal line intensity, occurrence of geomagnetic crochets and sudden commencement storms, Ap index, and E and F_2 layer ionospheric indices, and that where known, these indices show a similar 3-peaked pattern for solar cycles 12-19 (Figs. 18 & 19).

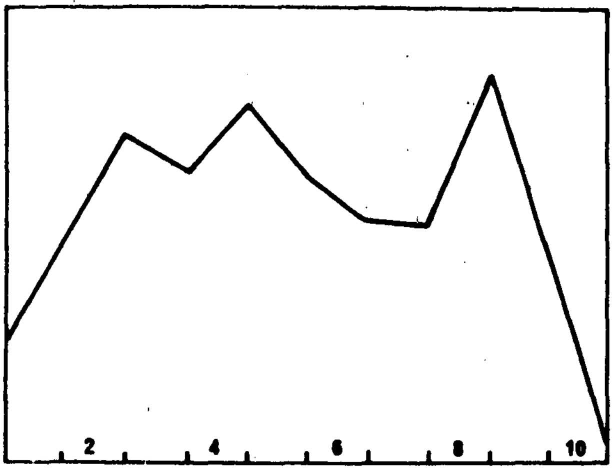

a. Areas of Sunspots over 1500 Millionths During 7 Cycles (Greenwich, 1954).

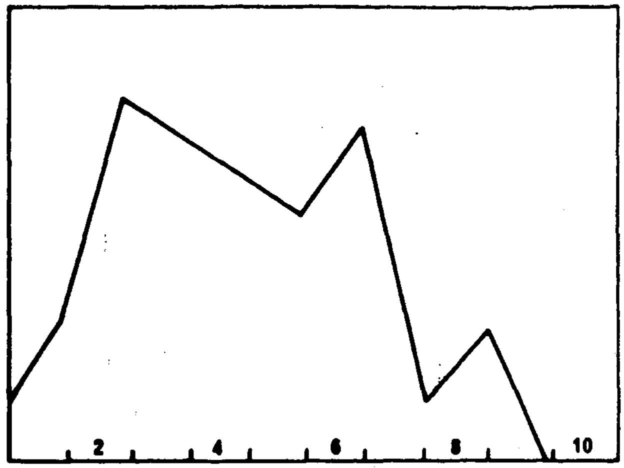

b. Frequency of Sunspots with Area Greater Than 1500 Millionths (Newton, 1958).

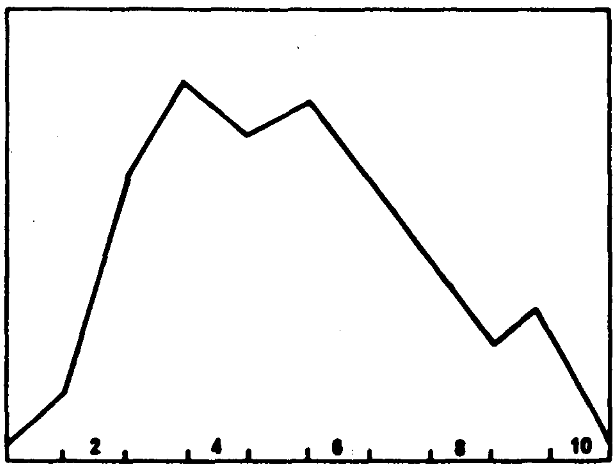

c. F_2 Layer Ionospheric Index (Minnis and Bazzard, 1958; see Rubashev 1964).

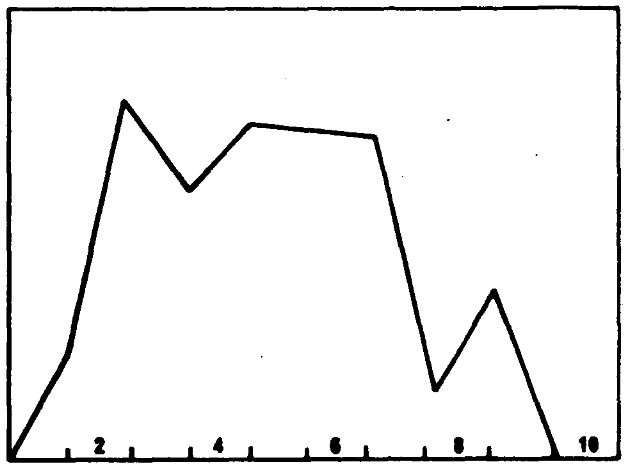

d. Frequency of Large Flares (Kleczek, 1952).

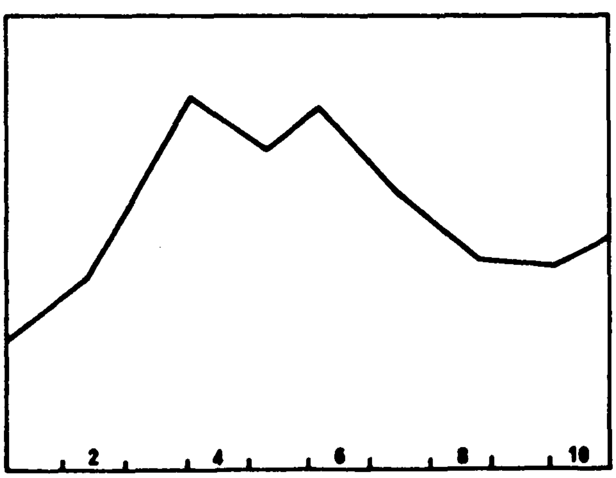

e. E Layer Ionospheric Index (Minnis and Bazzard, 1959; see Rubashev, 1964).

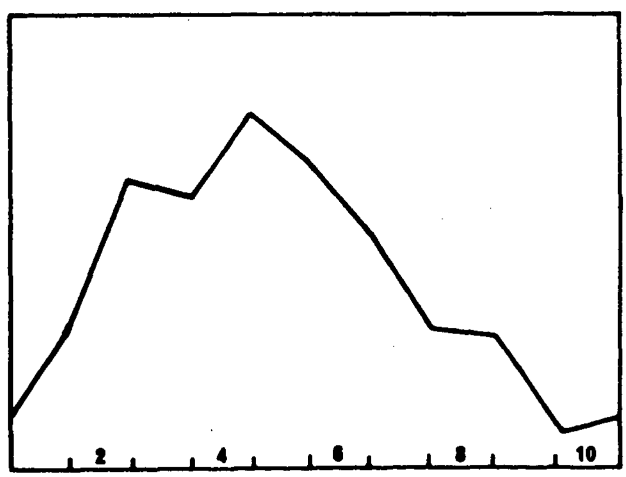

f. Distribution of Sudden Commencement Geomagnetic Storms (Newton, 1958).

Figure 18. Distribution of Major Solar Geophysical Activity by Phase of the Eleven Year Cycle.

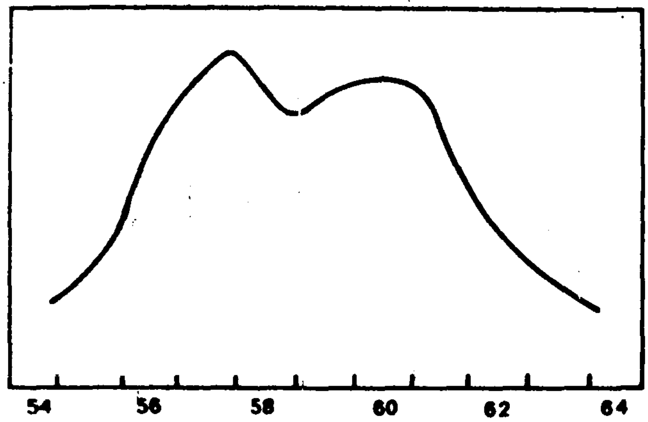

a. Intensity of 5303Å green coronal line averaged around the limb (Gnevishev,1968).

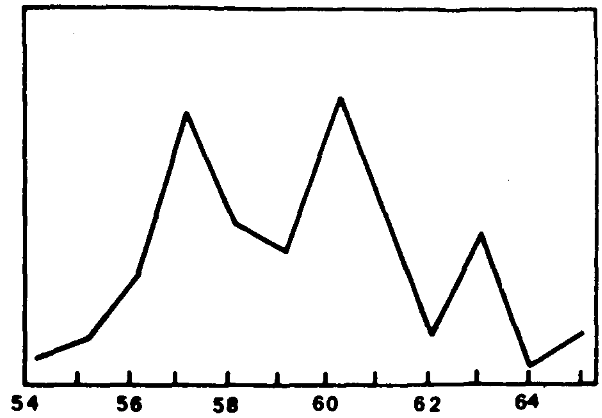

b. Number of Polar Cap Absorptions, 1954-1964 (Hakura, 1967).

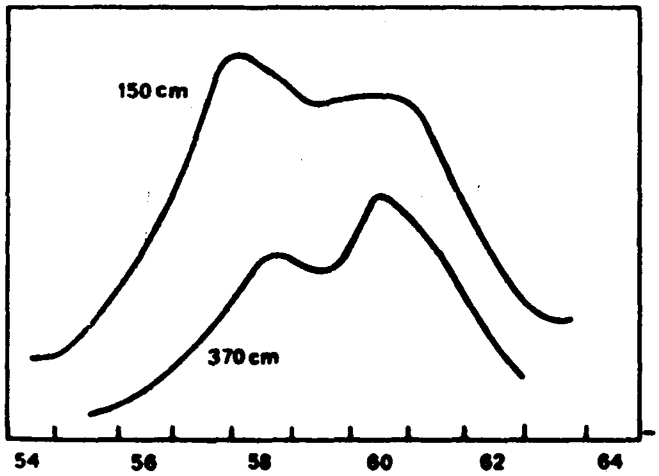

c. Meter Wavelength Solar Radio Flux, 1954-1963 (Genvishev, 1967).

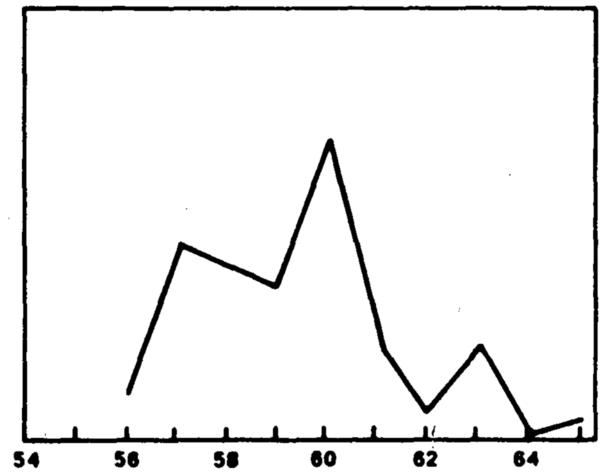

d. Number of Radio Type IV Bursts, 1955-1964 (Hakura, 1967).

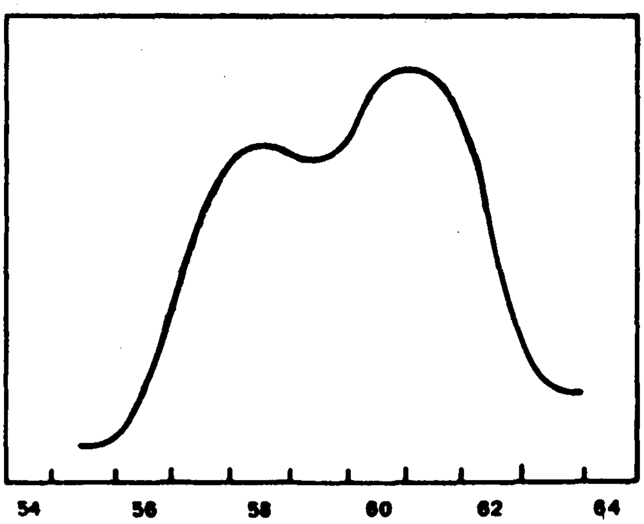

e. Geomagnetic A_p Index 1953-1963. (Anatalova and Gnevishev, 1968).

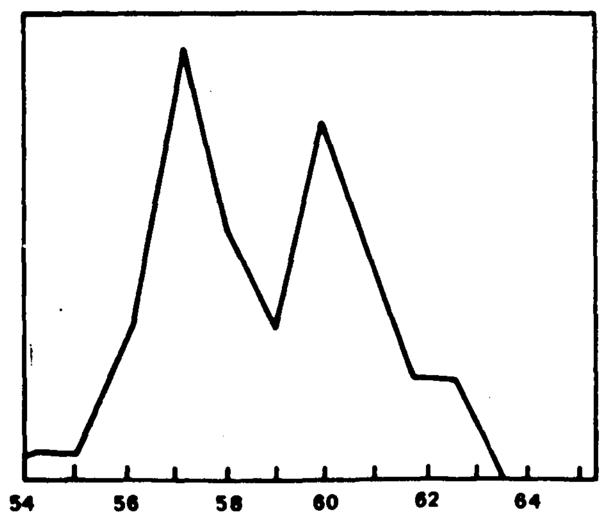

f. Number of Geomagnetic Crochets, 1954-1964 (Pinter, BAC, 1967).

Figure 19. Characteristics of Major Solar-Geophysical Activity During the 19th Cycle, by Phase of 11-Year Cycle.

III ULTRA LONG RANGE FORECASTING

Missions such as the Apollo Telescope Mount, the Manned Orbital Workshop, Lunar Bases and Planetary Missions require predictions of solar activity several years or decades in advance. Such ultra long range forecasting can be based on the rate of occurrence of proton events during the 11 year cycle, coupled with the long term modulation of solar activity, referred to as the 80-90 year cycle. Even though the sunspot number is not a good indicator of individual events, sunspot number may be a satisfactory index of the yearly integrated intensity of solar particles above 20 MeV (Fichtel and McDonald, 1967). A satisfactory correlation between these quantities can be shown for the years 1955 through 1965. Thus estimates of the expected yearly intensities of solar proton can be made from projections of yearly sunspot numbers. Therefore predictions of cycles 20, 21 and 22 are presented in Figure 20 and Table 30. based on several lines of evidence.

There are several important parameters of solar activity which depend upon the long cycle:

1. Maximum sunspot number
2. Length of cycle (7-17 years)
3. Spot lifetime (Kopecky, 1967)
4. Number of large spots (Kopecky, 1967) (Eygenson 1946, 1948)
5. North-South asymmetry of sunspots
6. Magnitude of sunspot magnetic fields (Xanthakis, 1967)

The maximum and minimum of the long cycle have been estimated by secular smoothing, moving averages and other methods (Rubashev, 1964) (Gleissberg, 1969) (Vitinsky, 1968). The latter two authors find the most recent smoothed maximum in 1938-1940. Extrapolation would place the next long cycle minimum in the 1980's.

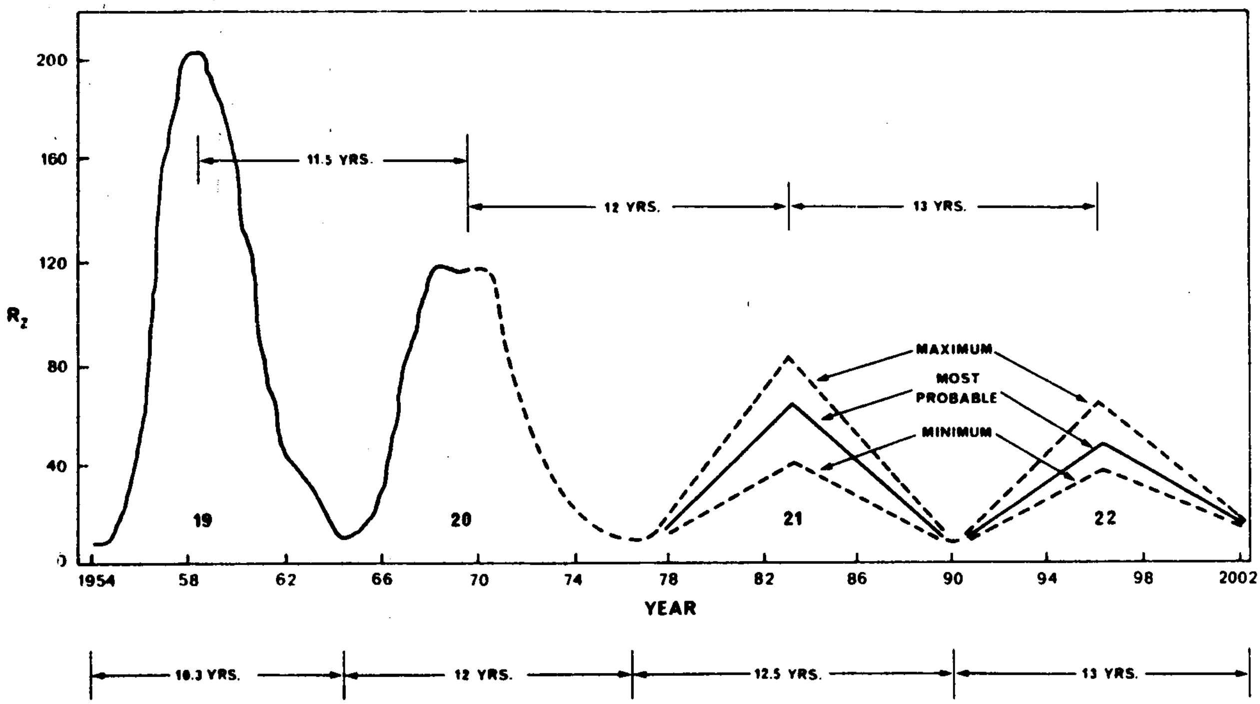

Figure 20. Forecasts of Cycles 20, 21 and 22, Based on Planet Positions, (Jose, 1965) (Wood, 1968); the Long Solar Cycle (Bezrukova, 1962), (Bonov, 1968) and 2000 Years of Sunspot and Auroral Data, (Schove, 1955). (Composite: see Table

Table 30. Ultra Long Range Forecasts of Cycles 20, 21 and 22. R_m=smoothed maximum sunspot number. T_{max}, T_{min}: dates of maximum, minimum.

	CYCLE 20			CYCLE 21			CYCLE 22	
	T_{max}	R_m	T_{min}	T_{max}	R_m	T_{min}	T_{max}	R_m
Bezrukova, 1962	1969-70	-	-	1982	120	-	1994	80
Bonov, 1968	1968.4	128	1976.5	1984.1	52	1990.6	1996.6	47
Jose, 1965	1967	120	1977	1984	60	1990	1995	60
Schove, 1955	1972.5	100	1978.5	1984.5	140	1989.5	1994.5	120
Wood, 1968	1969	120	1976	1983±1	60	1989	1995.5	40

CONCLUSIONS

Active longitudes are populated by large long-lived sunspots of mean area >500 millionths, a group which includes nearly all active centers. The active longitudes are stable over periods longer than a solar 11-year cycle, although activity appears at one longitude or another at different times within a cycle, perhaps due to the latitude drift of sunspots.

Major proton events occur in two major peaks one year before and two years after the peak sunspot number R_m followed by a smaller peak occurring 3-4 years after R_m. Most characteristics of major solar activity follow the same three-peaked cycle including: areas of giant sunspots, frequency of giant sunspots, frequency of large flares, occurrence of geomagnetic crochets, green coronal line intensity, A_p index, SSC storms and E and F_2 layer ionospheric indices. Where known, these indices show a similar 3-peaked pattern for solar cycles 12-19.

Ultra long range forecasting can be based on the long term modulation of solar activity. Even though sunspot number is not a good indicator of individual events, it may be a satisfactory index of the yearly integrated intensity of high energy solar particles. Predictions of the lengths and amplitudes of cycles 20, 21 and 22 are presented based on several independent lines of evidence. Parameters which depend on the long cycle include: peak sunspot number, length of cycle, spot lifetime, number of large spots, north-south asymmetry of sunspots, and magnitude of sunspot magnetic fields.

BIBLIOGRAPHY

Antalova, A. and M. N. Gnevishev, "Principal Characteristics of the 11-Year Solar Activity Cycle," Soviet Astronomy-AJ 9, No. 2, pp. 198-201 (Sept.-Oct. 1968).

Anderson, C. N., "Notes on the Sunspot Cycle," J. Geophys. Res. 59, No. 4, pp. 455-461 (Dec. 1964).

Anderson, K. A., "Preliminary Study of Prediction Aspects of Solar Cosmic Ray Events," NASA TN D-700, Washington (April 1961).

Bezrukova, A. Y., "On the Epoch of the Maxima of the 11-Year Cycles 20, 21 and 22," Soln. Dannye pp. 69-74 (August 1962).

Bezrukova, A. Y., "Longitudinal Distribution of Areas of Sunspot Groups in the 19th Cycle of Solar Activity," Soln. Dannye pp.58-60 (Feb. 1961).

Blizard, J. B., "Solar Activity and Planetary Configurations," Bull. Am. Astron. Soc. 1, No. 3 (1969).

Blizard, J. B. and B. C. Epstein, "The Persistence and Rotation Rate of Flare Centers," Denver Research Institute Report, 12 pp. (December 1965).

Bonov, A. D., "Prognosis of the 11-Year Cycles No. 20, 21 and 22 of the Solar Activity," Soln. Dannye pp. 68-73 (Oct. 1968).

Bumba, V. and V. N. Obridko, "Bartels' Active Longitudes, Sector Boundaries and Flare Activity," Sol. Phys. 6, No. 1, pp. 104-110 (Jan. 1969).

Dewey, E. R., "A Key to the Sunspot Planetary Relationship," Cycles, pp. 233-238 (Oct. 1968).

Dodson, H. W., Hedeman, E. R. and Stewart, F. L., "Solar Activity During the First 14 Months of the IQSY," Science 148, p. 1328 (1965).

Eckert, W. J., Brouwer, D., and Clemence, G. M., "Coordinates of the Five Outer Planets, 1653-2060," Astro. Papers Am. Ephemeres and Nautical Alm. XII, Washington, D. C. (1951).

Gleissberg, W., "The Duration of the Zonal Spot Activity," Sol. Phys. 4, No. 1, pp. 93-95 (May 1968).

Gnevishev, M. N., and A. I. Ohl, "On the Manifestation of the 11-Year Cycle of Solar Activity in the Brightness of the Nightglow," Planet. Spa. Sci. 16, pp. 1311-1312 (1968).

Goldberg, L., "Ultraviolet and X-Rays from the Sun," Ann. Rev. Astron. Astrophys. 5, 279-324 (1967).

Gopasyuk, S. E., Ogir, M. B., and Tsap, T. T., "The Relationship Between Photospheric and Chromospheric Processes in the Active Region during Flares," NASA TT F-251, Washington, D.C. (Sept. 1965).

Hachenberg, O., "RF Emission of the Sun: The Slowly Varying Component," in Solar System Radio Astronomy, ed. by J. Aarons, Plenum Press, NY, (1965).

Hakura, Y., "Polar Cap Absorptions and Associated Solar-Terrestrial Events Throughout the 19th Solar Cycle," NASA TMX-55812, Goddard (June 1967).

Haurwitz, M. W., "Solar Longitude Distributions of Proton Flares, Meter Bursts and Sunspots," Astrophys. J. 151, pp. 351-364 (Jan. 1968).

Kimura, H., "On the Harmonic Analysis of Sunspot Relative Numbers," Monthly Notices R.A.S. 73, pp.543-552 (1913).

Kopecky, M., "The Periodicity of the Sunspot Groups," Adv. in Astron. and Astrophys. 5, pp. 189-266 (1967).

Leighton, R. B., "A Magneto-Kinematic Model of the Solar Cycle," Astrophys. J. 156, pp. 1-26 (April 1969).

Link, F., "Manifestations de L'Activite Solair dans le Passe Historique," Planet. Spa. Sci. 12, pp. 333-48 (1964).

Link, F., "Auroral and Climatic Cycles in the Past," J. B. A. A. 78, No. 3, pp. 195-205 (April, 1968).

Losh, H. M., "Distribution of Sunspots in Longitude," Publ. Obser. Univ. of Mich 7, No. 5, pp. 127-145 (Sept. 1938).

Newkirk, G., "Structure of the Solar Corona," Ann. Rev. Astron. and Astrophys. 5, pp. 213-266 (1967).

Newton, H. W., "The Face of the Sun," Penguin Books, Inc., Baltimore, MD. (1958).

Pratt, T. E., "Longitudinal Persistence of Major Solar Flares," NASA TM-X-53782 (Oct. 15, 1968).

Rubashev, B. M., "Problems of Solar Activity," NASA TT F-244 (Dec. 1964).

Shove, D. J., "The Sunspot Cycle 649 B.C. to A.D. 2000," J. Geophys. Res. 60, pp. 127-146 (1955).

Van Hoven, G., P. A. Sturrock, and P. Switzer, "A Statistical Analysis of Flare Events and Its Implications Concerning the Sun's Internal Rotation," Report No. SUIPR 267, Institute for Plasma Research, Stanford University, California (Nov. 1968).

Vitinsky, Y. I., "On the Epochs of Extrema of the 80-90 Year Cycles of Solar Activity," Soln. Dannye pp. 90-95 (Feb. 1968).

Vitinsky, Y. I., "On the Problem of Active Longitudes of Sunspots and Flares," Sol. Phys. 7 pp. 210-216 (1969).

Vitinsky, Y. I., "Solar Activity Forecasting," NASA TT F 289 (1965).

Waldemeier, M., "The Sunspot Activity in the Years 1610-1960," Zurich Schulthess, 1961.

Ward, F., "Determination of the Solar Rotation Rate from the Motion of Identifiable Features," Astrophys. J. 145, p. 416 (1966).

Warwick, C. S., "Longitude Distribution of Proton Flares," Astrophys. J. 141, pp. 500-504 (Feb. 15, 1965).

Wilcox, J. M. and K. H. Schatten, "Longitude Distribution of Proton Flares as a Function of Recurrence Period," Astrophys. J. 147, pp. 364-367 (1967).

Xanthakis, J., "The Different Indices of Solar Activity and the Time of Rise," from Solar Physics, ed. by J. Xanthakis Interscience Publ., N.Y. 1957; pp. 157-228.

9. LONG RANGE PREDICTIONS OF THE SOLAR CYCLE

K. D. WOOD, Ph.D.

9. LONG RANGE PREDICTION OF THE SOLAR CYCLE

by K. D. Wood, Ph. D.

Recent studies by Bigg indicate conclusively that Mercury, Venus, earth and Jupiter have detectable small effects on short-term solar activity (less than one "11-year" cycle). The present study assumes that planet effects on the sun may also be useful in explaining the long-term history of solar activity and in making long-term forecasts. Some possible physical mechanisms for the effects are suggested.

This report is concerned chiefly with forecasting times of high mean annual Zurich sunspot numbers (R_z) rather than locating exactly the peak of a sunspot curve; some such curves have rather flat tops. Years in which the mean annual R_z is within 10% of the peak are listed in Table 31.

The cycles peaks have been numbered by Waldmeier starting with Cycle No. 1 in 1761. To include less accurately known data back to 1700, cycle numbers 0, -1, -2, -3, and -4 have been assigned for use in this report.

A study of sunspot cycle lengths based on mean annual sunspot data, if they are caused by planet effects, can involve at the most only the six outer planets (Mars, Jupiter, Saturn, Uranus, Neptune, and Pluto) because the inner planets (earth, Venus, Mercury) have orbital periods of one year or less. For the physical effects here considered, Mars, and usually Pluto, may be shown to have very minor effects, negligible with good accuracy. Hence, the sunspot cycle analysis and forecasting problem, as treated here, involves only four planets: Jupiter, Saturn, Uranus and Neptune. These four planets may have several simultaneous effects. The analysis is clarified by considering the planets two at a time. Hence, the table of synodic periods of all planets, considered two at a time (Table32) is considered useful for comparison of sunspot cycles and planet effects. Note in Table 32 that synodic periods are not constants to four or even three significant figures, because of the eccentricity of the planet orbits and the misalignment of their perihelia. For example, five recent (since 1850) synodic dates of Jupiter and Saturn were 1862.00, 1881.27, 1901.75, 1921.67 and 1940.88, giving synodic periods of 19.27, 20.48, 19.92, and 19.11, or a mean of 19.8 (as calculated from mean circular orbits) ± 0.7 as noted in the table. Since four or more planets are involved in most planet effects, times when three or four planets are nearly in line may also be of significance. One such time is the Jupiter-Uranus-Neptune near-triple-conjunction about 1830 (a time when the Jupiter-Saturn cycle was NOT related to the sunspot cycle). This near-triple conjunction will occur again about 1989. Jupiter-Saturn-Uranus near-conjunctions occurred around 1763, 1800, 1900, and 1940 and will not occur again till after 2000. The only recent (since 1750) Jupiter-Saturn-Neptune near-triple-conjunction was about 1880 and this was also the time of a long and weak (low R_z) sunspot cycle, differing from the ten year Jupiter-Saturn cycle.

Possible physical reasons for these striking "coincidences" are considered in Part II of this report, and their use in long-range predictions is considered in Part III.

II. PHYSICAL EFFECTS OF THE PLANETS ON THE SUN

For the purposes of this study, dealing with only a few hundred years, the solar system center of mass may be considered to have zero acceleration, or constant velocity.

Because of the planets, the center of mass of the sun travels in a series of spiral paths within a region of about two solar radii from the center of mass of the solar system, as sketched in Figure 21. With excellent accuracy the spiral paths may be calculated from the known masses, orbit radii, and periods of the planets Jupiter, Saturn, Uranus, and Neptune.

The apparent complexity of the spiral path is greatly reduced by calculating and plotting separately the Jupiter-Saturn effect, and the Uranus-Neptune effect as sketched in Figure 22.

If the solar system center of mass is used as a location of x, y, and z axes fixed in inertial space, the vector $\vec{R}_{\odot z}$ from the origin of these axes to the center of mass of the sun is seen in Figure 21 to be nearly zero in 1951, but the displacement from one year to another (e.g., $\vec{R}_{\odot z_{1951}} - \vec{R}_{\odot z_{1950}}$) is never zero. The sun center is always moving, and most of its velocity is due to Jupiter, with a major perturbation by Saturn (minor perturbations by Uranus and Neptune). The magnitude of the sun center velocity vector $\vec{V}_{\odot z}$ since 1900 is seen in Figure 3 to be nearly a sine wave of period equal to the Jupiter-Saturn synodic period of about 20 years; this graph is very similar to the graph of sunspot number R_z vs time for some periods (e.g., since 1900) when the sunspot cycle averages about 10 years (for other periods of time it is not, presumably because of the effects of Uranus and Neptune, as described later). Figure 23shows also the separate effects of these four planets on the speed of the sun center.

The sun center has a velocity $\vec{V}_{\odot z}$ relative to fixed axes, but it also has a velocity relative to axes rotating with the displacement vector $\vec{R}_{\odot z}$, designated x', y', and z'. The sun thus behaves like a rotating body on a rotating platform, located at a variable distance $R_{\odot z}$ from the center of the rotating platform, and moving with velocity $\vec{V}_{rt}$ relative to the platform's rotating axes. Let $\vec{\omega}_{\odot z}$ be the angular velocity of rotating axes (the angular velocity of the vector $\vec{R}_{\odot z}$). The velocity and acceleration of points on the sun's surface change as the sun rotates, depending on the planet-determined velocities and postions of the sun.

This is explained in principle in many text books on dynamics; the notation and equations used here are from Berman, pages 91-94. The velocity observed by a rotating observer $\vec{V}_{rt}$ is related to the velocity seen by a fixed observer $\vec{V}_{fx}$ (which is the velocity plotted in Figure 23) by the equation

$$\vec{V}_{fx} = \vec{V}_{rt} + \vec{\omega}_{\odot z} \times \vec{R}_{\odot z} \qquad (1)$$

The acceleration viewed by a fixed observer $\vec{A}_{fx}$ is related to the acceleration $\vec{A}_{rt}$ viewed by a rotating observer by the equation

$$\vec{A}_{fx} = \vec{A}_{rt} + \vec{\omega}_{\odot z} \times \vec{\omega}_{\odot z} \times \vec{R}_{\odot z} + 2\vec{\omega}_{\odot z} \times \vec{V}_{rt} \qquad (2)$$

where $-\vec{\omega}_{\odot z} \times \vec{\omega}_{\odot z} \times \vec{R}_{\odot z}$ is the centrifugal acceleration, and

$-2\vec{\omega}_{\odot z} \times \vec{V}_{rt}$ is called the Coriolis acceleration.

Relative velocities and Coriolis accelerations for the sun center and for two points on the sun's surface are shown in Figure 24.

Considering one planet only, say Jupiter, the sun moves in a near circular elliptic orbit at a mean radius of 1.06 solar radii ($\pm$ 4.8% due to Jupiter's orbit eccentricity) with a velocity of $2\pi \times 1.06$ solar radii in 11.86 years and $|\vec{\omega}_{\odot z}| = 2\pi/11.86$ radians per year on the average, with the same variation due to eccentricity. Essentially, the only acceleration of the sun center, considering Jupiter to act alone, would be the centripetal acceleration $\vec{\omega}_{\odot z} \times \vec{\omega}_{\odot z} \times \vec{R}_{\odot z}$ (in the direction of Jupiter). Points on the surface of the sun, because of its rotation, have two components of velocity relative to axes x', y', and z' which rotate with $\vec{R}_{\odot z}$, one due to rotation of the sun about its own axis and one due to the difference between the velocity $\vec{V}_{\odot z}$ and the velocity $\vec{\omega}_{\odot z} \times \vec{R}_{\odot z}$ due to rotation of the radius vector $\vec{R}_{\odot z}$ at a rate of $\vec{\omega}_{\odot z}$. The second velocity is much smaller, but since there is change in direction by 180° every half-revolution of the sun, a small Coriolis acceleration disturbance at the sun's surface is involved.

Considering two planets, say Jupiter and Saturn, the disturbances are greatly magnified. For this case, the sun moves in the path of Figure 22(a) and it has a velocity which is not perpendicular to the radius vector $\vec{R}_{\odot z}$, so large Coriolis disturbances at the sun's surface may be expected.

Uranus and Neptune effects (involving the additional motions sketched in Figure 22(b)) give a combined displacement about equal to the Saturn displacement (as shown in Table 33, discussed later), when Uranus and Neptune are near conjunction.

It is evident from the above that an equation can be written for the sun center Coriolis acceleration referred to axes rotating with the sun radius vector. Such an equation would involve positions of the four giant planets, their orbit eccentricities, and the angles between the planet positions and their perihelion positions. For 11 of the 24 cycles studied in detail, sunspot cycle peaks are related to Jupiter-Saturn conjunction or opposition times. For others, a comparison is in progress. Development of this equation (or series of equations) is beyond the scope of this report.

Coriolis accelerations due to the planet-determined sun center velocity combined with rotational sun surface velocities are probably not the only Coriolis effect on sunspots; there are quite possibly also important effects due to velocity gradients and angular velocity gradients within the sun.

In addition to the Coriolis acceleration associated with the sun center velocities shown in Figure 23, there is a sun center acceleration $\vec{A}_{\odot Z} = d\vec{V}_{\odot Z}/dt$ shown by Wood and Wood to require consideration of the inner planets as well as the outer planets for reasonably accurate calculations. The direction of $\vec{A}_{\odot Z}$ for a particular planet is the same as the direction of the planet, whereas the velocity $\vec{V}_{\odot Z}$ for each planet is nearly at 90° to the planet direction as noted in Table 33. The next higher derivative $d\vec{A}_{\odot Z}/dt$, designated the "jerk" by Wood and Wood, was found to depend almost entirely on the inner planets.

A summary of the effects of various planets on the sun and on the sun center motion is presented in Table 33 and the relative effects of various planets on some factors is illustrated graphically in Figure 25 Table 33 lists in the first three columns for each planet (except Mars) the mass ratio relative to the earth, the mean planet orbit radius (semi-major axis of the ellipse), and the factor $(1 + e)$, where e is the orbit eccentricity. Note that the mass of Mercury is indicated as uncertain by a factor of two. Its size is known, but because it has no known satellites, its mass is not known, though the mass can be estimated by assuming various values for a specific mass comparable with earth and Mars and an estimated "adopted" value is the one usually given in Tables. The next six columns of Table 33 are calculated values of mr^n where n is an exponent selected in accordance with the quantity to be compared. For instance, n = -2 if it is desired to compare the solar accelerations due to the planets, or n = 1 if it is desired to compare the displacements from the solar system center of mass due to each planet.

Table 33 thus compares the separate effects of planets on solar displacement, solar velocity, solar accelerations, and solar jerk. Also included is the relative tidal bulge at the surface of the sun due to each planet with n = -3. For sun center accelerations Jupiter dominates, but four other planets are involved. For tidal bulge of the sun due to each planet, Saturn (as well as Mercury, Venus, earth, and Jupiter) is seen to have a small but not negligible effect. The sun center jerk depends only on Mercury, Venus, earth, and Jupiter. Whether Mercury has the largest or smallest effect of these four planets depends on the uncertain mass of Mercury. It is possible that the mass of Mercury can be determined by statistical isolation of these effects.

Each planet has a mr^{-3} effect not only because of tidal bulge but also because of the torque on the sun due to such solar oblateness as may exist.

III. PLANET POSITIONS AND TIMES OF HIGH SOLAR ACTIVITY FROM 1700 TO 1968

The approximate positions, neglecting planet orbit eccentricity, of the four giant planets relative to the first point of Aries for the three hundred year period from 1700 to 2000 are shown in Figure 26, including only one typical Saturn orbit in the interest of clarity, but including the positions of Jupiter-Saturn conjunctions because they appear to be related to solar activity. For each Jupiter orbit the position of Jupiter at times of high solar activity is also shown as well as the Waldmeier sunspot cycle number. It is interesting to note that for cycles (0 to 4) and (15 to 20) Jupiter is about 90 degrees ahead of a Jupiter-Saturn conjunction or opposition when the sunspot cycles peak and these eleven cycles are over half of the cycles plotted. For cycles 5, 6, and 7 the position of Jupiter at sunspot cycle peak seems to be related to the mean direction of Uranus and Neptune, and Uranus and Neptune are nearly in conjunction at this time. For the other cycles (8 through 14) the Jupiter position at cycle peak is nearly uniform in the region from 80 to 100 degrees from the first point of Aries. The reason for the different conditions for cycles (8 to 14) from all the other cycles is not clear at this time, and needs further investigation, but it may well be noted that all of these cycles occur between Uranus-Neptune conjunction and Uranus-Neptune opposition. If it is assumed Jupiter, Saturn, Uranus, and Neptune are major factors determining the mean annual sunspot number, it would be reasonable to expect that the next three cycles (21, 22, and 23) would be related to Uranus-Neptune positions, like cycles 5, 6, and 7. It is concluded from the study thus far, that sun surface Coriolis acceleration changes with solar rotation can be used to explain the Jupiter locations shown by cycles 8 through 14 in Figure 26 This demonstration will require additional work. Matching of other cycles about 179 years apart is shown in Figure 27, along with planet conjunctions and oppositions and a more specific prediction. Figure 28 is a study of mismatch of magnitude and timing. Figure 29 shows why Jupiter and Saturn have a large effect about 3 years prior to conjunction.

IV. CONCLUSIONS

These studies show that a dominant cause of the sunspot cycle is probably the Coriolis acceleration of the sun center caused primarily by the four planets Jupiter, Saturn, Uranus, and Neptune. The Coriolis acceleration of the sun center is shown to produce turbulence at the sun's surface. At times when Uranus and Neptune are near conjunction, sunspot cycles peak at a time when Jupiter is a few years ahead of the mean position of Uranus and Neptune, and the Saturn effect is minor. At other times the Jupiter-Saturn effect predominates but is modified by the Uranus-Neptune effect.

This conclusion supplements the finding of Bigg that sub-cyclic solar activity is associated with the periods of the inner planets (Mercury, Venus, earth) with possibly some contribution by Jupiter. Bigg suggests that tidal distortions of the sun may be an important factor in sub-cyclic solar activity, but sun-surface turbulence generated by Coriolis accelerations of the sun due to the inner planets should also be investigated as a contributing factor to general level of disturbances caused by the outer planets.

Use of these facts permits predicting the cycle timing and magnitude for the next 40 years as follows: there will be several long weak cycles such as occurred between 1790 and 1830. The next cycle peak is expected to occur about 1983 ± 2 years and the mean annual Zurich sunspot number R_z is expected to be between 40 and 80.

V. REFERENCES

Berman, Arthur I. The Physical Principles of Astronautics. Wiley 1961, 350 pages.

Bigg, E. K. Influence of the Planet Mercury on Sunspots. Astron. J. 74, 4, May 1967.

Chernosky and Hagan. Sunspot Number and Its Variations for 1700-1957. 1958 J. Geophys. Res. 63, pp. 779-784.

ESSA (Environmental Sciences Services Administration, U.S. Dept. of Commerce), Environmental Data Service Publication IER-FB-286, issued June 1968, with data through May 1968 on page 6.

Flammarion, G. C., and Danjon, A. The Flammarion Book of Astronomy. Simon and Schuster: New York, 1964, 670 pages.

Jose, Paul D. Sun's Motion and Sunspots. 1965 Astron. J. 70, 3, p. 193.

King-Hele, D. G. Letter to the Editor of Nature. Nature, January 15, 1966, pp. 285-286.

Waldmeier, M. 1941 Astron. Mitt. Zurich, 140, 551.

Wood, R. M., and Wood, K. D. Solar Motion and Sunspot Comparison. Nature 208, No. 5006, October 9, 1965, pp. 129-131.

VI. SUMMARY OF NOTATION

Vectors denoted by arrows over symbols. For example, $\vec{a}$ = vector acceleration. Magnitudes designated by bars on both sides of the vector symbol; thus $|\vec{a}|$ = magnitude of acceleration; x denotes the vector or cross-product of two vectors; thus $-2\vec{\omega} \times \vec{v}$ = two times the vector product of angular velocity and linear velocity = Coriolis acceleration.

a	=	acceleration
A	=	acceleration of sun center
d	=	differential
e	=	orbit eccentricity
m	=	mass of planet relative to mass of earth
r	=	radius of mean planet orbit, in astronomical units (earth orbit radii)
$R_{\odot z}$	=	distance to sun center from center of mass of solar system
R_z	=	Zurich sunspot number (also called Wolf Number)
t	=	time
v	=	speed = magnitude of velocity vector $\vec{v}$ = $\lvert\vec{v}\rvert$
V	=	speed of sun center = $\lvert\vec{V}\rvert$
x, y, z	=	mutually perpendicular axes fixed in inertial space at the center of mass of the solar system: x axis in the direction of the first point of Aries, y and z axes in the "invariant" plane of the solar system ≈ plane of orbit of Jupiter
x', y', z'	=	axes through the center of mass of the solar system rotating with the vector $\vec{R}$ to the center of the sun
ω	=	angular velocity

Subscripts:

⊙	=	sun, z = relative to z axis, v = vertical,
ss	=	solar surface, 1, 2, etc. = points,
c	=	Coriolis, fx = viewed by fixed observer,
rt	=	viewed by rotating observer.

TABLE 31. Years of Peak Mean Annual Sunspot Numbers and Lengths of Cycles, from Chernosky and Hagan. Years within 10% of Peak also included to Study Variability

Cycle No. [a]	Peak Year and Frac. [b]	Peak and Near-Peak Years	R_z, Annual Mean of Monthly Means	Cycle Length, Years	Variation
-4	1705.5	1705	54	12	
-3	1718.2	1717	58	10	
-2	1727.5	1727	113	11	
-1	1738.7	1738	106	13	
0	1750.3	1751	83	10	
1	1761.5	1761	85.9	8.5	± 0.5
2	1769.7	1769	106.1		
		1770	100.8	8.5	± 0.5
3	1778.4	1778	154.4	9.5	± 0.5
4	1788.1	1787	132.0		
		1788	130.9	16	± 2
5	1805.2	1802	45.0		
		1804	47.5		
		1805	42.2	13	± 2
6	1816.4	1816	45.8		
		1817	41.1	13	± 1
7	1829.9	1829	67.0		
		1830	71.0	7.5	± 0.5
8	1837.2	1837	138.3		

Cycle No. [a]	Peak Year and Frac. [b]	Peak and Near-Peak Years	R_z, Annual Mean of Monthly Means	Cycle Length, Years	Variation
9	1849.1	1848	124.3	11	
10	1860.1	1859	93.8	11.5	± 0.5
		1860	95.7		
11	1870.6	1870	139.1	10.5	± 0.5
		1882	59.7		
12	1883.9	1883	63.7	13	± 1
		1884	63.5		
13	1894.1	1893	84.9	10	± 1
		1894	78.0	13.5	± 0.5
14	1907.0	1907	62	10	
15	1917.6	1917	103.9		
16	1923.4	1928	77.8	11	
				9.5	± 0.5
17	1937.4	1937	114.4		
		1938	109.6	9.5	± 0.5
18	1947.7	1947	151.6	10.5	± 0.5
19	1957.5	1957	189.9		
		1958	184.6	10.5	± 0.5
20[c]		1968	105		

a Assigned by Waldmeier, except 0 to -4
b Used by Jose
c Estimated from ESSA Pub. IER-FB-286

TABLE 32. Calculated Planetary Synodic Periods in Years for Mean Circular Orbits, with Estimated Corrections for Orbit Eccentricity

Equation: $T_2/T_{syn} = T_2/T_1 - 1$, where T_2 = longer period, T_1 = shorter, T_{syn} = synodic period. Eccentricity of the orbit for T_1 tends to dominate the departures from circular orbit calculations except when T_2 is nearly the same as T_1; perihelia directions relative to synodic directions are also an important factor. Mars omitted as irrelevant to the sunspot problem.

Planet	r mean	e^{T_2}	Mercury	Venus	Earth	Jupiter	Saturn	Uranus	Neptune
Mercury	.387	.206	0.241	0.396 ± .07[4]	0.317 ± .06[4]	0.246 ± .05	0.243 ± .05	0.242 ± .05	0.241 ± .05
Venus	.723	.007		0.615	1.59 ± .01	0.770 ± .005	0.626 ± .994	0.620 ± .004	0.615 ± .004
Earth	1.000	.017			1.000	1.092 ± .017	1.035 ± .017	1.012 ± .017	1.006 ± .017
Jupiter	5.20	.0482				11.86	19.8 ± 0.7[1]	13.8 ± 0.5	12.8 ± 0.45
Saturn	9.54	+.054 .001					29.5	46 ± 0.5[2]	36 ± 0.2[2]
Uranus	19.2	+.048 .003						84.0	171[3]
Neptune	30.0	+.009 .003							165

(1) Mean for last five synodic periods (≈ 100 years) from Amer. Ephemeris & Naut. Almanacs.

(2) Mean of last four synodic periods based on plots from Amer. Ephemeris & Naut. Almanacs.

(3) Plots of Amer. Ephemeris & Naut. Almanac data permit estimating the current synodic period as (1992.2±0.3) - 1821.8 = (170.4±0.3) years (±0.3 here denotes uncertainty of graphical solution). Over a large number of periods averaging 171 years, variation would be about ± 6 years.

(4) Variability believed to have changed substantially for times covered by this study, partly because of Mercury perihelion direction changes. Most statistically observed sunspot cycle periods are multiples of the above periods.

TABLE 33. Summary of Relative Magnitudes of Various Planet Effects on the Sun

Data from 1961 Explanatory Supplement to American Ephemeris and Nautical Almanac, p. 491

Symbol	Mass Ratio $m_p/m_0=m$	Orbit Radius, semi-Major r	Eccent. Corr. factor 1 + e	Displacement from SSCM mr		Velocity $mr^{-0.5}$		Acceleration mr^{-2}		Tidal Bulge mr^{-3}		Jerk $mr^{-3.5}$	
Planet				mean	max / min	mean	max / min	mean	max / min	mean	max / min	mean	max / min
Mercury	.033 to .066*	0.387	1.2056					.33	.64 / .15	.86	2.00 / .33	1.37	3.50 / .50
Venus	0.817	0.723	1.0068					1.56	1.58 / 1.54	2.17	2.21 / 2.12	2.49	2.55 / 2.43
Earth	1.000	1.000	1.0167					1.000	1.03 / .97	1.000	1.05 / .95	1.000	1.067 / .933
Jupiter	318.0	5.203	1.0484	1660	1740 / 1590	139.5	143 / 136	11.75	12.9 / 10.7	2.25	2.60 / 1.95	.985	1.162 / .834
Saturn	95.2	9.54	1.0557	907	955 / 860	30.8	31.7 / 30.0	1.045	1.165 / .940	.11	.13 / .09		
Uranus	14.6	19.18	1.0472	280	293 / 268	3.33	3.41 / 3.25						
Neptune	17.3	30.05	1.0086	520	524 / 516	3.16	3.19 / 3.13						
Pluto	0.8 to 1.0	39.44	1.2502	35	49 / 23								
Directions of above magnitudes:				-p		-p+90°		p		p		p+90°	

p = planet direction, -p = opposite to planet. * Estimated by S. H. Dole, Habitable Planets for Man, Figure 11.

Values less than 1% of the greatest value in each column are omitted for clarity. Mars is less than 1% in all columns and is omitted

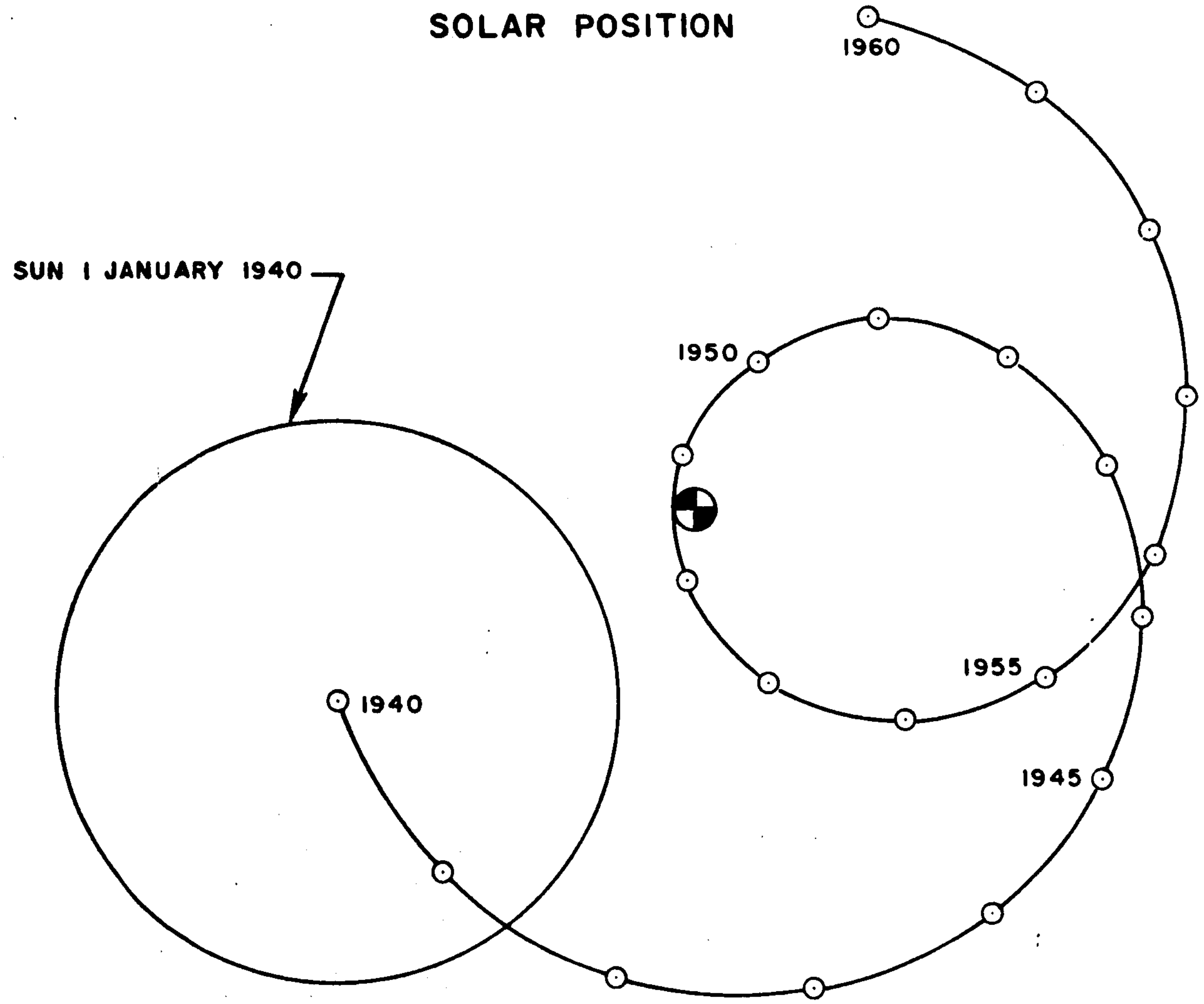

Figure 21. Sun Center Position Relative to Solar System Center of Mass, 1940 to 1960. Based on Flammarion page 51. This Chart Courtesy R. M. Wood

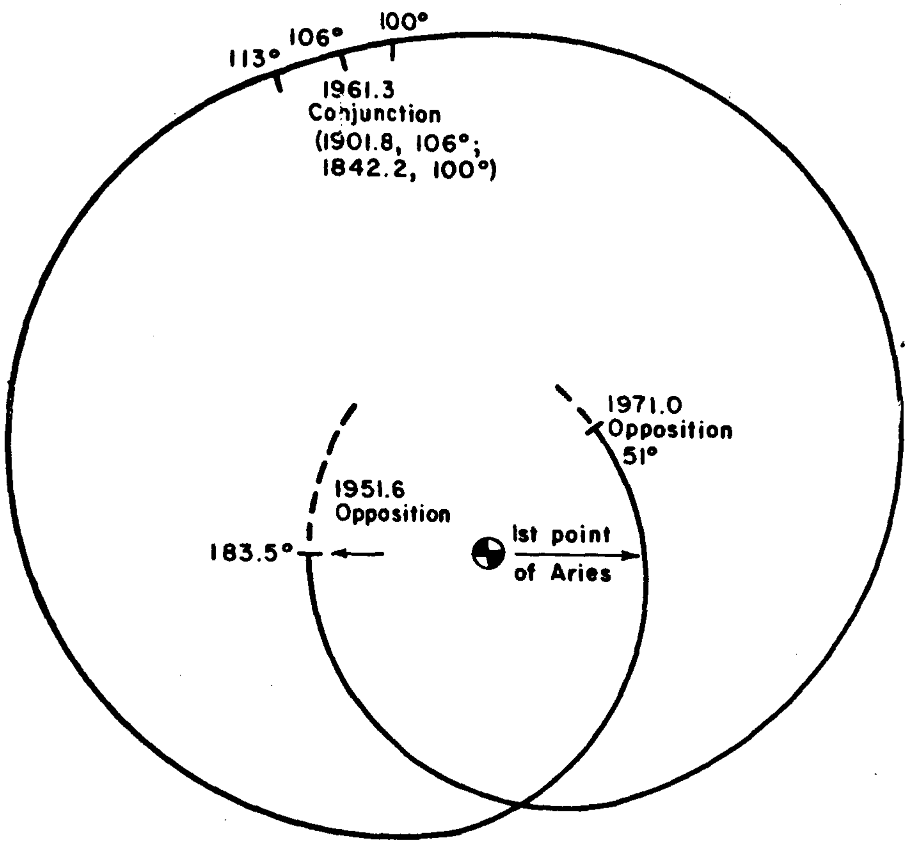

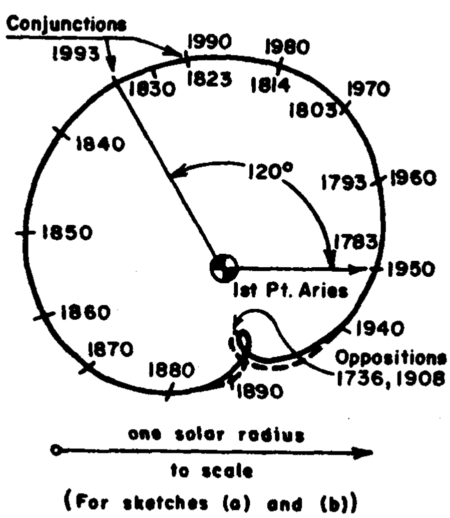

(a) Typical sun center position changes for one opposition-to-opposition period of Jupiter and Saturn. Three periods returns sun to nearly same point.

(b) Sun center position changes due to Uranus and Neptune.

Figure 22. Effect of 2-Planet Combinations on Position of Sun Center Relative to Solar System Center. Positions not Accurately to Scale

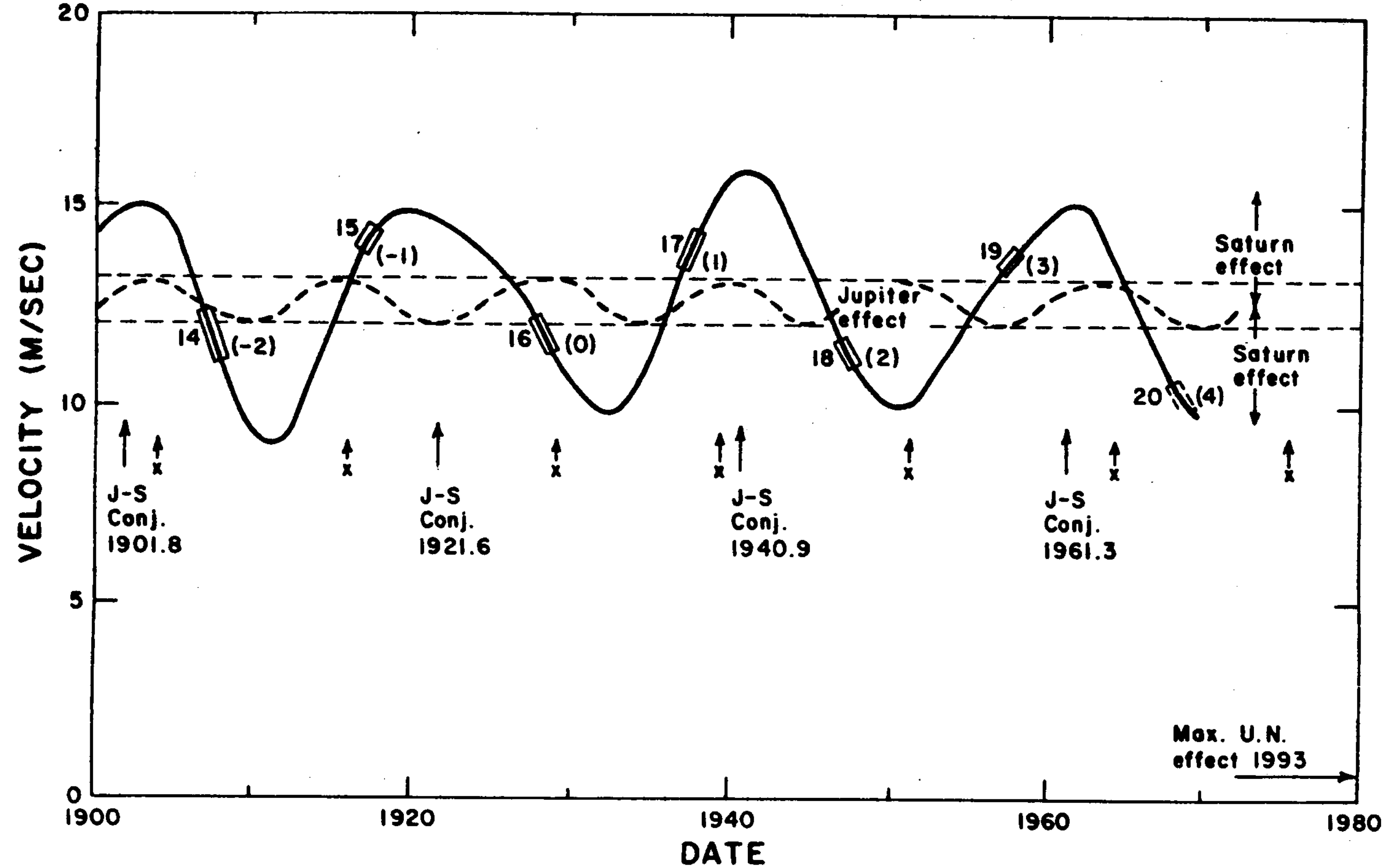

Figure 23. Magnitude of Sun Center Velocity Vector, 1900 to 1970. Magnitudes of Separate Effects of Jupiter and Saturn, and of the Combined (Uranus + Neptune) Effect also Shown. Small Rectangles indicate Years of Solar Activity within 10% of the Cycle Peak, Identified by Waldmeier Cycle Number, with Approximately Matching Earlier Cycle Number in Parentheses. x = Jupiter Perihelion Position, Applicable to Recent Cycles Only, not to Earlier Cycles

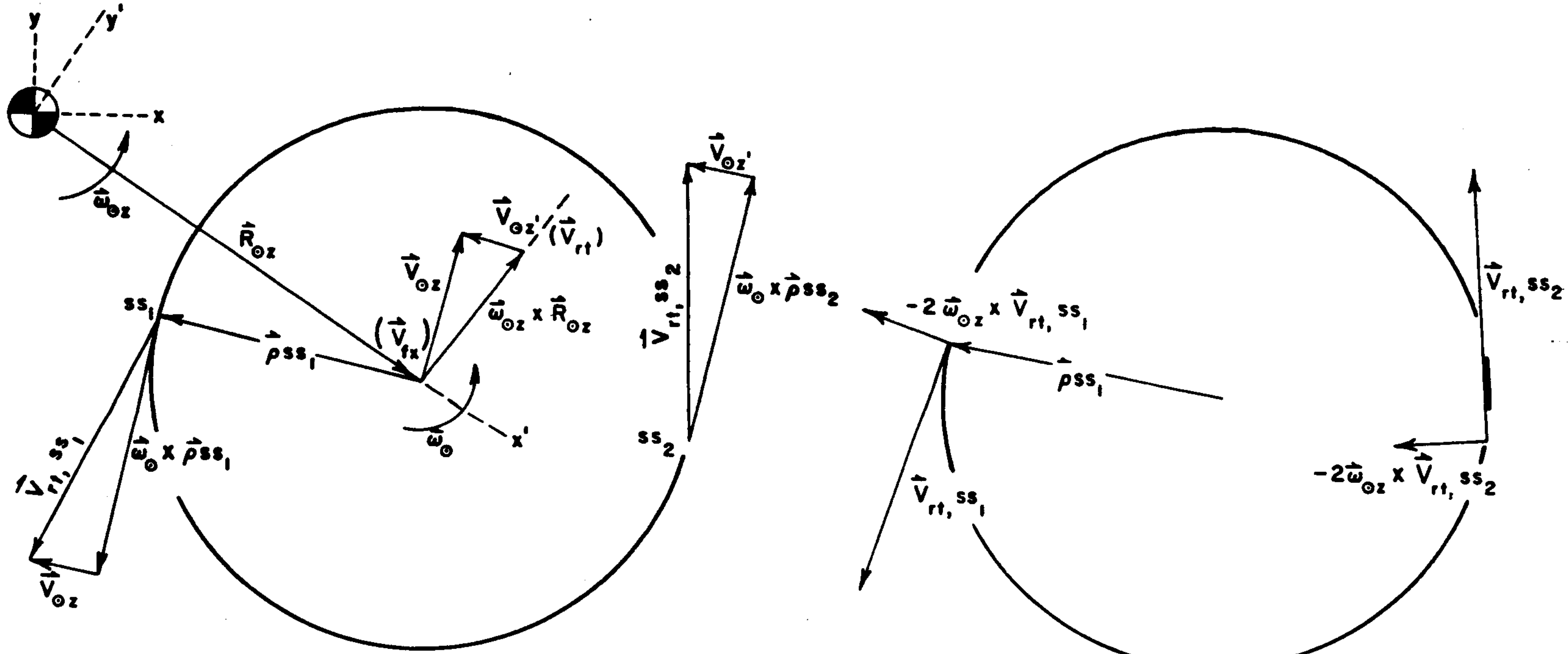

(a) Velocities

(b) Relative velocities plus Coriolis acceleration

Figure 24. Vector Diagram (a) for Finding Sun Surface (ss) Velocities Relative to Axes Rotating with $\vec{R}_{\odot z}$ and (b) for Finding the Corresponding Coriolis Accelerations

Displacement $|\vec{R}_{\odot z}|$

(AND "Coriolis Velocity")

$|2\vec{\omega}_{\odot} \times \vec{R}_{\odot z}|$

Velocity $|\vec{V}_{\odot z}|$

(AND Coriolis Acceleration)

$|2\vec{\omega}_{\odot} \times \vec{V}_{\odot z}|$

Acceleration $|\vec{A}_{\odot z}|$

(AND Coriolis Jerk)

$|2\vec{\omega}_{\odot} \times \vec{A}_{\odot z}|$

Tidal Bulge

(AND Approximate

Solar Oblateness Torque)

Jerk $|\dot{\vec{A}}_{\odot z}|$

(AND Coriolis $|\ddot{\vec{A}}_{\odot z}|$)

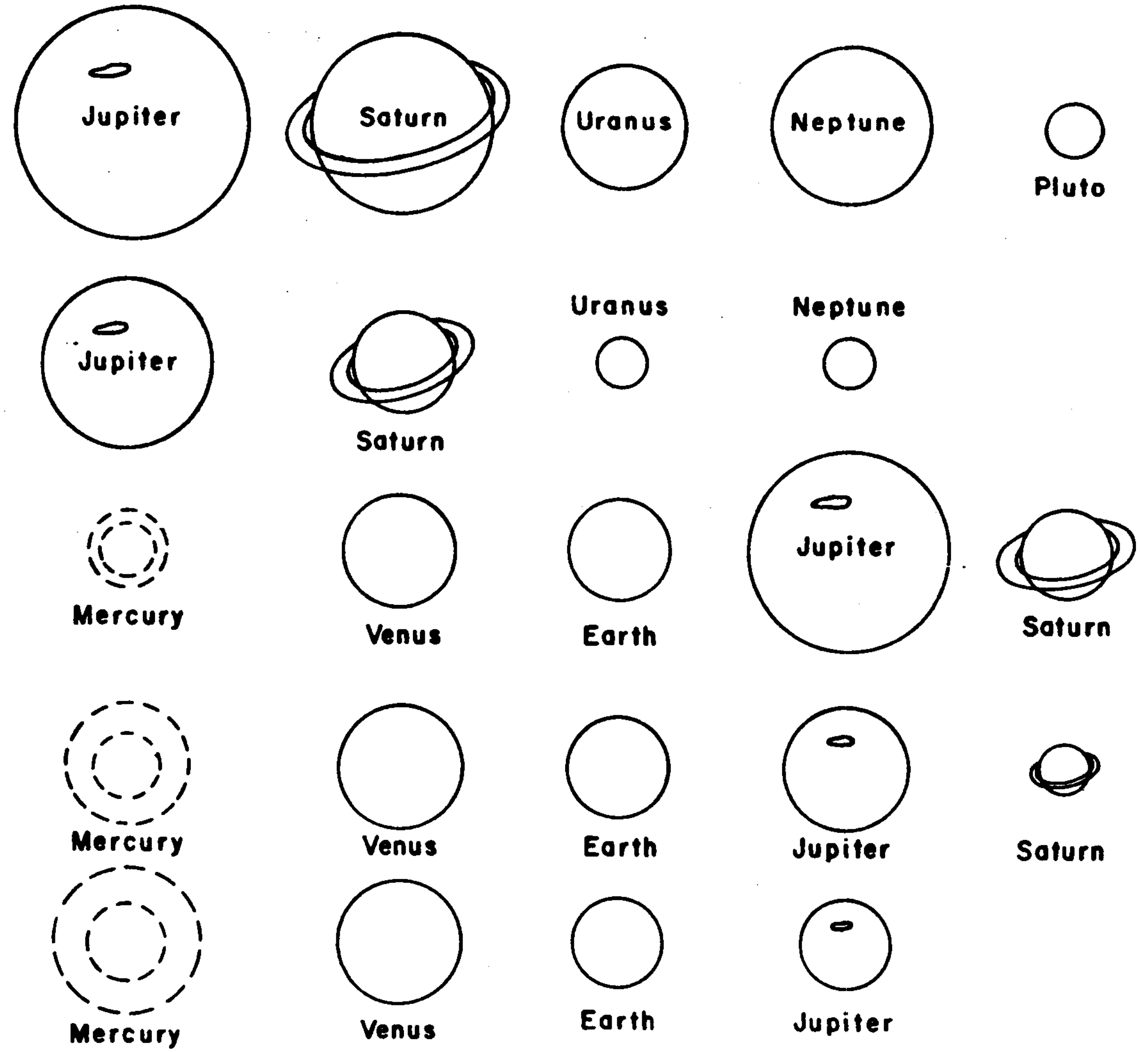

Figure 25. Volumes of Spheres Showing Relative Magnitudes of Planet Effects on the Sun.

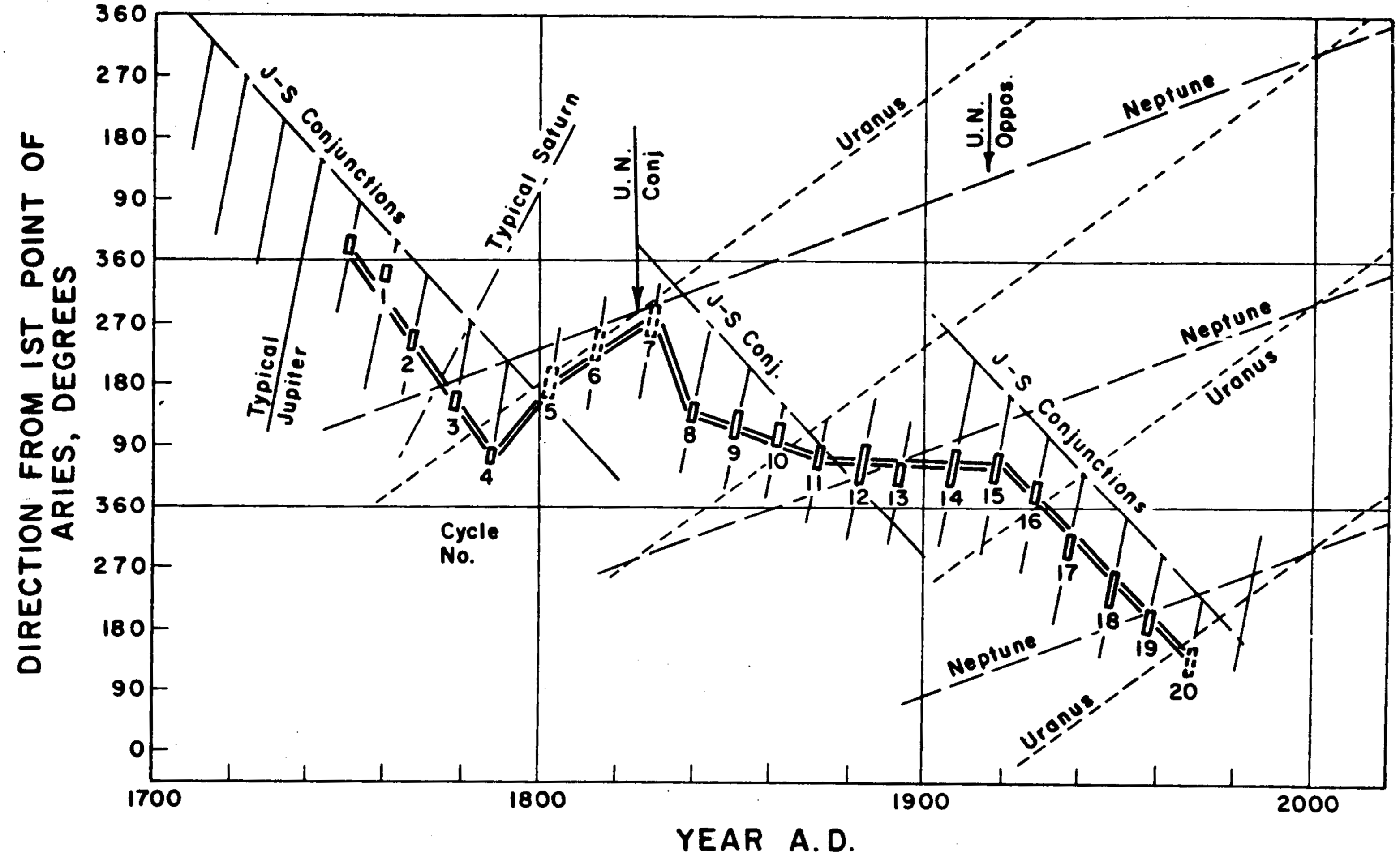

Figure 26. Positions of Jupiter at Sunspot Maxima Relative to Jupiter-Saturn Conjunctions and to Uranus and Neptune Positions. A Graph Like This Enlarged by a Factor of About Eight was Used in the Estimates of Near-Double Conjunctions and Near-Triple Conjunctions in the Text

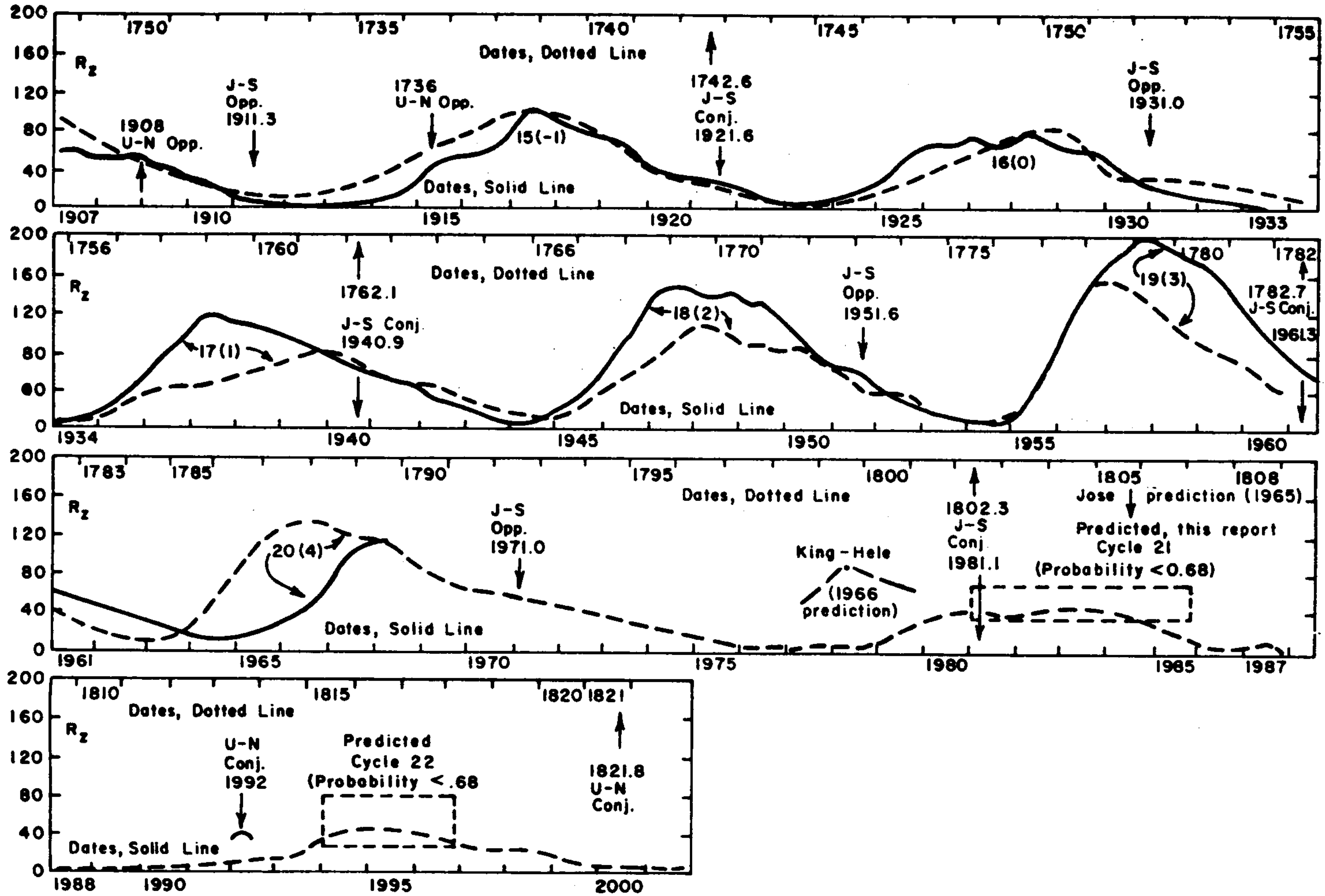

Figure 27. Matching of Sunspot Cycles 178.7 Years (Nine Jupiter-Saturn Conjunctions) Apart and Forecast Compared with Earlier Cycles. Graphs from Waldmeier, Cycle Numbers Noted (Earlier in Parentheses). See Figure 8 for Study of Mismatching

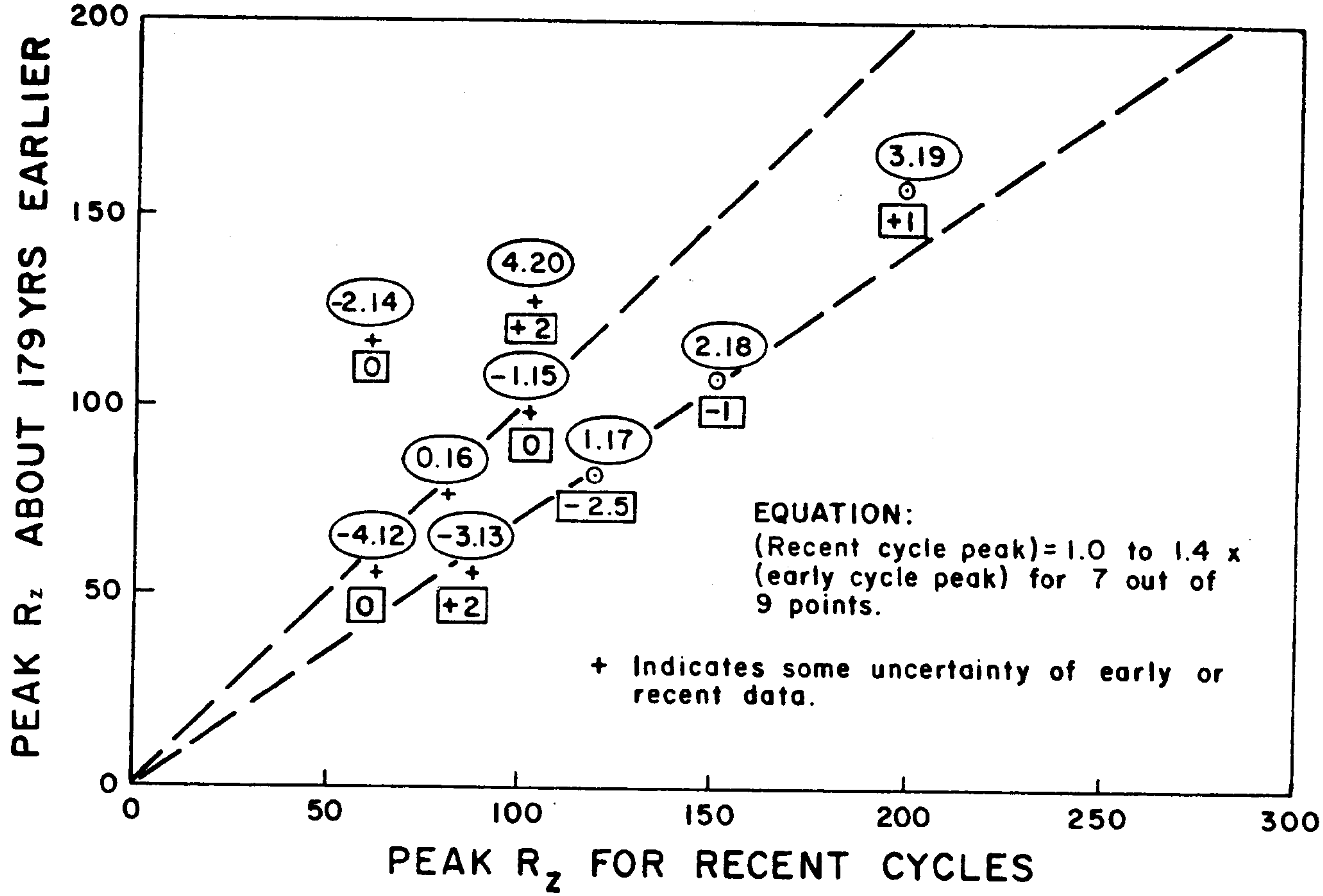

Figure 28. Study of Magnitude of Mismatch Between Recent Cycles and Cycles About 179 Years (Nine Jupiter-Saturn Conjunctions) Earlier. Part of the Higher Recent Readings May be Due to More Accurate Recent Observing. Data from Figure 1. Cycle Numbers Encircled. Lateness of Recent Cycle in Years Indicated in Boxes

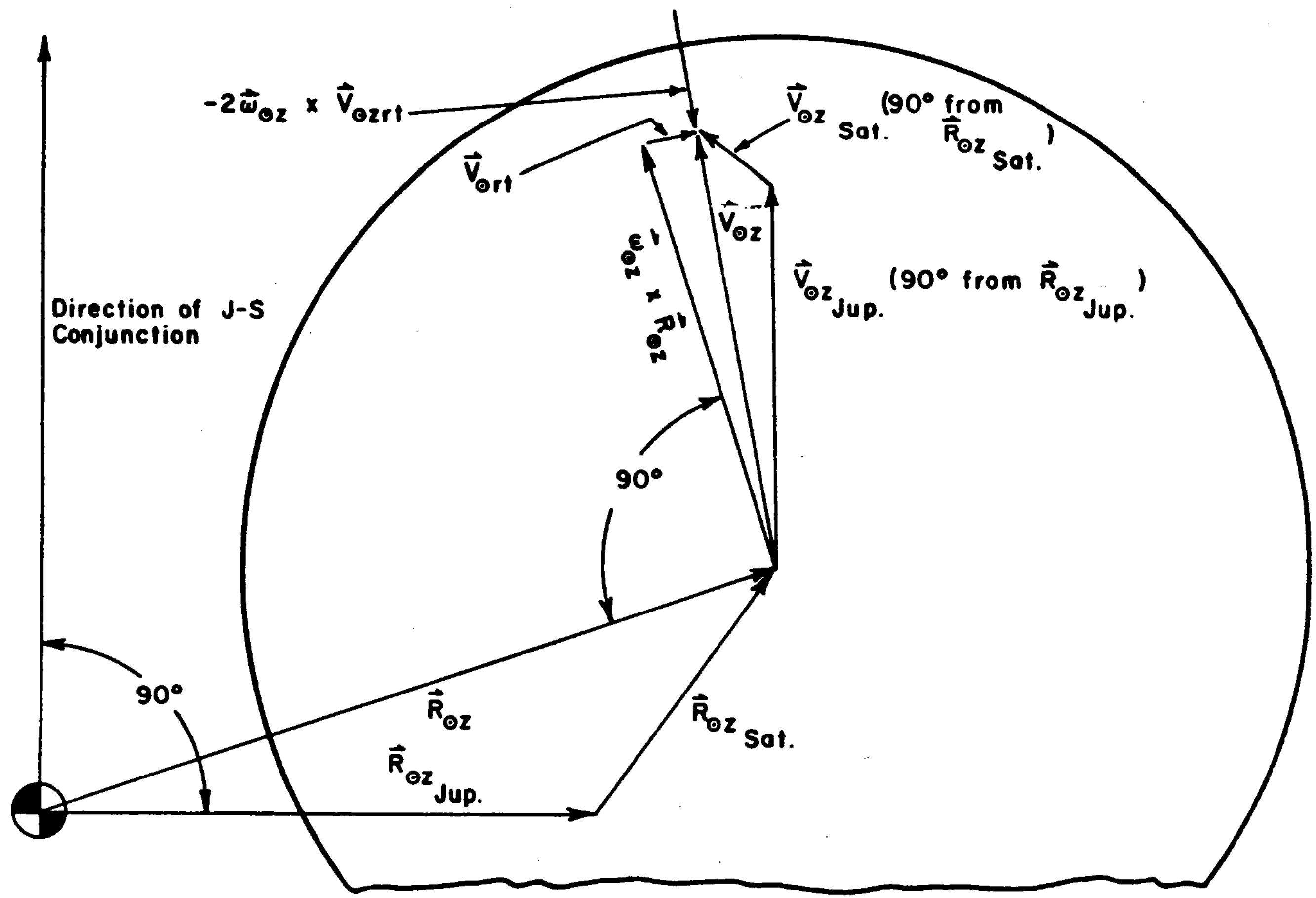

Figure 29. Addition of Separate Jupiter and Saturn Effects on Sun Center Velocities to Find Coriolis Acceleration of Sun Center, (a Turbulence Generating Factor Near the Sun's Surface) About Three Years Prior to Jupiter-Saturn Conjunction, when Uranus and Neptune are Near Opposition and have Small Effects. At Jupiter-Saturn Conjunction $\vec{V}_{\odot zrt} = 0$ and Sunspots Due to Jupiter and Saturn do not Occur (Provided Uranus and Neptune are Near Oppositions).

10. CONCLUSIONS AND RECOMMENDATIONS

10. CONCLUSIONS AND RECOMMENDATIONS

One of the most important conclusions of the study is that localized density increases occur in the corona in alignment with planetary conjunctions. The density increases are detected by increased radio and X-ray emission on the exact day of conjunction. Other solar parameters such as sunspot and plage area also increase but the correlation is not as precise because of a lag of a day or two. Following successive excitations, an active center develops, possibly as the result of standing waves, or shock waves. In a fully developed active center on a second or later rotation, a further conjunction of tidal planets may trigger a proton event.

Ten individual active centers have been analyzed for 2 or 3 months by daily radio emission. Thirty-six conjunction dates showed radio flux increases, even though integrated over the entire disk. All of these active centers produced one or more proton events, and eight produced ground level events. Although there may be alternative explanations, unstable regions in the sun are sensitive to solar displacement or tidal effects. While the initial tidal effects may be so small as to be barely measurable (Trellis, 1966) (Wood and Wood, 1965), the result is an amplified waveform due to the steep gradients of density and temperature in the sun's corona. X-ray daily flux was analyzed 3 months before four major events of cycle 20, involving 24 conjunction dates for which significant X-ray flux increases occurred, even when averaged over the whole face of the sun. The X-radiation of one of these active centers was also studied at the Naval Research Laboratory. It was concluded that:

"Below 20 Å (radiations which affect the lower E and D regions of the ionosphere), a detectable X-ray background began to appear in late 1965. The first large spot to develop (March 1966) increased the 8-20 Å flux by 50 times; yet this spot occupied less than one-thousandth of the disk area. We conclude that the corona immediately over this spot had an X-ray brightness 5000 times as great as the surrounding corona. A factor of 2 in the enhanced emission may be attributed to increased temperature. The remaining increase of 2500 must be due to the greater density of the condensed corona over the active region - a fiftyfold increase in density, since X-ray brightness varies with the square of the density."*

The daily radio maps at 9.1 cm. wavelength were examined for the March 1966 active region, and the source of the radio flux confirms Friedman's conclusion about the localized source of the hard X-ray flux. The radio increase on conjunction dates is also localized in the major active center, and not distributed over the disk of the sun. The July 1966 and March 1969 active centers were also studied by means of the radio maps, with the same conclusion, but such analyses took place too late to be included in the body of the report.

An empirical approach was used to evaluate the role of solar system dynamics in solar activity. Both tidal effects and jerk are dominated by Jupiter, Venus and Mercury and Earth, and conjunctions of these four planets seem to be the triggering mechanism for proton events. The relative importance of these two processes cannot be determined without further study. A detailed study was made of the large active centers and their proton events of solar cycles 14 thru 20 to determine planetary positions and the sequence of conjunctions preceding proton events or flares. Tables of significant planetary conjunctions (supplemented by 16 charts for selected proton events) were prepared for the period 1876-1970, and compared to solar activity during the same period.

*Friedman, H., "Energetic Solar Radiations," paper delivered at the Joint IQSY/COSPAR Symposium on the IQSY, London, July 1967.

The discussion concentrates on events later than 1900 because:

1. A complete 59.5 year Jupiter-Saturn cycle is covered, and almost one-half of a Uranus-Neptune cycle.
2. Seven-planet tidal forces have been computed from 1900-1959 (Bollinger, 1960).
3. Sunspot polarities from 1913 and magnetic field strengths from 1917 are available (Hale and Nicholson, 1938).
4. Daily maps of the chromosphere and prominences are available from Meudon Observatory from 1919 to date (d'Azambuja).
5. Systematic sunspot observations were made by both Greenwich and Mt. Wilson Observatories from 1917.

Projections of solar activity for the 1969-1970 period were prepared, as well as ultra-long forecasts of proton flux and sunspot number for cycles 20, 21 and 22.

A study was made of the latitudes of solar activity to observe if there are cyclic variations related to planetary positions above or below the solar equator. Recent increased activity in the sun's southern hemisphere may be related to a long cycle of the north-south positions of planets. (Rubashev, 1964) (Vitinsky, 1965). The long period of the N-S asymmetry restricts investigation due to lack of data on flare location in earlier solar cycles, although sunspot and geomagnetic storm data are available. The role of active solar longitudes was discussed. It was concluded that they are stable over several 11-year cycles, but that activity changes from one to another within a cycle.

A solar equatorial coordinate system was developed. The position of the planets was determined relative to the plane of the solar equator, since the ecliptic plane is not significant in this context. The distance of planets above or below the solar equatorial plane affects the sunspot number and probably the north-south distribution of spots and flares. It may be due to precessional torques on a fluid oblate sun.

The ascending nodes of at least seven planets lie within the range 240° and 260°. The clustering suggests that there may be related seasonal and long-period variations in solar activity. Tables were prepared showing dates of ascending and descending nodes, greatest latitude north and south in the solar equatorial coordinate system for all of the planets.

Ten criteria have been established for the occurrence of major proton flares. Most of the features listed below have been recorded over the 130 year period of quantitative solar observations. Thus it is feasible to study earlier solar cycles and determine major proton flare activity, on the basis of one or more of these criteria. The ten criteria are:

(1) Flare activity follows a closely spaced sequence of tidal planet conjunctions.

(2) The plage region must be in second or later passage.

(3) The sunspot area must be greater than 500 millionths.

(4) The penumbra must enclose umbra of opposite polarity.

(5) The flare causes a short wave fade (SWF) or crochet which follows the time of the flare maximum intensity.

(6) The flare covers a large part of the sunspot umbrae.

(7) The flare is accompanied by the loop prominence system.

(8) The spot group must be magnetically complex.

(9) The flare occurs at an active Carrington longitude.

(10) The flare must occur near one of the three peaks of major activity in the 11 year cycle.

Although events before 1942 were included because of the magnetic storm record, the strong seasonal effect makes them of little value. On the other hand, the area of large sunspots correlates strongly with significant planetary conjunctions. Every case investigated shows a peak sunspot area on the day of the triggering planetary conjunction including: Feb. 1942, Feb. 1956, Jul. 1959, Nov. 1960, Mar. 1966, Jul. 1966 and Mar. 1969. (In about half of the events the spot group is on the far side of the sun at the time of the triggering conjunction.) Therefore it is indeed possible to investigate conclusively the major centers of activity back as far as 1874, through the daily Greenwich records of sunspot area.

Recommendations. Several improvements have already been incorporated in the 120-Day Solar Flare Prediction. These include use of all nine planets starting Sept. 1968. It has been found that alignment of several planets other than Mercury, Venus, Earth and Jupiter has a definite effect on solar activity. Examples would be the activity of March-April 1966, which appears related to the alignment of Saturn, Uranus and Pluto, and February-April 1969, at which time Jupiter and Uranus had the same longitude. The influence of Jupiter and Saturn together has been discussed by several authors (Nelson, 1952) (Wood, this report). Considerable time was spent investigating influence of the outer planets on formation of large sunspots, magnetic storms,

storms, and other major solar-terrestrial events over the time period 1870 to present, but the results were not very definitive, primarily because of an inadequate amount of data, or in the case of geomagnetic storms, the strong seasonal effect.

The second improvement in the prediction system has been to utilize several solar active longitudes with attention to the phase of cycle 19 when they were most active (Bezrukova, 1961).

The third important improvement has been to concentrate on second and later rotation of an active center for flare and particularly proton event predictions. Studies during the IGY showed that of 1556 spot groups listed by Zurich, only 652 were flare active (at least one flare); 30% of these lasted 1/2 rotation, 43% lasted 1 rotation, 23% lasted 2 rotations and only 3.4% lasted 3 rotations. It was found that of this group of 652 active centers, 87% of the flares occurred on the second or third rotation (Smith and Smith, Solar Flares, 1965). Proton events show a similar concentration in late rotations. Therefore before 1969, although several active centers were successfully predicted, flares and proton events occurred on later rotation than had been predicted. The long slow development of active centers is an ultimate advantage for men in space, because the warning time is greatly increased. On the other hand it has been a disadvantage in this study. Analysis of a sufficient number of active regions for two and three months has been exceedingly time consuming, and has precluded a planned statistical analysis of centers and events. In addition, applicable statistics are more complex because the birth of active centers and triggering of proton events both correlate with planetary configurations and/or conjunctions. Therefore it is recommended that a suitable statistical analysis be performed. It should now be possible to determine the relative importance of the different planets by the relative increases on conjunction dates of solar radio and X-ray flux. Also events can be listed by the energy spectrum (rigidity) versus the planets involved (See Table 9). However other factors must be compensated for, such as active longitudes, phase of 11-year cycle, relative activity of cycle (peak sunspot number, and so on).

New monitoring techniques have completely changed the outlook for long range prediction. Ten-cm. radio flux has been used as an index throughout the report because of its reliability and continuous record from 1947. However, since the IGY, continuous daily series have been available at several other wavelengths which reveal conditions lower in the chromosphere, and would therefore be more sensitive indicators. Daily flux is now reported in the IAU Quarterly Bulletin for the following frequencies:

> 8800-9400 Mc/S - Sagamore Hill, Gorky, Heinrich Hertz, Irkutsk, Nagoya; 10,700 Mc/sec-Penn State, 15,000 Mc/S-Kislovodsk; and 17,000 Mc/S, Tokyo.

Furthermore, the development of active centers can be studied more effectively on radio spectroheliograms. There is a continuous series (almost daily) of radio flux contours of specific active centers at 9.1 cm. wavelength from Stanford since 1958.

X-ray flux variations are more temperature and pressure sensitive, and now have been monitored daily for six years, and hourly in three bands since late 1968. Apparently X-ray spectroheliograms will become available on a daily monitoring basis in the near future. The time development of active centers will be far more straightforward with such techniques for several reasons. First, monitoring will not be restricted to the face of the sun visible from earth. Secondly, planet effects on solar activity will be far above the threshold detection of today.

11. APPENDIX: SOLAR EQUATORIAL COORDINATES

11. APPENDIX: SOLAR EQUATORIAL COORDINATES

The north-south distribution of sunspots and flares is influenced by the distance of planets above or below the solar equator. It may be due to precessional torques on a fluid oblate sun. A coordinate transformation is performed from the heliocentric ecliptic system to the heliocentric solar equatorial system. The orbital elements of all nine planets are calculated in the new solar equatorial system. The ascending nodes of seven planets are concentrated within twenty-degrees. Similarly, the perihelia of five planets are located in one quadrant. The implications of such grouping is discussed. The applicability of the solar equatorial coordinate system is demonstrated with experimental data.

I. TRANSFORMATION TO SOLAR EQUATORIAL COORDINATES

The conversion from heliocentric ecliptic coordinates to solar equatorial coordinates involves a rotation about the intersection of the planes of the ecliptic and the solar equator. The intersection is the longitude of ascending node of the solar equator on the ecliptic (λ_s). We find that $\lambda_s = 73° \ 40'$, and that the inclination of the solar equator to the ecliptic is $\epsilon = 7° \ 15'$ (Explanatory Supplement to the American Ephemeris, 1961).

First, we make the following definitions:

λ = heliocentric longitude measured counterclockwise from vernal equinox along the ecliptic plane

β = heliocentric latitude north of ecliptic plane

λ_N = heliocentric longitude of ascending node of planet orbit on ecliptic plane

i = inclination of orbit plane to ecliptic plane

α' = azimuthal angle of planet in orbit plane, measured counter-clockwise from the ascending node.

Then we have, for any point P along the orbit:

$$\sin \beta = \sin i \sin \alpha' \qquad \text{(see Figure)}$$

$$\cos \beta \cos(\lambda - \lambda_N) = \cos \alpha' \qquad \text{(Smart, 1961)}$$

therefore

$$\sqrt{1 - \cos^2 \beta} = \sin i \ \sin \alpha'$$

$$1 - \cos^2 \beta = \sin^2 i \ \sin^2 \alpha'$$

$$\cos \beta = \pm \sqrt{1 - \sin^2 i \sin^2 \alpha'}$$

and hence,

$$\sin \beta = \sin i \sin \alpha' \tag{1}$$

$$\cos(\lambda - \lambda_N) = \pm \frac{\cos \alpha'}{\sqrt{1 - \sin^2 i \sin^2 \alpha'}} \tag{2}$$

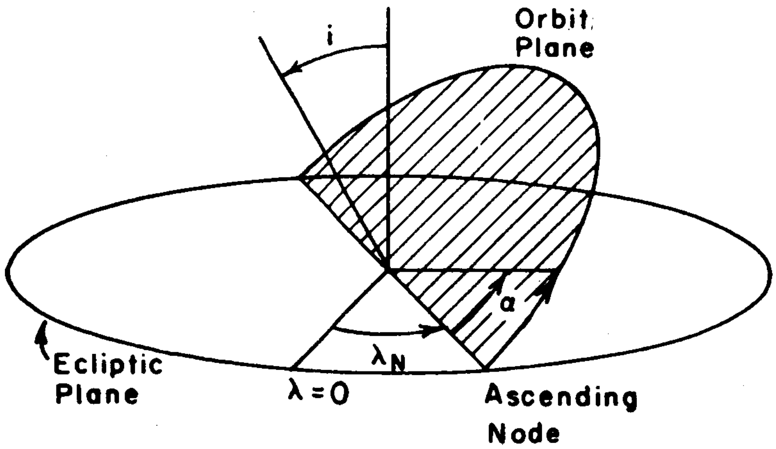

Figure 30. Planet Orbital Plane in Relation to Ecliptic Plane

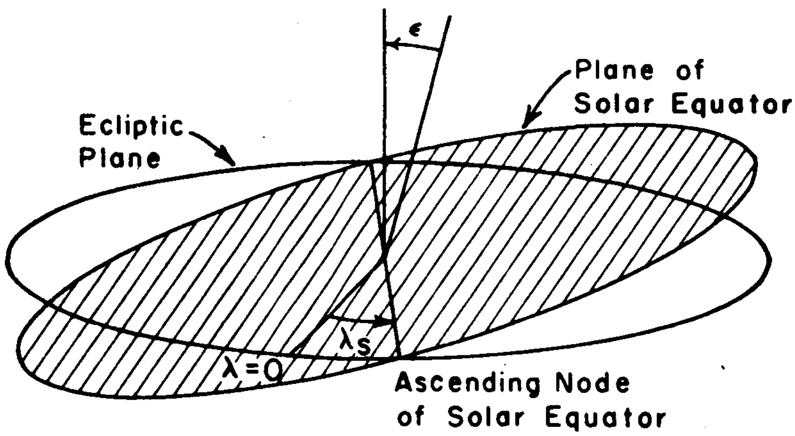

Figure 31. Plane of Solar Equator in Relation to Ecliptic Plane

Now, to transform from ecliptic to solar equatorial coordinates, we let the zero of solar equatorial longitude ℓ be defined as the ascending node λ_s of the solar equator, and let solar longitude be measured counterclockwise around the solar equator. We define b = solar latitude, the angle north of the solar equator (see Figure 31). Also we again define ϵ = angle of inclination of the solar equator to the ecliptic. Then we have,

$$\sin b = \cos \epsilon \sin \beta - \sin \epsilon \cos \beta \sin (\lambda - \lambda_s) \qquad (3)$$

$$\cos b \cos \ell = \cos \beta \cos (\lambda - \lambda_s) \qquad (4)$$

When the planet crosses the solar equator, we have b = 0, whence from equation (3)

$$0 = \cos \epsilon \sin \beta - \sin \epsilon \cos \beta \sin (\lambda - \lambda_s) \qquad (5)$$

The solutions of equation (5) give the latitude β and longitude λ at which the planet crosses the solar equator. Knowing β and λ, the solar longitude ℓ at the "crossing point" is given by equation (4), with b = 0:

$$\cos \ell = \cos \beta \cos (\lambda - \lambda_s) \qquad (6)$$

Thus for a given planet the values in equation (5) and (6) are tabulated near the ascending node and an accurate solution may be obtained graphically or analytically by interpolation. After the ascending node has been found, the inclination may be found as the greatest latitude north or south at an angle ± 90° from the node. The results for all nine planets are shown in Table 34. The ascending node and inclination of Pluto should be regarded as tentative, since considerable extrapolation was necessary from the ephemerides which are available for less than 40° longitude of Pluto's orbit.

TABLE 34. Orbital Elements of the Planets in the Solar Equatorial Coordinate System. Columns 5 (Inclination) and 6 (Longitude of Ascending Node to the Solar Equator) were Calculated Using the Method in the Text. Other Data from Explanatory Supplement to the American Ephemeris and Nautical Almanac, 1961

1	2	3	4	5	6	7
Planet	Siderial Period (Tropical Years)	Synodic Period (Days)	Eccentricity	Inclination (to Solar Equator)	Longitude Asc. Node	Longitude Perihelion
Mercury	0.24085	115.88	0.205627	3° 21'	327.°9	76.83309
Venus	0.61521	583.92	0.006793	3° 47'	253.°2	131.00831
Earth	1.00004	--	0.016726	7° 10'	254.°4	102.25253
Mars	1.88089	779.94	0,093368	5° 34'	262.°7	335.32269
Jupiter	11.86223	398.88	0.048435	6° 00'	249.°2	13.67823
Saturn	29.45772	378.09	0.055682	5° 25'	237.°9	92.26447
Uranus	84.01331	369.66	0.047209	6° 24'	254.°5	170.01083
Neptune	164.79345	367.48	0.008575	6° 21'	240.°9	44.27395
Pluto	247.686	366.72	0.250236	(12°)	(309°)	224.16024

The ascending nodes of seven planets lie within the range 240° to 260° (Figure 32) (Table 34). The clustering suggests that there may be related seasonal variations in solar activity, and may also have implications for the origin of the solar system.

The different orientation of the nodes of Mercury may be related to regression of the nodes due to general relativity, solar oblateness, or a solar quadrupole moment (Dicke and Goldenberg, 1967) (Gilvarry and Sturrock, 1967) (Roxborough, 1967) (O'Connell, 1968).

The correlation between the nodes of the planets suggests strong interaction or interrelationships between the planets. It has recently been shown that the maximum possible number of resonances occurs between the planets of the solar system (Molchanov, 1968). The solar system is compared to the satellite systems of Jupiter and Saturn, which contain minimal resonances. The solar system resonances are shown in Table 35 where multiples of many siderial periods and synodic (conjunction) periods of the major planets are shown to be equivalent to the long period of solar activity (Jose, 1965).

There is also a concentration of planetary perihelions. The perihelions of all planets (except Pluto and Mars) are within 157°; five important eccentric planets have perihelions in the same quadrant (Figure 33. (Pluto and Mars would be the least important planets affecting solar activity.) There could be high spring tides when the planets are located in this quadrant, if tidal effects are predominant. On the other hand, if solar displacement is important the timing and orientation of aphelion passage could be significant. There is a suggestion of this during solar cycle 19 (the most active on record) at which time three major planets passed aphelion: Jupiter, 1957; Saturn, 1959, and Neptune, 1959 (see Table 37).

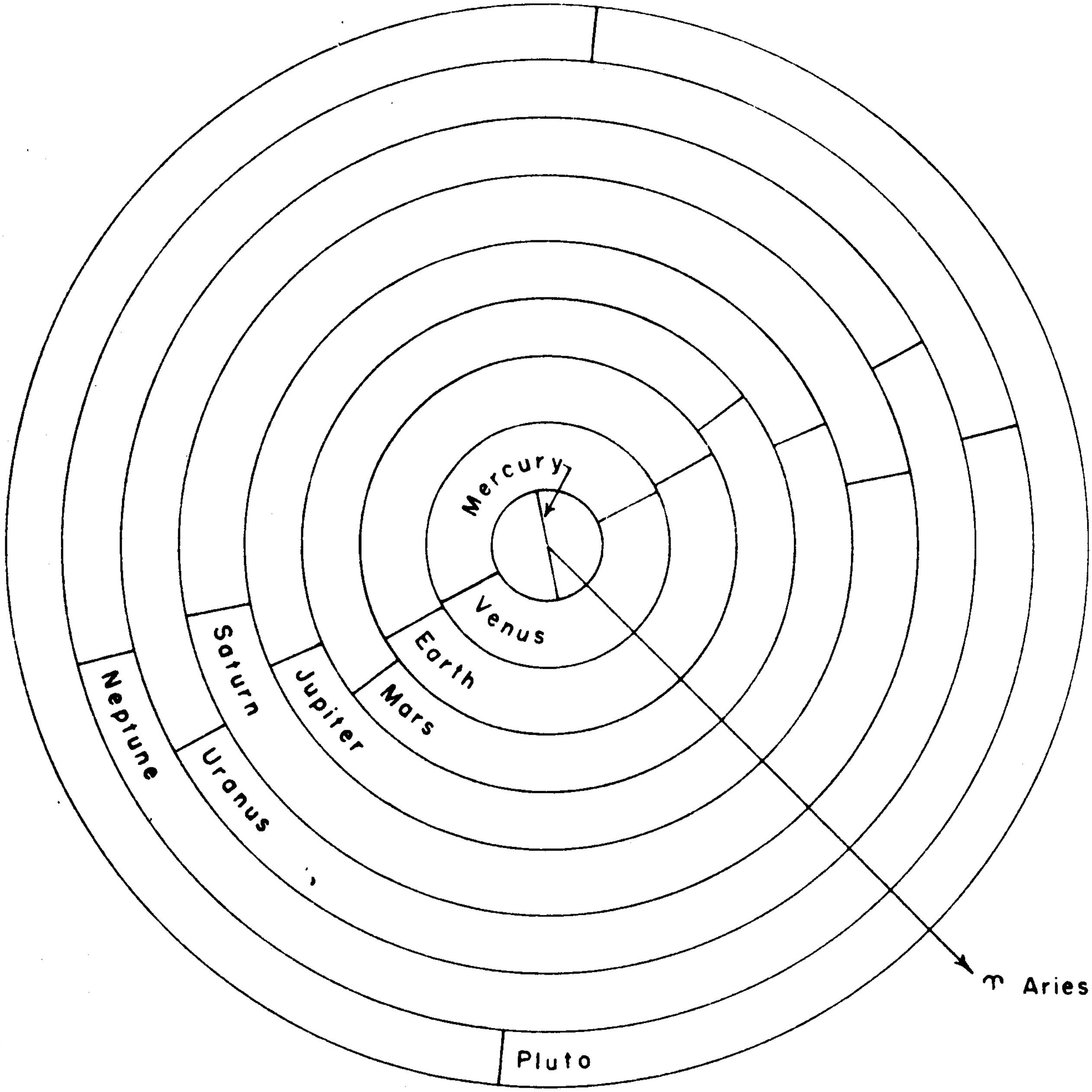

Figure 32. Ascending Nodes of the Planets with Respect to the Solar Equator (schematic)

Table 35. Short Period Resonances of the Inner Planets. (Explanatory Supplement to the Astronomical Ephemeris, 1961.)

PERIOD	TROPICAL YEARS
46 Siderial Revolutions of Mercury	11.079
18 Siderial Revolutions of Venus	11.074
11 Siderial Revolutions of Earth	11.000
6 Siderial Revolutions of Mars	11.286

Table 36. Long Period Resonances of the Outer Planets. (Explanatory Supplement to the Astronomical Ephemeris, 1961.) For longer periods, see "Time and Astronomic Cycles," C. M. Stacey, pp. 999-1003, Encyclopedia of Atmospheric Physics and Astrogeology, Reinhold N.Y., 1967.

PERIOD	TROPICAL YEARS
6 Siderial Revolutions of Saturn	176.746
15 Siderial Revolutions of Jupiter	177.933
9 Synodic Periods, Jupiter - Saturn	178.734
14 Synodic Periods, Jupiter - Neptune	178.923
13 Synodic Periods, Jupiter - Uranus	179.562
5 Synodic Periods, Saturn - Neptune	179.385
4 Synodic Periods, Saturn - Uranus	181.455
1 Synodic Period, Uranus - Neptune	171.40

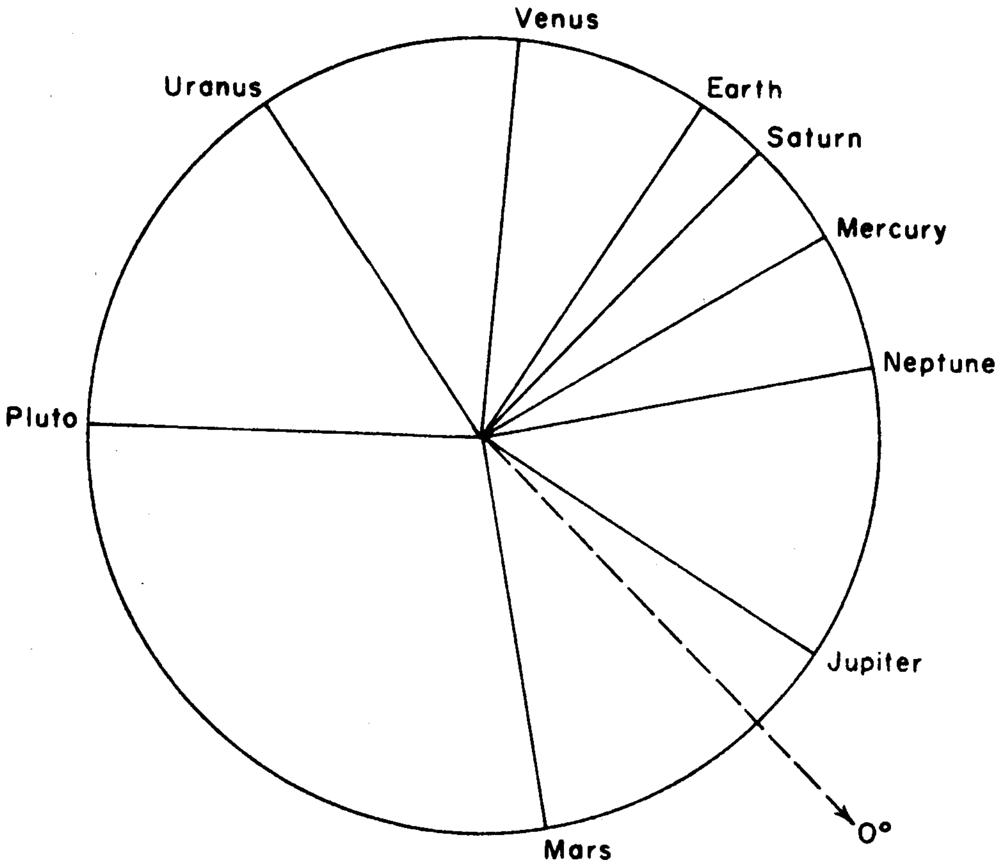

Figure 33. Perihelion Longitudes of the Planets. (Explanatory Supplement to the Astronomical Ephemeris and the American Ephemeris and Nautical Almanac.)

TABLE 37. Outer Planet Dates of Perihelion and Aphelion Passage, Nodal Passage and Greatest Latitudes North and South in the Solar Equatorial Coordinate System. Dates Derived from the Orbital Elements in Table 1 and the Planetary Ephemerides of the American Ephemeris and Nautical Almanac (yearly)

Planet	Perihelion	Asc. Node	Gr. Lat. N.	Desc. Node	Gr. Lat. S.	Aphelion
Jupiter	June 1, 1904	July 8, 1900	June 4, 1903	Feb. 21, 1906	Feb. 24, 1909	May 10, 1910
	Apr. 17, 1916	May 19, 1912	Apr. 12, 1915	Dec. 31, 1917	Jan. 1, 1921	Apr. 4, 1922
	Mar. 16, 1928	Mar. 26, 1924	Feb. 24, 1927	Nov. 11, 1929	Nov. 10, 1932	Feb. 19, 1934
	Jan. 11, 1940	Feb. 1, 1936	Jan. 2, 1939	Sep. 20, 1941	Sep. 20, 1944	Dec. 18, 1945
	Nov. 20, 1951	Dec. 15, 1947	Nov. 13, 1950	July 27, 1953	July 30, 1956	Oct. 23, 1957
	Sep. 26, 1963	Oct. 22, 1959	Sep. 17, 1962	June 7, 1965	June 6, 1968	Sep. 3, 1969
Saturn	Feb. 21, 1915	1896	June 27, 1905	Sep. 11, 1912	May 9, 1919	1900
	Sep. 8, 1944	Oct. 27, 1926	Nov. 26, 1934	Feb. 3, 1942	Oct. 7, 1948	Dec. 6, 1929
	Jan. 30, 1974	Mar. 29, 1956	Apr. 25, 1964	July 19, 1971	Mar. 6, 1978	May 29, 1959
Uranus	May 20, 1966	1986	June 6, 1923	Sep. 20, 1945	July 20, 1965	Apr. 1, 1925
Neptune	Sep. 15, 2042	Feb. 20, 1971	1847	1888	July 23, 1929	July 26, 1959
Pluto	Aug. 5, 1989	1946	2008	1822	1884	1865

III. NORTH-SOUTH ASYMMETRY OF SOLAR ACTIVITY

It has long been known that solar activity is not equally divided between the northern and southern hemispheres of the sun. Previous to 1850, sunspots were more numerous in the northern hemisphere; from 1865-1910 they predominated in the southern hemisphere, and from 1910-1938 again in the northern hemisphere (Rubashev, 1964). Apparently now the northern excess is coming to an end, since cycle 20 shows increasing southern activity. If sunspots (and associated solar activity) are influenced by planetary position, then their slow swing in latitude may be due to the similar slow swing in the combined influence of all the planets which exert an effect on the sun. Any such influence would need to be referred to planetary latitude with respect to the solar equatorial plane. Referring to Tables 34, 36 and 37 we find that the slowest important planets, Uranus and Neptune, reached their greatest latitudes north only 10 years apart in 1672 and 1682, in the solar equatorial coordinate system. We will now note a remarkable fact in the history of solar observations. The most extreme case of north-south asymmetry occurred between 1672 and 1704, when no spots were observed in the solar northern hemisphere (Rubashev, 1964, p. 38). During this entire time period two or more outer planets were north of the solar equator. Two years before Uranus reached the descending node, Saturn passed its ascending node, and Jupiter's northern position was apparently phased for the generation of southern spots.

Recently it has been shown by computer analysis that the orbital position of the planet Mercury influences the sunspot number (Bigg, 1965). He found an amplified Mercury effect when other planets (Venus, Earth, or Jupiter) was on the same side of the sun as Mercury. Bigg was searching for an increase in effect at Mercury's perihelion but found a very complex curve of sunspot number with the orbital position of Mercury. The author states "two conspicuous minima occur near the greatest latitudes north and south of the ecliptic plane." If the solar equatorial plane is used as a reference level instead of the ecliptic plane, involving a 100° rotation for Mercury's orbit, we find that the "two conspicuous minima" occur at the nodes of Mercury's orbit with respect to the solar equator. In other words, there is a sinusoidial component of the sunspot number with minima at Mercury's nodes and maxima at the orbital points where Mercury is farthest north and south of the solar equator. With this interpretation, Bigg's computer results for Mercury are in basic agreement with earlier results (Clayton, 1947) showing a small but consistent influence of Mercury's north and south positions on sunspot numbers. A similar latitude effect has also been demonstrated for Venus and the Earth (Clayton, 1947), provided the latitude of the planet is referred to the solar equator.

TABLE 38 Inner Planet Dates of Perihelion and Aphelion Passage, Nodal Passage and Greatest Latitudes North and South in the Solar Equatorial Coordinate System. Dates Derived from the Orbital Elements in Table 1 and the Planetary Ephemerides of the American Ephemeris and Nautical Almanac (yearly)

Planet	Perihelion	Asc. Node	Gr. Lat. N.	Desc. Node	Gr. Lat. S.	Aphelion
Venus	Jan. 29, 1966	Sep. 3, 1965	Oct. 29, 1965	Dec. 25, 1965	Feb. 19, 1966	Oct. 9, 1965
	Sep. 10, 1966	Apr. 16, 1966	June 11, 1966	Aug. 6, 1966	Oct. 1, 1966	May 21, 1966
	Apr. 23, 1967	Nov. 26, 1966	Jan. 22, 1967	Mar. 20, 1967	May 14, 1967	Jan. 1, 1967
	Dec. 4, 1967	July 9, 1967	Sep. 4, 1967	Oct. 30, 1967	Dec. 25, 1967	Aug. 14, 1967
	July 16, 1968	Feb. 19, 1968	Apr. 15, 1968	June 11, 1968	Aug. 5, 1968	Mar. 25, 1968
	Feb. 26, 1969	Sep. 30, 1968	Nov. 26, 1968	Jan. 22, 1969	Mar. 18, 1969	Nov. 5, 1968
Earth	Jan. 3, 1966	June 6, 1966	Sep. 8, 1966	Dec. 7, 1966	Mar. 6, 1966	July 5, 1966
	Jan. 2, 1967	June 6, 1967	Sep. 8, 1967	Dec. 7, 1967	Mar. 6, 1967	July 5, 1967
	Jan. 4, 1968	June 6, 1968	Sep. 8, 1968	Dec. 7, 1968	Mar. 6, 1968	July 2, 1968
	Jan. 3, 1969	June 6, 1969	Sep. 8, 1969	Dec. 7, 1969	Mar. 6, 1969	July 5, 1969
Mars	Jan. 16, 1966	Nov. 2, 1963	Mar. 27, 1964	Sep. 2, 1964	Feb. 1, 1965	Feb. 6, 1965
	Dec. 4, 1967	Sep. 19, 1965	Feb. 13, 1966	July 20, 1966	Dec. 19, 1966	Dec. 26, 1966
	Oct. 21, 1969	Aug. 7, 1967	Jan. 1, 1968	June 6, 1968	Nov. 7, 1968	Nov. 12, 1968

CONCLUSIONS

Solar activity has been studied to observe if there are cyclic variations related to planetary position above or below the solar equator. In order to study this phenomenon, a solar equatorial coordinate system was developed. The orbital elements of all nine planets were determined relative to the plane of the solar equator, since the ecliptic plane used for observational purposes is irrelevant in this context.

In the solar equatorial coordinate system, the ascending nodes of seven planets lie within the range 240° to 260°. The concentration suggests that there may be related seasonal variations in solar activity. In addition, the planets Jupiter, Neptune, Mercury, Saturn and Earth all have eccentric orbits and are in perihelion in the same heliocentric quadrant between the perihelion of Jupiter (13°.67823) and the earth (102°.25253). A concentration of planets in this quadrant could cause exceptionally strong planetary tides (if tides are the mechanism of planetary influence on solar activity).

The applicability of the solar equatorial coordinate system is demonstrated by solar activity data correlated to the north-south positions of inner and outer planets. Tables are presented giving dates of ascending and descending nodes, greatest latitudes north and south, and perihelion and aphelion passage in the solar equatorial coordinate system for the major planets.

REFERENCES

Allen, C. W., "Astrophysical Quantities," Univ. of London, Athlone Press, London, 1963.

American Ephemeris and Nautical Almanac, U. S. Government Printing Office (yearly).

Bigg, E. K., "Influence of the Planet Mercury on Sunspots," Astronom. J. 72, pp. 463-466 (May 1967).

Clayton, H. H., "Solar Cycles," Smithsonian Misc. Coll 106 #2 Misc. Publ. 3870, Washington, D. C. (March 5, 1947).

Dicke, R. H. and Goldenberg, H. M., "Solar Oblateness and General Relativity," Phys. Rev. Letters 18, p. 313 (1967).

Explanatory Supplement to the Astronomical Ephemeris and the American Ephemeris and Nautical Almanac, Her Majesty's Stationery Office, London, 1961.

Gilvarry, J. J. and Sturrock, P. A., "Solar Oblateness and the Perihelion Advances of Planets," Nature 216, No. 5122, p. 1283 (December 30, 1967).

Goldreich, P. and Schubert, G., "Differential Rotation in Stars," Astrophys. J. 150, p. 57 (1967).

Jose, P. D., "Sun's Motion and Sunspots," Astronom. J. 70, #3 pp. 193-200 (April 1965).

Kopecky, M., "The Periodicity of the Sunspot Groups," Adv. Astron. and Astrophysics Vol. 5 (1967).

Molchanov, A. M., "The Resonant Structure of the Solar System," Icarus 8, 203-215 (1968).

O'Connell, R. F., "Regression of the Node of the Orbit of Mercury due to a Solar Quadrupole Moment," The Astrophysical Journal 152, L11-12 (April 1968).

"Planetary Positions 1800-1940, 1940-1960, and 1960-1980," Her Majesty's Stationery Office, London 1958, 1960, 1961.

Roxborough, I. W., "Solar Oblateness," Nature 216, No. 5122, p. 1286 (December 30, 1967).

Rubashev, R. M., "Problems of Solar Activity," NASA TTF-244 Washington, D. C. 1964.

Shapiro, I. I., "Solar Rotation and Planetary Orbits," Icarus 4, p. 549 (1965).

Shapiro, I. I., in "Dynamics of Satellites," (ed. by M. Roy) p. 257, Academic Press, N. Y., 1963.

Smart, W. M., "Spherical Astronomy," Cambridge University Press, 1962.

Wollars, E. W. and Clemence, G. M., "Spherical Astronomy," Academic Press, N. Y., 1966.